DISSERTATION

Defence held on 12/09/2019 in Esch-sur-Alzette
to obtain the degree of

DOCTEUR DE L'UNIVERSITÉ DU LUXEMBOURG EN BIOLOGIE

by

Simone LARSEN

Born on 20 July 1991 in Denmark

PHENOTYPIC CHARACTERIZATION OF CELLULAR MODELS OF VPS35-ASSOCIATED MUTATION IN PARKINSON'S DISEASE

Dissertation defence committee

Dr Rejko KRÜGER, dissertation supervisor
Professor, Université du Luxembourg

Dr Stephen Wood
Associate Professor, Griffith University

Dr Anne GRÜNEWALD, Chairman
Associate Professor, Université du Luxembourg

Dr Philip SEIBLER
Professor, University of Lübeck

Dr Alexander SKUPIN, Vice Chairman
Université du Luxembourg

Affidavit

I hereby confirm that the PhD thesis entitled "Phenotypic characterization of cellular models of VPS35-associated mutation in Parkinson's disease" has been written independently and without any other sources than cited.

Luxembourg, the …………………………..   …………………………………………
                                                                          Name

Table of Contents

Abbreviations:

β2AR	β2 adrenergic receptor
AD	Alzheimer's disease
AMPAR	α-amino-3-hydroxy-5-methyl-4-isoxazolepropionic acid receptor
APP	amyloid precursor protein
CCCP	carbonyl cyanide 3-chlorophenylhydrazone
CIMPR	cation-independent mannose 6-phosphate receptor
CMA	chaperone-mediated autophagy
CRISPR	clustered regularly interspaced short palindromic repeats
DA	dopamine
DAT	Dopamine transporter
DMEM	Dulbecco's Modified Eagles Medium
DMSO	dimethylsulfoxide
DRD1	dopamine receptor D1
Drp1	dynamin related protein 1
ER	endoplasmic reticulum
ETC	electron transport chain
GABA	gamma-aminobutyric acid
GCase	Glucocerebrosidase
HEK293T	human embryonic kidney 293T
hrs	hours
ICC	immunocytochemistry
iPSC	induced pluripotent stem cell
KD	knock down
KI	knock in
KO	knock out
LAMP	lysosome associated membrane protein
LRRK2	leucine-rich repeat kinase 2
LTP	long term potentiation
MAM	mitochondria associated membrane
MAPL	mitochondria associated protein ligase
MEF	mouse embryonic fibroblasts
MFN	mitofusin 2
MMP	mitochondrial membrane potential
MDV	mitochondria derived vesicle
min	minutes
MPTP	1-methyl-4-phenyl-1,2,3,6-tetrahydropyridine
NMDAR	N-methyl-D-aspartate receptor
PD	Parkinson's disease
PINK1	PTEN-induced putative kinase 1
PMA	purmorphamine
RBD	REM sleep behavior disorder
REM	rapid eye movement
RME-8	receptor-mediated endocytosis 8
ROS	reactive oxygen species
smNPC	small molecule neuronal precursor cell
SNX	sorting nexin

TOM	translocase of the outer membrane
TGN	trans-Golgi network
TH	tyrosine hydroxylase
TMRE	tetramethylrhodamine, ethyl ester
VDAC1	Voltage-dependent anion-selective channel 1
VPS	vacuolar protein sorting
WASH	Wiskott-Aldrich syndrome protein and scar homolog
WT	wild type

Summary

Parkinson's disease was first described more than 200 years ago and yet the aetiology of the disease is not fully understood. Cellular phenotypes include mitochondrial impairment, lysosomal clearance dysfunction with α-synuclein accumulation and intracellular trafficking alterations. In most cases PD develops sporadically and the causes are yet unknown. However, in 10% of the cases, PD is inherited and the cause is genetic. Currently, 23 *PARK* loci have been identified within genes causing PD (Del Rey *et al.*, 2018). Here, we focus on *PARK17,* where a point mutation leading to an amino acid exchange p.D620N in VPS35 has been found to cause an autosomal-dominant form of PD.

Fibroblasts from a patient carrying the p.D620N mutation and from two age and gender-matched control were derived from a skin biopsy. Functional analyses of these fibroblasts revealed that mitochondrial membrane potential (MMP) was decreased in the patient cells compared to controls without any alteration of mitochondrial morphology (Appendix 1).

Next, the fibroblasts were reprogrammed into induced pluripotent stem cells (iPSCs),that were characterised in detail (Manuscript I). The iPSCs were first differentiated in small molecule neuronal precursor cells (smNPCs) (Reinhardt *et al.*, 2013), where we analysed mitochondrial function and lysosomal clearance capacity (Appendix 2). We found no significant difference in MMP between patient and control smNPCs. However, we observed a decreased autophagic flux and lower levels of mature Cathepsin D protein, a lysosomal hydrolase responsible for the degradation of α-synuclein. Nonetheless, we found no difference in α-synuclein protein level.

In order to study the impact of p.D620N on PD-related neuronal phenotypes we differentiated the smNPCs in this more disease-relevant cell population. We generated a neuronal culture enriched in dopaminergic neurons (Manuscript II). We found that the mitochondrial network was fragmented with smaller mitochondria and less branching. Mitochondria had lower MMP and increased intra-mitochondrial reactive oxygen species (ROS) levels. In addition, mitochondrial respiration was impaired which resulted in lower production of ATP. After CCCP treatment, mitophagy was induced in the patient neurons to the same level as in the control neurons. However, while in the control neurons the autophagosomes containing mitochondrial fragments were successfully cleared, in the patient neurons they accumulated and were not cleared properly. In line with this observation, the autophagic flux was decreased and late endosome/lysosomal mass was decreased. This decreased autophagic flux was accompanied by an increase of α-synuclein protein levels.

We further wanted to pinpoint how p.D620N VPS35 caused mitochondrial impairment in patient neurons. Accumulation of α-synuclein has been shown to induce similar mitochondrial alterations. Therefore, we measured α-synuclein protein levels in the mitochondrial and the cytosolic fraction and found that it was increased in both fractions to the same ratio. However, when we knocked down α-synuclein to the levels of the controls, it was not sufficient to rescue the decreased MMP and increased ROS level in the patient neurons. We conclude that α-synuclein accumulation in the mitochondrial fraction was not sufficient to cause the observed phenotype.

Recently, an increased LRRK2 kinase activity was identified in p.D620N VPS35 mutant monocytes and erythrocytes from patients, as well as brains from homozygous mice. Therefore, we hypothesized that pathological LRRK2 kinase activity may induce mitochondrial impairment. We measured the phosphorylation levels of Rab10, one of LRRK2 kinase substrates, however, no significant difference between patient and control neurons was observed.

In this study, we show for the first time that p.D620N VPS35 causes PD-related cellular phenotypes in patient-derived neurons. The patient-derived neurons displayed impaired mitochondria and lysosomal clearance, with accumulation of α-synuclein.

1. Introduction

Parkinson's disease (PD) is the second most common neurodegenerative disease and is characterised as a progressive movement disorder with a broad spectrum of motor and non-motor symptoms (Jankovic, 2008). The diagnosis of PD can only be confirmed *post mortem* based on the presence of Lewy bodies and neurites in the brain. Clinically, PD is diagnosed by four criteria: bradykinesia, resting tremor, rigidity and postural instability (Jankovic, 2008). Moreover, patients typically have a good and sustained response to levodopa (or L-Dopa) treatment.

According to the American Parkinson Foundation, it affects approximately ten million patients worldwide with a prevalence of 1% in people older than 60 years in Europe (von Campenhausen *et al.*, 2005). Since 1990, the number of PD patients has more than doubled worldwide and is foreseen to continue to dramatically increase in the next generations, which will ultimately increase the cost of healthcare (Dorsey *et al.*, 2018).

This disease was first described over 200 years ago by James Parkinson in the *Essay of the Shaking Palsy* in 1817. Even though our understanding of the disease improved, there is still no curative treatment for PD available, nor a way to prevent it. In order to do so, we need to understand better the underlying molecular mechanisms involved in the pathophysiology of the disease to identify potential biomarkers for prevention or pathways impaired for treatment.

1.1. Parkinson's disease

1.1.1. Clinical phenotype and risk factors

The three cardinal motor symptoms are bradykinesia, unilateral resting tremor and rigidity (Jankovic, 2008).

Bradykinesia is defined as a slowness of movement and is directly correlated with the degree of dopamine loss (Lozza *et al.*, 2002). It is essential for the diagnosis of the patient. Bradykinesia is clinically assessed by loss of amplitude and speed in repetitive finger taping and hand pronation-supination movement (Jankovic, 2008). Another common clinical feature in PD in resting tremor. It is a shaking with a frequency between 4 and 6 Hz and commonly appears in the hands in a pronation-supination manner, more pronounced on one side. Most patients experience resting tremor at the early onset of the disease (Hughes *et al.*, 1993) and it is one of the most disabling feature for the patients. Patients can experience rigidity of the limbs, which can be accompanied by pain, especially in the shoulders (Stamey *et al.*, 2008).

Some patients suffer from postural instability, it occurs relatively late after the disease onset (Jankovic, 2008) and it is the major cause of falls in PD, together with freezing. Freezing is as well very disabling for the patients, it occurs mainly in patients without tremor (Macht *et al.*, 2007). The main form of freezing is the freezing of gait, characterised by a transient inability to walk (Bloem *et al.*, 2004).

The motor symptoms can be accompanied by a variety of non-motor symptoms that can occur prior to the disease diagnosis or concomitantly. For example, hyposmia, rapid eye movement (REM) sleep behaviour disorder (RBD), depression and constipation can precede the onset of motor symptoms and can be caused by other neuronal degeneration (Schapira *et al.*, 2017). On the other hand, cognitive decline occurs concomitantly or later in the disease progression in the majority of patients (Schapira *et al.*, 2017).

PD usually occurs sporadically or in approximately 5-10% of all cases, is inherited genetically. The main risk factor of PD is age but some environmental factors combined with genetic predisposition can increase the risk of developing PD. Up to date, 23 loci have been identified and for most of them genes were identified that co-segregate with PD in families (**Table 1**). The first gene associated with PD was *SNCA*, coding for α-synuclein, the main protein aggregated in Lewy bodies (Polymeropoulos *et al.*, 1997). Point mutations in *SNCA* or multiplication of the gene cause an autosomal-dominant form of PD (**Table 1**). Other genes have been associated with autosomal-dominant form of PD such as *LRRK2, EIF4G1* and *VPS35* (**Table 1**). The LRRK2 p.G2019S variant is the most common cause of autosomal-dominant PD in the Western hemisphere. Several genes have been associated with autosomal-recessive form of PD such as *PRKN*, *PINK1*, *DJ-1* and *DNAJC6* (**Table 1**). Furthermore, some genes have been associated with greater risk of developing PD, such as *GBA*, which is the most common risk factor (Sidransky *et al.*, 2009).

Table 1: List of *PARK* genes

Locus	MIM No.	Inheritance	Chr.	Gene	Mutation	First described by
PARK1	601508	AD	4q21-23	***SNCA***	PM	Polymeropoulos et al., 1997
PARK2	600116		6q25.2-27	***PRKN***	Del/Ins/Dupl /Tripl/PM	Kitada et al., 1998
PARK3	602404	AD	2p13	-	-	Gasser et al., 1998

Locus	MIM No.	Inheritance	Chr.	Gene	Mutation	First described by
PARK4	605543	AD	4q21-23	*SNCA*	Dupl, Tripl	Singleton et al., 2003
PARK5	191342	AD	4p14	*UCH-L1*	PM	Leroy et al., 1998
PARK6	605909	AR	1p35-36	*PINK-1*	PM	Valente et al., 2004
PARK7	606324	AR	1p36	*DJ-1*	Del, PM	Bonifati et al., 2002
PARK8	607060	AD	12cen	*LRRK2*	PM	Zimprich et al., 2004
PARK9	606693	AR	1p36	*ATP13A2*	PM	Ramirez et al., 2006
PARK10	606852	AD	1p32	*-*	-	Hicks et al., 2001
PARK11	607688	AD	2q36-37	*GIGYF2*	PM	Lautier et al., 2008
PARK12	300557	nd	Xq21-25	*-*	-	Pankratz et al., 2003
PARK13	610297	AD	2p12	*Omi/HtrA2*	PM	Strauss et al., 2005
PARK14	610297	AR	22q13	*PLA2G6*	PM	Gregory et al., 2008
PARK15	610297	AR	22q12-13	*FBXO7*	PM	Di Fonzo et al., 2008
PARK16	613164	AR	1q32	*-*	-	Satake et al, 2009
PARK17	614203	AD	16q13	*VPS35*	PM	Zimprich et al., 2011
PARK18	614251	AD	3q27.1	*EIF4G1*	PM	Chartier-Harlin et al., 2011
PARK19	615528	AR	1p31.3	*DNAJC6*	Del, PM	Edvardson et al., 2012
PARK20	615530	AR	21q22.11	*SYNJ1*	PM	Quadri et al., 2013
PARK21	614334	AD	3q22.1	*DNAJC13*	PM	Vilariño-Güell et al., 2014
PARK22	616710	AD	7p11.2	*CHCHD2*	PM	Funayama et al., 2015
PARK23	616840	AR	15q22.2	*VPS13C*	PM	Lesage et al., 2016

Overall, PD is a very heterogeneous disease and patients do not all suffer from the same clinical phenotypes, making it difficult to treat. Lately, clinicians have been trying to stratify the disease by endophenotypes in order to find the best personalised treatment for each patient (Krüger *et al.*, 2017). Studying the monogenic forms of PD as prototypes could help decipher the underlying mechanisms of each endophenotype of the disease.

1.1.2. Pathophysiology

PD is characterised by two main hallmarks: degeneration of dopaminergic (DA) neurons in the *substantia nigra pars compacta* and presence of α-synuclein-positive inclusions in the soma (Lewy bodies) and in neurites (Lewy neurites) of the remaining neurons. A-synuclein inclusions start in the brain stem and spread to the forebrain and the midbrain, when the motor symptoms begin, and spread further to the whole brain according to the Braak staging (Braak *et al.*, 2006). Other type of neurons degenerate as well in PD, such as cholinergic neurons in the pedunculopontine nucleus and noradrenergic neurons in the locus coeruleus (Bolam and Pissadaki, 2012). There seems to be a higher susceptibility in neurons with long axons and unmyelinated arborisation.

However, DA neurons of the *substantia nigra pars compacta* are selectively dying, which is the main cause of the motor symptoms experienced by patients. DA neurons are particularly susceptible to death because of their autonomous pacemaker activity (Surmeier and Sulzer, 2013). Indeed, DA neurons are highly active cells that need a lot of energy to sustain their activity and to transport molecules, proteins or organelles along their long axon, projecting in the striatum. This high energy need will consequently increase the production of mitochondrial reactive oxygen species (ROS), which is detrimental to the neurons (Brichta and Greengard, 2014).

So far, clinicians have been focusing on a dopamine replacement strategy as a treatment for motor symptoms. However, this strategy is only a symptomatic treatment, and treatment is not yet in place to either slow down or revert the disease, nor to prevent it. We need to better understand the molecular and cellular pathomechanisms to identify new pathways involved and subsequently to find new treatments.

1.2. Cellular pathways dysregulated in PD

In order to better understand the pathomechanisms underlying DA neurodegeneration, scientists have been using monogenic forms of the disease. Indeed, they hypothesise that they can serve as relevant prototypes of the disease for studying different pathways involved. Some *PARK* genes are involved in mitochondrial homeostasis, some in lysosomal clearance and protein aggregation and finally some in endosomal trafficking and synaptic function (Antony *et al.*, 2013) (**Fig. 1**).
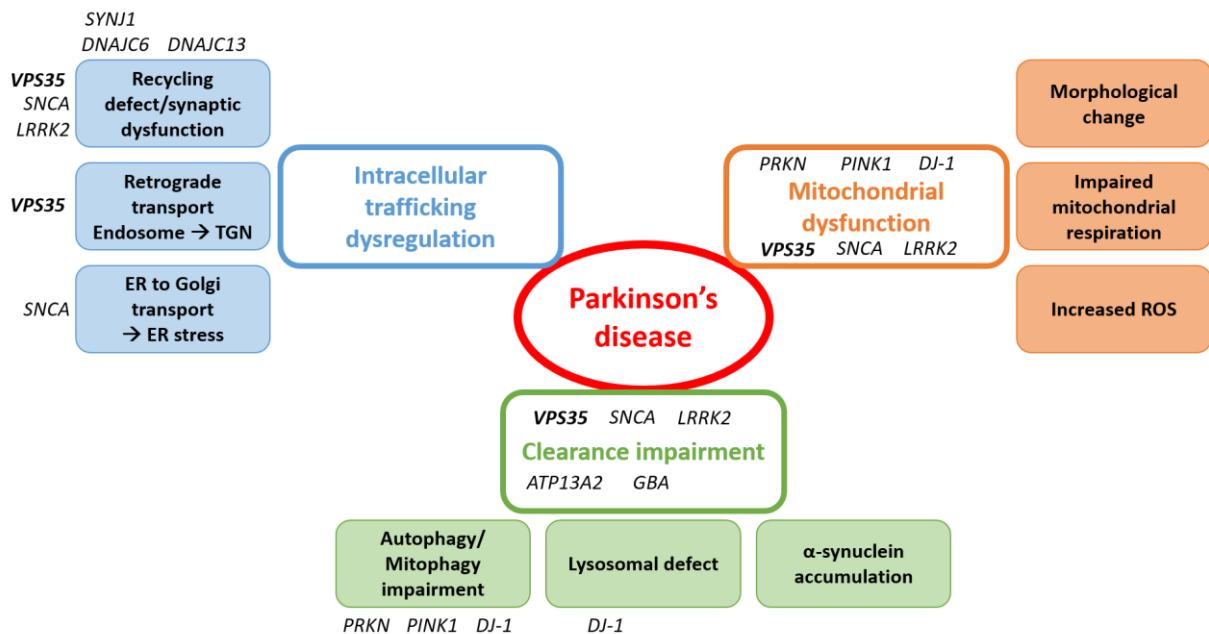
<u>Figure 1</u>: Schematic overview of cellular pathways involved in PD pathomechanisms and PD-linked genes associated. All the pathways mentioned in the thesis are summarized in this scheme and references can be found in the text.

1.2.1. Mitochondrial impairment

The first evidence of the link between mitochondrial dysfunction and Parkinson's disease came from an observation of two cases of drug abuse where patients developed a severe parkinsonism (Langston *et al.*, 1983). MPTP was injected intravenously and was converted in MPP+ in the brain which can enter selectively dopaminergic neurons by the dopamine transporter (DAT) (Storch *et al.*, 2004). MPP+ inhibits complexes I, III and IV of the electron transport chain which leads to impaired mitochondrial respiration and decreased ATP production (Nicklas *et al.*, 1985). Other environmental factors such as exposition to pesticides

have been associated with mitochondrial respiration deficiency. Indeed, rotenone is a pesticide which inhibits complex I activity and further leads to mitochondrial respiration deficiency (Jackson-Lewis *et al.*, 2012). Mitochondrial respiration dysfunction is tightly linked to impaired mitochondrial membrane potential (MMP) and increased mitochondrial ROS. ROS forms close to complex I and III, where electrons escape the electron transport chain (Quinlan *et al.*, 2013). Mitochondrial respiration impairment further leads to decreased ATP production and dopaminergic neuronal death (reviewed in Grünewald *et al.*, 2019).

An impairment of mitochondrial respiration was also found post-mortem in the *substantia nigra* of PD patients with reduced complex I, II and IV activities (Bindoff *et al.*, 1989). Later, several mitochondrial associated genes were found to be mutated in PD patients and segregated within families. Among those, mutations in the *PRKN*, *PINK1* and *DJ-1* genes were found to cause early-onset autosomal-recessive PD (reviewed in Larsen *et al.*, 2018). Interestingly, the proteins encoded by these genes are involved to a different extent in mitochondrial quality control (**Fig. 1**).

Indeed, DJ-1 is a redox sensor and plays a crucial role of scavenging mitochondrial ROS which confirms the implication of elevated ROS levels in dopaminergic neurodegeneration (Grünewald *et al.*, 2019). Omi/HtrA2 is a mitochondrial chaperone implicated in the mitochondrial unfolded protein response and leads to the degradation of oxidised and unfolded proteins in the inner membrane space of the mitochondria (Moisoi *et al.*, 2009). Mutations in *Omi/HtrA2* have been linked to PD as rare variants with substantial effect (Strauss *et al.*, 2005; Unal Gulsuner *et al.*, 2014). On the other hand, Parkin and PINK1 are essential proteins for the induction of mitophagy. Mitophagy has been described for the first time while characterising the functional impairment of Parkin and Pink1 deficiency in the context of PD (Narendra *et al.*, 2008; Youle and van der Bliek, 2012). Recently, both proteins have also been linked to another type of mitochondrial quality control involving the budding of vesicles from the mitochondrion. These mitochondria derived vesicles (MDV) engulf localised oxidised proteins (Soubannier *et al.*, 2012) or selective cargoes such as MAPL (mitochondria-associated protein ligase) (Braschi *et al.*, 2009) or Drp1 (Wang *et al.*, 2015). These MDVs are then redirected towards the lysosome or the peroxisome. The two cargoes identified so far have been shown to be transported in VPS35 positive vesicles, suggesting that the retromer plays a role in mitochondrial quality control, which will be discussed later on.

The first level of mitochondrial quality control is morphology change. Indeed, mitochondria are highly dynamic organelles capable of travelling anywhere in the cell according to energy

demands. Mitochondria undergo several cycles of fission and fusion to maintain their homeostasis. Two mitochondria can fuse in order to dilute their content which requires fusion proteins MFN1, MFN2 and OPA1. For example, mitochondria accumulate mitochondrial DNA (mtDNA) mutations and ROS over time. In order to decrease the impact of mutated mtDNA or ROS, one mitochondrion can fuse with another one (reviewed in Larsen *et al.*, 2018). If this is not enough to rescue the defective mitochondrion, it can undergo fission to isolate the dysfunctional part, which implicates the fission protein Drp1. During fission, MMP decreases and Drp1 forms a spiral around the mitochondrion. The defective depolarised mitochondrion then undergoes mitophagy in order to be cleared (reviewed in Larsen *et al.*, 2018). The balance between fission and fusion is essential to maintain mitochondria integrity. Interestingly, several studies report excessive fragmentation of mitochondrial network in models of PD (reviewed in Burbulla *et al.*, 2010), suggesting an unbalance of fission/fusion.

Other PD-associated genes have been linked to mitochondrial dysfunction, even though they were not initially described as being mitochondria-related; e.g. *SNCA* and *LRRK2* (**Fig. 1**). α-Synuclein and LRRK2 are associated with vesicular trafficking and can be found in the endosomal pathway. However, α-synuclein has been shown to colocalise with mitochondria in several studies. How exactly they interact is still debated. Di Maio *et al.*, showed that toxic forms of α-synuclein can interact with TOM20, impairing mitochondrial protein import (Di Maio *et al.*, 2016). Overexpression of α-synuclein thus led to reduced respiration, increase ROS and loss of MMP. This interaction was confirmed in post-mortem brain tissue from PD patients where an increase α-synuclein-TOM20 interaction was found. On the other hand, α-synuclein is found to be located in region of ER-mitochondria contacts (mitochondria associated membranes, MAM) (Guardia-Laguarta *et al.*, 2014). In this study, PD-associated mutations in α-synuclein caused an increased association with MAM and led to an increase mitochondrial fragmentation.

LRRK2 interacts with key regulators of mitochondrial dynamics such as Miro1, Drp1, MFN2 and OPA1. Indeed, when MMP drops, LRRK2 removes Miro1 from mitochondria to stop its transport (Hsieh *et al.*, 2016). Miro1 is responsible for the transport of mitochondria along microtubules and variants of Miro1 have recently been linked with PD (Grossmann *et al.*, 2019). The removal of Miro1 is necessary for the induction of mitophagy. LRRK2 interacts with Drp1, MFN2 and OPA1 and modulates their activity (reviewed in Ryan *et al.*, 2015). The PD-associated LRRK2 G2019S mutation, resulting in an increase of kinase activity, exacerbates

Drp1 phosphorylation and activation leading to an enhanced mitochondrial fragmentation (Niu *et al.*, 2012).

Interestingly, the retromer has also been linked to the regulation of mitochondrial morphology via MDV sorting (reviewed in Larsen *et al.*, 2018), which will be explained further later.

1.2.2. Clearance impairment and protein aggregation

Cells use different strategies to effectively degrade long-lived proteins and organelles which involve the lysosomal compartment. Autophagy is one of the main strategies and three different types exist, depending on how the content is delivered to lysosomes. Macroautophagy is the most common form and also the most studied and depends on the elongation of a double membrane structure called phagophore. It is not specific and is defined as a bulk degradation of cytoplasmic content including proteins and organelles. When the phagophore closes, the structure containing cytoplasmic components is called the autophagosome which will subsequently fuse with the lysosome for degradation. Macroautophagy will hereafter be referred to as autophagy. Microautophagy is not well characterised and is defined by the invagination of the lysosomal membrane itself. It will therefore sequester small amount of cytoplasmic content. Chaperone-mediated-autophagy (CMA) is a selective form of autophagy. It involves receptors on the endosomal/lysosomal membrane (LAMP2A) and in the cytosol (Hsc70) which targets specific proteins carrying the KFERQ amino acid sequence. Proteins are then translocated directly into the lysosome across the membrane. In the lysosomal lumen, the acidic environment and several hydrolases are responsible for the degradation of its content. Endocytosed membranous proteins present in the endosomal system can be degraded upon fusion of the late endosome with lysosome.

The normal degradation route of α-synuclein is the lysosomal system and in case of increased α-synuclein burden, the autophagy system is recruited. Indeed, soluble α-synuclein as well as aggregated forms can be engulfed by bulk autophagy and further be degraded in the lysosomal lumen. Furthermore, α-synuclein can be directly targeted by LAMP2A for CMA mediated degradation as it contains the KFERQ amino acid sequence (Cuervo *et al.*, 2004). In the lysosomal lumen, α-synuclein is degraded by several enzymes including Cathepsin-D (Qiao *et al.,* 2008).

Impairment of the autophagy pathways have been linked to several genetic cases of PD, leading to α-synuclein accumulation (**Fig. 1**). Indeed, α-synuclein overexpression in

mammalian cell lines and transgenic mice results in decrease of autophagy induction by interfering with Atg9 localisation (Winslow *et al.*, 2010). Atg9 is essential for the initiation of autophagy, procuring membranes for the phagophore formation. Furthermore, α-synuclein aggregates reduces the autophagosome clearance in neurons treated with pre-formed fibrils (Tanik *et al.*, 2013). A53T mutant and dopamine modified α-synuclein has an increased affinity for LAMP2A and inhibits its translocation in the lysosome, therefore decreasing CMA-mediated degradation of various misfolded proteins (Cuervo *et al.*, 2004; Martinez-Vicente *et al.*, 2008).

PD-linked p.G2019S mutation of *LRRK2* inhibits CMA in the same way (Orenstein *et al.*, 2013). Furthermore, LRRK2 p.G2019S and p.R1441C mutant dopaminergic neurons display accumulation of autophagic vacuoles and increased mitophagy in mice (Ramonet *et al.*, 2011), which was confirmed in induced pluripotent stem cells (iPSCs) -derived neurons from PD patients carrying the mutant *LRRK2* (Sánchez-Danés *et al.*, 2012). In addition, *LRRK2* variants result in enlarged lysosomes and reduced lysosomal capacity in astrocytes (Henry *et al.*, 2015). LRRK2 seem to have a regulatory role in autophagy clearance and lysosomal function and size, which leads to α-synuclein accumulation. Mutations in *GBA*, the most common risk factor of PD, leads as well to impaired lysosomal activity. Indeed, *GBA* encodes for the lysosomal enzyme glucocerebrosidase (GCase) and the mutations compromise its activity. In IPSC-derived neurons from patient carrying the p.N370S mutant, lysosomal protein degradation is impaired which leads to α-synuclein accumulation (Mazzulli *et al.*, 2011). In turn, accumulation of α-synuclein result in dysfunctional lysosome by disrupting the trafficking of GCase from the ER to the lysosome (Mazzulli *et al.*, 2016). Interestingly, decrease of GCase activity has been shown also in post-mortem brain from sporadic PD patients, resulting in impaired lysosomal function and accumulation of α-synuclein (Murphy *et al.*, 2014). PD-linked mutations in the lysosomal protein ATP13A2 leads to impaired lysosomal acidification, reduced lysosomal degradation and decreased clearance of autophagosome in PD patient fibroblasts (Dehay *et al.*, 2012; Usenovic *et al.*, 2012). Furthermore, it also leads to accumulation of α-synuclein in mice (Usenovic *et al.*, 2012).

In addition, the retromer has been implicated in the sorting of key proteins for autophagy and lysosomal function (reviewed in Mohan and Mellick, 2017), which will be explained later on.

Mitochondria-associated proteins, linked to PD have also been shown to play a role in autophagy regulation (**Fig. 1**). As already mentioned, Parkin and Pink1 are responsible for the induction of mitophagy, thereby regulating the engulfment of mitochondria by autophagosomes. Also, loss of DJ-1 leads to reduced basal autophagy in knock out (KO) mice

(Krebiehl *et al.*, 2010). Furthermore, iPSC-derived neurons from patients with a loss of DJ-1 show decreased GCase activity in the lysosome with accumulation of α-synuclein protein level (Burbulla *et al.*, 2017).

All this highlights the relevance of lysosomal and autophagic dysfunction in the pathogenesis of PD (**Fig. 1**).

1.2.3. Defective intracellular trafficking

Intracellular trafficking includes two distinct pathways: the exocytic and endocytic pathway (Tokarev *et al.*, 2009). The exocytic pathway consists of proteins synthesised in the cytoplasm that are translocated in the endoplasmic reticulum (ER) and further transported to the trans-Golgi network (TGN) for sorting. The final destination varies from endosome, lysosome, back to the ER or to the plasma membrane for exocytosis. The endocytic pathway comprises proteins internalised at the plasma membrane through clathrin-dependent or independent endocytosis. Here, the sorting takes place in the early endosome with similar final destinations.

The first evidence that defective intracellular trafficking was a hallmark of PD pathogenesis came from the finding that mutations or multiplication in *SNCA* gene led to synaptic dysfunction (Vidyadhara *et al.*, 2019) (**Fig. 1**). Indeed, α-synuclein was demonstrated to be a synaptic protein, regulating clathrin-mediated endocytosis and therefore the endocytosis of synaptic vesicles (Vargas *et al.*, 2014). Some studies also suggest that α-synuclein could regulate exocytosis (Lautenschläger *et al.*, 2017). Overexpression of α-synuclein affects dopamine transporter trafficking, leading to a dopamine dyshomeostasis (Kisos *et al.*, 2014). Furthermore, it has been demonstrated that α-synuclein accumulation has detrimental effect on ER to Golgi trafficking of lysosomal enzyme GCase (Mazzulli *et al.*, 2016) and that aggregated forms could disrupt the retromer complex (Chung *et al.*, 2017). PD-associated variants of *VPS35*, component of the retromer complex, lead to intracellular mistrafficking of both exocytic and endocytic pathways (reviewed in Mohan and Mellick, 2017), which will be detailed later on. Interestingly, LRRK2 overexpression can rescue the VPS35 p.D620N synaptic deficit in drosophila larvae (Inoshita *et al.*, 2017). Indeed, LRRK2 and VPS35 can both be found in the endocytic compartment and seem to have similar roles in terms of synaptic vesicle recycling and dopaminergic synaptic release. LRRK2 p.G2019S mice display accumulation of clathrin-coated vesicles and lowered synaptic vesicle density in dopaminergic terminals (Xiong *et al.*, 2018). LRRK2 regulates synaptic vesicles endocytosis by

phosphorylating dynamin and endophilin A-1, which mediate the fission of clathrin-coated vesicles with the plasma membrane and recruits other proteins essential for the uncoating of clathrin. Moreover, LRRK2 phosphorylates synaptojanin 1 (Soukup *et al.*, 2016) and auxilin (Nguyen and Krainc, 2018), both responsible for the uncoating of clathrin. Interestingly, variants of synaptojanin 1 (*SYNJ1*) and auxilin (*DNAJC6*) have been linked to autosomal-recessive early-onset PD (Edvardson *et al.*, 2012; Quadri *et al.*, 2013). Mutations in *DNAJC6* lead to a lowered auxilin expression which causes synaptic vesicle endocytosis dysfunction (Yim *et al.*, 2010). Indeed, KO mice displayed increased number of clathrin-coated vesicles and empty cages at the synapse. Mutations in SYNJ1 cause impaired phosphatase activity and subsequently impaired synaptic vesicle endocytosis (Krebs *et al.*, 2013; Quadri *et al.*, 2013). Furthermore, fibroblasts from patients with *SYNJ1* mutations displayed defective endocytic trafficking, suggesting a role of synaptojanin outside of the synapse as well (Quadri *et al.*, 2013).

DNAJC13 mutations have also been linked to PD, causing autosomal-dominant PD (Vilariño-Güell *et al.*, 2014; Gustavsson *et al.*, 2015). Unlike the other DNAJC proteins variants, mutations in *DNAJC13* causes toxic gain-of-function of RME-8, leading to endolysosomal cargo trafficking deficits (Norris *et al.*, 2017). Moreover, RME-8 has been shown to regulate retromer complex activity by regulating the localization of the WASH complex (Wiskott-Aldrich syndrome protein and scar homolog) and the recruitment of SNX dimer, essential for cargo trafficking (Freeman *et al.*, 2014). However, this genetic link between *DNAJC13* and PD have been challenged by (Deng *et al.*, 2016), finding mutations in *TMEM230* in the same families.

LRRK2 also plays an important role in the late endosomal maturation and fusion with lysosomes. Indeed, in drosophila, mutations in LRRK2 impairs interaction with Rab7 (Dodson *et al.*, 2012) and reduce Rab7 activity in mammalian cells, consequently impairing late endosomal trafficking events (Gómez-Suaga *et al.*, 2014).

Curiously, DA neurons from *PRKN* patients displayed increased intracellular dopamine suggesting that dopamine packaging or metabolism might be impaired (Jiang *et al.*, 2012). Parkin have been associated with the endosomal system but its role in synaptic vesicle endocytosis remains to be explored. However, parkin has been showed to ubiquitinate VPS35 and other endosomal proteins, most likely to regulate their activity (Martinez *et al.*, 2017; Williams *et al.*, 2018). In *PRKN* deficient cells, the membrane association of VPS35 and SNX1 was impaired, suggesting an impaired retromer-mediated trafficking (Song *et al.*, 2016).

Indeed, Parkin regulates Rab7 activity by ubiquitination, a protein essential for retromer association with endosomes (Priya *et al.*, 2015).

Interestingly, deficit in exocytic pathways leads to all the above-mentioned impairment, *e.g.* mitochondrial dysfunction, decreased clearance and dysregulated synaptic function, putting trafficking deficit in the centre of PD pathogenesis (Vidyadhara *et al.*, 2019) (**Fig.1**). Growing number of endocytic membrane trafficking genes have been associated with risk of developing PD (Bandres-Ciga *et al.*, 2019). Further studies are needed to understand the role played by endocytic PD-linked proteins in the pathogenesis. Here, we will focus on the role of VPS35 p.D620N variant in PD phenotypes.

1.3. VPS35 and the retromer complex

The endosomal trafficking is a highly orchestrated system, essential for intracellular protein homeostasis. The retromer is one of the main sorting platform of the endosomal system. Deficiency in retromer sorting has been linked to several neurodegenerative diseases, including PD (Vagnozzi and Praticò, 2019).
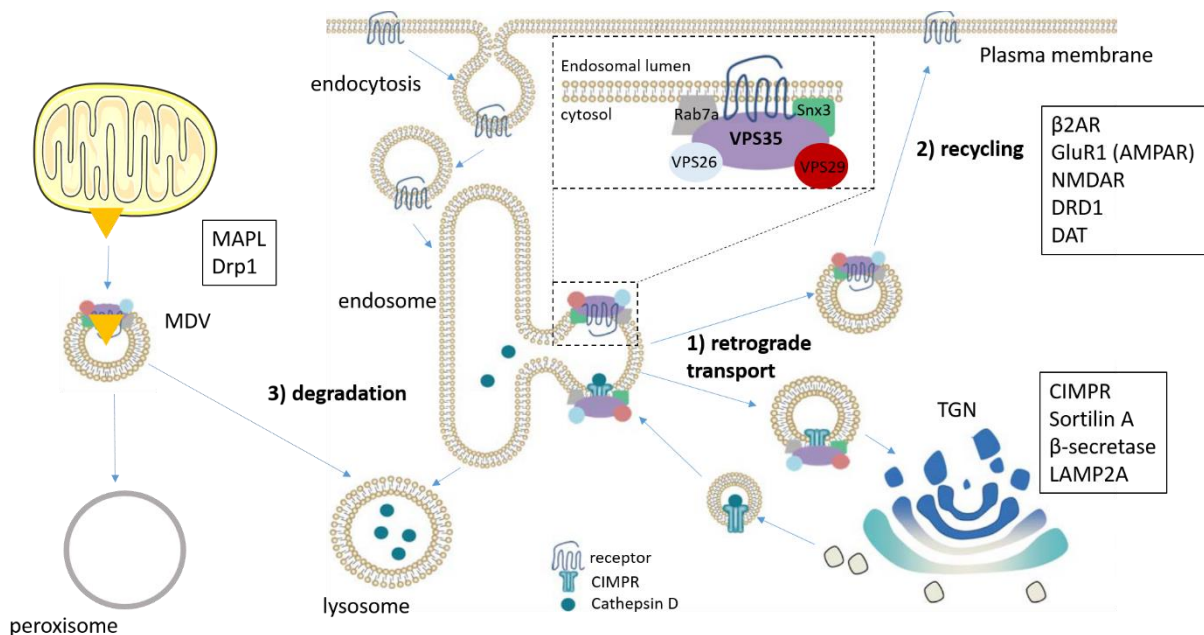

Figure 2: Schematic overview of retromer trafficking functions and cargoes known to be targeted. All the pathways mentioned in the thesis are summarized in this scheme and references can be found in the text. Figure adapted from (Williams *et al.*, 2017).

1.3.1. Retromer function

The retromer complex was first discovered in 1998 and is a heteropentamere ubiquitously expressed and highly conserved across species (Seaman *et al.*, 1998). It is composed by the cargo recognition complex of vacuolar protein sorting VPS35, VPS29 and VPS26A or VPS26B and a membrane associated heterodimer of SNX-Bar proteins (**Fig. 2**) (Griffin *et al.*, 2005). The retromer is recruited to endosomal membranes through Rab5 and Rab7 (Rojas *et al.*, 2008).

It was originally thought to convey only retrograde transport of hydrolase receptors from endosome to the TGN (Seaman *et al.*, 1998). Indeed, the first cargo described was cation-independent mannose 6-phosphate receptor (CIMPR) which is a receptor for the lysosomal hydrolase Cathepsin D. CIMPR binds pro-Cathepsin D in the TGN and delivers it to the endosomal system where it is cleaved into mature Cathepsin D. The retromer is responsible for the retrograde transport of unoccupied CIMPR back to the TGN (Arighi *et al.*, 2004). To date, three distinct pathways of endosomal trafficking have been found: 1) retrograde trafficking from endosomes to TGN, 2) recycling of endocytosed transmembrane receptors from early endosomes back to the plasma membrane and 3) degradation pathways towards lysosomes (**Fig. 2**) (Cui *et al.*, 2018).

The endosomes form a sorting hub in the cell where cargo proteins are sorted towards the different locations. In order to do so, tubulations enriched in cargo molecules are generated from the endosome. The machinery implicated in the tubulation are mostly SNX-BAR proteins that undergo oligomerisation on the endosome membrane surface. How exactly the tubulations are formed is still under investigation but seem to implicate SNX-BAR proteins, microtubules and associated motor proteins (Cui *et al.*, 2018). In addition, recent work showed that RME-8, encoded by *DNAJC13,* is required for SNX-1 mediated membrane tubulation (Freeman *et al.*, 2014). The budding process is realised by fission and implicates the dynamin GTPase. Studies in yeast have identified Vps1 and Mvp1 as key players in that process. However, the mechanism in mammalian cells remains elusive (Cui *et al.*, 2018) but might implicate EHD1 (Cai *et al.*, 2014) and the WASH complex (Derivery *et al.*, 2009). Indeed, the WASH complex interacts directly with VPS35 and dynamin/Arp2/3 complex, a regulator of β-actin network. The WASH complex has been showed to be essential for the sorting of several retromer cargoes. The vesicles then fuse with the final destination organelle.

The retrograde pathway has been described firstly for CIMPR sorting (**Fig. 2, pathway 1**). Since then, several cargoes have been identified such as LAMP2A. Indeed, LAMP2A is

implicated in CMA and is localised in the late-endosome/lysosome. After translocation of the cargo in the late-endosome/lysosome, LAMP2A needs to be retrieved in order to avoid degradation. The retromer is responsible for the retrieval of LAMP2A and recycling back to the TGN. In VPS35 knock down (KD) mice, LAMP2A protein level and LAMP2A positive vesicles were decreased specifically in the ventral midbrain and not in other brain regions (Tang *et al.*, 2015*a*). In addition, the retromer, in cooperation with the WASH complex has been shown to mediate the trafficking of Atg9A from the TGN to the autophagosome. Atg9A is responsible for bringing membrane to the autophagosome. If the WASH complex is KD, Atg9A accumulates in the TGN and autophagy induction is impaired (Zavodszky *et al.*, 2014). This shows that the retromer has a regulatory role in cellular homeostasis and clearance with its implication in the sorting of the lysosomal hydrolase receptor CIMPR, the CMA protein LAMP2A and the autophagy protein Atg9A.

Furthermore, the retromer has been shown to recycle several neurotransmitter receptors such as glutamate receptors AMPAR and NMDAR (Choy *et al.*, 2014), and adrenergic receptor β2AR (Temkin *et al.*, 2011) (**Fig. 2, pathway 2**). Loss of VPS35 leads to excitatory transmission deficit. This suggests that the retromer plays an important role in synaptic integrity and function. Recently, the retromer has been suggested to be implicated in dopaminergic transmission. Indeed, loss of VPS35 led to decrease in synaptic vesicle pool and to an abnormal morphology of synaptic boutons in dopaminergic neurons of drosophila (Inoshita *et al.*, 2017). In addition, retromer has been shown to recycle both dopamine receptor DRD1 (Wang *et al.*, 2016*a*) and dopamine transporter DAT (Wu *et al.*, 2017). This strongly suggests that the retromer plays an essential role in neurotransmission and synapses integrity, including dopaminergic transmission.

If retromer fails to retrieve the cargo from the endosomal system, the late endosome will fuse with the lysosome and cargoes will get degraded (**Fig.2, pathway 3**). The retromer is essential to maintain protein homeostasis and transport cargoes away from the degradative pathways.

Interestingly, the retromer has been linked to MDV, a form of mitochondrial quality control (Braschi *et al.*, 2009; Wang *et al.*, 2015) (**Fig. 2, pathway 3**). Indeed, so far two cargoes have been found to be transported from the mitochondrion towards the lysosome or the peroxisome for degradation and both involves the retromer. The first identified was mitochondrial associated protein ligase (MAPL or Mul1) that was showed to be transported in VPS35 positive vesicles towards the peroxisome (Braschi *et al.*, 2009) or the lysosome (Tang *et al.*, 2015*b*). MAPL is a SUMO E3 ligase that regulates mitochondrial dynamics by stabilizing the fission

protein Drp1 and inducing the degradation of the fusion protein Mfn2. In cell lines or mice where VPS35 is downregulated, MAPL protein levels increases leading either to mitochondrial fission increase and fragmented morphology (Braschi *et al.*, 2009, Tang *et al.*, 2015*b*). Even more recently, the retromer has been shown to directly bind to Drp1 complexes at the mitochondrial membrane and sort the MDVs towards the lysosome for degradation. Here, the retromer mediates the retrieval and degradation of Drp1 complexes so that new Drp1 complexes can form on the mitochondrial membrane, therefore leading to increased fission (Wang *et al.*, 2015). This demonstrates that the retromer has a regulatory role in mitochondrial quality control and dynamics.

As shown here, the retromer plays an important role in trafficking proteins implicated in various cellular processes *e.g.* lysosomal degradation, mitochondrial morphology, synaptic function (**Fig. 1**). This confers a central role of the retromer in cellular homeostasis. The retromer efficiency might be even more of importance in neurons where the activity needs to be tightly regulated. If this sorting platform is dysregulated somehow, it could have tremendous impact on cellular viability. Indeed, loss of VPS35 in mice is lethal at embryonic stages, suggesting that the retromer is essential for cellular viability and might even play a role in development (Wen *et al.*, 2011).

1.3.2. VPS35 and association with neurodegenerative diseases

VPS35 deficiency has been associated with several neurodegenerative diseases such as Alzheimer's disease (AD) (Vardarajan *et al.*, 2012), frontotemporal lobar dementia (Hu *et al.*, 2010) and PD (Vilariño-Güell *et al.*, 2011, Zimprich *et al.*, 2011*a*).

Endosomal trafficking dysfunction has first been linked to AD by the observation that post-mortem brain tissue from AD patients displayed enlarged early endosomes (Cataldo *et al.*, 2000). Furthermore, VPS35 and VPS26 protein levels are reduced in the entorhinal cortex of AD patients, suggesting a perturbation in retromer function (Small *et al.*, 2005). Strikingly, the retromer is required for the sorting of the amyloid protein precursor (APP) receptor Sortilin A (Fjorback *et al.*, 2012). Sortilin A binds APP in the endosome and transport it to the TGN. Amyloidogenic processing of APP takes place in the endosome by β-secretase and γ-secretase, producing β-amyloid, one of the proteins aggregating in AD patient brains. In VPS35 deficient cells, an increased localisation of Sortilin A and APP in endosome is shown and therefore, more β-amyloid is produced. By recycling sortilin A, retromer decreases the

localisation of APP in endosome, therefore decreases β-amyloid levels. Furthermore, the retromer also regulates the subcellular localisation of β-secretase and transports it from the endosome towards the TGN (Wen *et al.*, 2011). Indeed, VPS35 and VPS26 KD in Tg2576 mice model resulted in an increased β-secretase activity in the hippocampus and higher β-amyloid levels. Overexpression of VPS35 could rescue AD-associated phenotypes in AD transgenic mice model (Li *et al.*, 2019). In addition, variants of retromer components have been linked with increased risk of developing AD (Vardarajan *et al.*, 2012).Together these results implicate the retromer as a key complex for regulating β-amyloid protein levels in neurons. Decreased retromer levels in AD brains most likely contribute to the β-amyloid burden.

The link between the retromer and PD was established by the independent findings of two groups, who discovered that the heterozygous point mutation p.D620N in *VPS35* led to autosomal-dominant form of PD (Vilariño-Güell *et al.*, 2011, Zimprich *et al.*, 2011*b*). Later, an additional *VPS35* variant was found in familial PD cases: p.P316S (Vilariño-Güell *et al.*, 2011). However, this variant was also discovered in a control subject, challenging its pathogenicity. Several nonsynonymous variants have also been reported in *VPS35* (p. R524W, p. H599R, p.M607V, p. I560T, p. L774M, p. G51S, p. R32S). In addition, nonsynonymous variant of VPS26 (p. K93E, p. M112V, p. K297X, p.R127H and p. N308D) and VPS29 (p. N72H) have also been discovered (reviewed in Cui *et al.*, 2018).

Here, we will further focus on the p.D620N mutation in *VPS35* and its relevance for PD pathogenesis.

1.3.3. p.D620N mutation in VPS35 and PD

The heterozygous VPS35 p.D620N mutation (PARK17) was found simultaneously by two groups in 2011 in an Austrian and a Swiss family by exome sequencing (Vilariño-Güell *et al.*, 2011, Zimprich *et al.*, 2011*b*). The mutation causes autosomal dominant inherited PD. The clinical phenotype of patients carrying the p.D620N mutation has been reported to be indistinguishable from sporadic PD with postural instability, resting tremor, bradykinesia and a good response to levodopa treatment (Vilariño-Güell *et al.*, 2011). The mean age of onset is 53 years old, ranging from 37 to 66 years old. The prevalence of this mutation is 0.1% in all familial cases, making it a very rare cause of PD (Rahman and Morrison, 2019). This mutation has been later found in Japanese and French populations (Ando *et al.*, 2012; Lesage *et al.*, 2012).

The p.D620N mutation in *VPS35* is a heterozygous point mutation G>A at the position 1858 of the gene. This point mutation resulted in an asp620-to-asn (D620N) amino-acid exchange in a highly conserved residue (Zimprich *et al.*, 2011*b*). It has been reported that the binding capacity of the mutant VPS35 with other members of the retromer complex was unaltered (Follett *et al.*, 2014). Also, the protein level of the retromer is unchanged compared to control and the endosomal localisation is maintained. However, enlarged endosomes sequestering around the nucleus have been shown in patient fibroblasts, suggesting an impairment in trafficking (Follett *et al.*, 2014). Indeed, the trafficking of the known cargo CIMPR have been shown to be impaired in cell lines overexpressing VPS35 p.D620N and in fibroblasts from patients, resulting in a decreased colocalisation of CIMPR with the TGN (Follett *et al.*, 2014; McGough *et al.*, 2014). The mistrafficking of CIMPR further led to decreased Cathepsin-D protein level. The association with WASH complex was also shown to be reduced in cell lines overexpressing the mutant VPS35, resulting in an increase localisation of ATG9A around the nucleus instead of a diffuse expression (Zavodszky *et al.*, 2014). This further led to a decrease of the number of autophagosomes in mutant VPS35 overexpressing cells. In mice overexpressing VPS35 p.D620N, the colocalisation between LAMP2A and VPS35 was decreased and reduced levels of LAMP2A were found (Tang *et al.*, 2015*a*), suggesting an impairment of CMA. This was accompanied by an increase of α-synuclein puncta in the mouse brain. All this suggest that VPS35 p.D620N leads to an impairment of autophagy and lysosomal clearance in a loss-of-function manner.

The pathogenicity of the mutation was shown by overexpressing VPS35 p.D620N in mice and in drosophila, which led to a loss of dopaminergic TH positive neurons (Tsika *et al.*, 2014; Wang *et al.*, 2014).

Moreover, the mitochondrial fragmentation observed in *VPS35* KD mice could be rescued by overexpression of WT VPS35 but not the mutant p.D620N (Tang *et al.*, 2015*b*). An increase interaction between VPS35 p.D620N mutant and Drp1 complex was shown, leading to an increase degradation of inactivated Drp1 complexes via MDVs (Wang *et al.*, 2015). This ultimately led to increased turnover of Drp1 on mitochondria and to a fragmented mitochondrial network. Furthermore, fragmented mitochondrial network accompanied by increased ROS, decreased MMP and decreased complex I and II activities were observed in fibroblasts from patient carrying the p.D620N mutation in VPS35 (Wang *et al.*, 2016*b*; Zhou *et al.*, 2017).

Recent work has shown that the VPS35 p.D620N mutation impairs AMPAR recycling in synapses and perturbs the synaptic transmission in mice cortical neurons overexpressing the

mutant protein (Munsie *et al.*, 2015). They further confirmed this finding in iPSC-derived DA neurons from patient carrying the p.D620N variant. Furthermore, the VPS35 p.D620N mutant does not affect the affinity of the retromer with DRD1 but fails to recycle it back to the plasma membrane (Wang *et al.*, 2016*a*). Moreover, impaired dopaminergic neurotransmission was shown in VPS35 p.D620N knock in (KI) mice with lower DAT levels and increased VMAT2 levels (Ishizu *et al.*, 2016; Cataldi *et al.*, 2018). This suggests that the VPS35 p.D620N mutation leads to an increased dopamine turnover. VPS35 p.D620N seems to alter synaptic homeostasis and function.

Previous studies have shown the impact of VPS35 p.D620N mutation on different cellular functions, *e.g.* autophagy and lysosomal clearance, mitochondrial morphology and function and synaptic homeostasis (**Fig. 1**). However, most of these studies were done on human tumour cell lines or rodent model overexpressing VPS35 p.D620N or in patient fibroblasts. Therefore, we need to understand how VPS35 p.D620N functions in patient-derived and disease-relevant cell type.

1.4. Patient-derived cellular models for p.D620N VPS35

So far, VPS35 has been shown to be implicated in various cellular pathways *e.g.* autophagy, mitochondrial homeostasis and synaptic turnover. However, the pathomechanisms of the p.D620N mutation has only been studied in artificial cell lines overexpressing the mutant protein, rodent and drosophila models, and patient-derived fibroblasts. The overexpression of the mutant protein in cell lines was very useful to study the binding capacity of p.D620N to known cargoes. However, it is essential to confirm these findings in a more physiological setting. Rodent models have the advantage that you can study the pathomechanism in DA neurons *in vivo* and thus can investigate the DA neuron-specific phenotype linked to p.D620N mutant. However, this model remains non-physiological with the overexpression of the p.D620N mutant and the fact that rodents do not display PD symptoms. Fibroblasts are a well-established model that are patient-derived and carry the genetic background of the patient, which is an advantage. This cellular model allowed further understanding of the impact of p.D620N on various cellular pathways, however not of neuron-specific phenotypes. Furthermore, fibroblasts express a very low level of α-synuclein. Consequently, there is a need for a better model that can combine advantages of each model cited above.

For this reason, we reprogrammed VPS35 p.D620N patient-derived fibroblasts and two age- and gender-matched controls into iPSCs. These iPSCs have the advantage of carrying the genetic background of the patient or healthy controls and have the ability to differentiate into any cell type of the organism.

PD is a neurodegenerative disease that causes a massive DA neuronal degeneration in the *substantia nigra*. For this reason, we differentiated the iPSCs first into small molecule neuronal precursor cells (smNPCs) (Reinhardt *et al.*, 2013). These smNPCs have the advantage to be easily expanded and banked in large quantities. The smNPCs were further differentiated into a neuronal culture enriched in midbrain DA neurons (Reinhardt *et al.*, 2013). This model will allow to study the impact of the p.D620N mutation on cellular pathways in a disease-relevant and patient-derived cell type.

1.5. Aim of the study

PD represents a growing social and economic burden to our society, as all of the treatments are symptomatic and not curative. PD was first described more than 200 years ago and, even though our understanding of the disease has improved, we still do not fully grasp its pathogenesis yet. For years, researchers have been focusing on mitochondrial impairment and α-synuclein toxicity as the primary causes of the pathophysiology. Recently, the focus has shifted towards endosomal trafficking with a growing number of genes associated with this pathway being linked to PD. Here, the aim is to decipher how an endosomal trafficking gene variant causing late-onset PD *e.g.* VPS35 p.D620N can induce a PD-like phenotype in a patient-derived disease-relevant cell type.

In order to do so, fibroblasts were derived from skin biopsies of a patient carrying the *VPS35* p.D620N mutation and two age- and gender-matched healthy individuals. These fibroblasts were reprogrammed into human iPSCs. We fully characterised the iPSCs and further differentiated them into smNPCs and neuronal culture enriched in midbrain DA neurons. We investigated for the first time mitochondrial function, morphology and clearance in VPS35 p.D620N patient-derived neurons. Moreover, we studied lysosomal mass and autophagy clearance capacity, as well as α-synuclein accumulation.

2. Results

2.1. Manuscript I

2.1.1. Preface

The first manuscript describes in detail the generation of the iPSCs used throughout my thesis. Fibroblasts from the index patient carrying the *VPS35* p.D620N mutation and from one age- and gender-matched control (Control 1) were reprogrammed into iPSCs using the Cytotune ™ iPS 2.0 Sendai Reprogramming kit (Thermo Fisher Scientific) according to manufacturer's protocol. Fibroblasts from the second age- and gender-matched control (Control 2) were reprogrammed using plasmid transfection-based reprogramming protocol developed by Christine Bus from Tübingen University. At least two clones of each line were sent for chromosomal analysis at Life&Brain GmBH (Bonn) using HumanOmni2.5 Exome 8 DNA Analysis Beadchip. No larger chromosomal aberrations were detected. One clone of each control and two clones of the patient were further characterised.

The gene expression of three pluripotency markers were tested by qPCR and the iPSCs were indeed expressing the pluripotent intracellular markers Nanog, Oct 3/4 and DNMT3B. Furthermore, we confirmed by immunocytochemistry (ICC) the expression of the intracellular markers Nanog and Oct3/4 and Sox2.

The ability of the iPSC clones to differentiate into cell types of the three germ layers was tested using the manufacturer's differentiation protocol (Human Pluripotent Stem Cell Functional Identification Kit, R&D Systems). We confirmed it by ICC using the ectodermal marker Otx2, the mesodermal marker Brachyury and the endodermal marker Sox17.

For this manuscript, I performed the reprogramming of all the lines as well as immunocytochemistry (ICC) and the three germ layer differentiation. François Massart extracted the RNA from the iPSC pellet that I procured him and converted it to cDNA. Gérald Cruciani performed the qPCR workflow on the automated platform HORST and analysed the results. I designed the figures and wrote the manuscript. Dr. Peter Barbuti and Prof. Rejko Krüger reviewed the manuscript.

2.1.2. Manuscript

Induced pluripotent stem cells (iPSCs) derived from a patient with Parkinson's disease carrying the p.D620N mutation in VPS35

Simone B. Larsen[1], Gérald Cruciani[1], François Massart[1], Peter A. Barbuti[1, 2, 5], George Mellick[3], Rejko Krüger[1, 4, 5]

[1] Luxembourg Centre for Systems Biomedicine (LCSB), University of Luxembourg, Esch-sur-Alzette, Luxembourg

[2] Department of Pathology and Cell Biology, Columbia University Medical Center, New York, NY, USA

[3] Griffith Institute for Drug Discovery, Griffith University, Nathan, Australia

[4] Parkinson Research Clinic, Centre Hospitalier de Luxembourg (CHL), Luxembourg

[5] Luxembourg Institute of Health (LIH), Strassen, Luxembourg

Abstract:

Fibroblasts were obtained from a 76-year-old man diagnosed with Parkinson's disease (PD). The disease is caused by a p.D620N mutation in *VPS35*. Induced pluripotent stem cells (iPSCs) were generated using the CytoTune™-iPS 2.0 Sendai Reprogramming Kit (Thermo Fisher Scientific). The presence of the c.1858G>A base exchange in exon 15 of *VPS35* was confirmed by Sanger sequencing. The iPSCs are free of genomically integrated reprogramming genes, express pluripotency markers, display *in vitro* differentiation potential to the three germ layers and have karyotypic integrity. Our iPSC line will be useful for studying the impact of the p.D620N mutation in VPS35 *in vitro*.

Resource table:

Unique stem cell line identifier	LCSBi001-A
Alternative name of stem cell line	VPS35 1_2
Institution	LCSB, University of Luxembourg, Belvaux, Luxembourg
Contact information of distributor	Rejko Krüger, rejko.krueger@uni.lu
Type of cell lines	Induced pluripotent stem cell line (iPSC)
Origin	Human
Additional origin info	Age: 76 years old Sex: male Ethnicity: caucasian
Cell Source	Dermal fibroblasts
Clonality	Clonal
Method of reprogramming	Transgene free (Cytotune™-IPS 2.0 Sendai Reprogramming kit)
Gene modification	YES
Type of modification	Familial, Spontaneous mutation
Associated disease	Parkinson's disease
Gene/locus	Vacuolar protein sorting 35 (*VPS35*)/ chromosome 16q11
Method of modification	N/A
Name of transgene or resistance	N/A
Inducible/constitutive system	N/A
Date archived/stock date	31/07/2019
Cell line repository/bank	N/A
Ethical approval	Ethical approval for the development of and research pertaining to patient-derived cell lines have been given by informed consent for the academic research project (CNER #201411/05): "Disease modelling of Parkinson's disease using patient-derived fibroblasts and induced pluripotent stem cells" (DiMo-PD).

Resource utility:

Parkinson's disease (PD) usually occurs sporadically, but in approximately 10% of the cases, a monogenic cause was identified. The VPS35 p.D620N (*PARK17*) mutation causes a late-onset autosomal-dominant form of PD (Vilariño-Güell et al., 2011; Zimprich et al., 2011). We aim to explore the molecular mechanisms underlying neurodegeneration in iPSC-derived neurons from one patient carrying p.D620N mutation in *VPS35*.

Resource details:

Dermal fibroblasts were obtained from a 76-year old man heterozygous for the p.D620N mutation in the *VPS35* gene. The patient was clinically diagnosed with PD at age 60, displaying typical signs of parkinsonism with rigidity and tremor as predominant symptoms. Reprogramming of the patient fibroblasts was performed by co-expressing the Yamanaka factors OCT3/4, SOX2, KLF4 and cMYC using the integration free CytoTune™-iPS 2.0 Sendai Reprogramming Kit (Thermo Fisher Scientific). Four weeks after transduction, we successfully generated an iPS cell line (**Fig. 1A**). Clones were picked and integration analysis with primers against Sendai virus backbone was performed at passage 8. The selected clones were free of integrated the viral DNA into their genome (**Fig. 1B**). Sanger sequencing confirmed the presence of a heterozygous c.1858G>A substitution in exon 15 of the *VPS35* gene corresponding to the p.D620N mutation (**Fig. 1C**). Using SNP-based karyotyping, no chromosomal aberrations were identified in the selected iPSC clone. (**Fig. 1D**).

Immunocytochemical (ICC) analyses showed the presence of the pluripotency markers OCT3/4 and NANOG, at the protein level (**Fig. 1E**). Pluripotency analysis confirmed that transcription of the endogenous pluripotency genes *NANOG*, *OCT3/4* and *DNMT3B* was upregulated compared to fibroblasts (**Fig. 1F**). *In vitro* differentiation using the Human Pluripotent Stem Cell Functional Identification Kit (R&D Systems) followed by ICC analyses with the mesodermal marker Brachyury, the endodermal marker Sox17 and the ectodermal marker Otx2 demonstrated the differentiation potential into all three germ layers (**Fig. 1G**).

Materials and methods:

Reprogramming of dermal fibroblasts:

Dermal fibroblasts carrying the heterozygous p.D620N mutation in VPS35 were collected at the Griffith Institute (Queensland, Australia) after informed consent of the patient. Fibroblasts derived from the skin biopsy were cultured in fibroblasts medium composed of Dulbecco's Modified Eagle Medium (DMEM) supplemented with 10% fetal bovine serum (FBS), 2 mM L-glutamine and 1% penicillin and streptomycin (Pen/Strep). The fibroblasts were transduced using the CytoTune-iPS 2.0 Sendai Reprogramming Kit (Thermo Fisher Scientific) with a multiplicity of infection (MOI) (KOS MOI=5, hc-Myc MOI=5, and hKlf4 MOI=3). Seven days post-transduction, cells were passaged under feeder-free conditions in a Matrigel™ (Corning)-coated plate. Freshly prepared E8 medium (DMEM F-12 + HEPES, 1% Pen/Strep, 1% Insulin-Transferrin-Selenium, 2 µg/L TGFβ1, 10 µg/L FGF2, 64 mg/L acid ascorbic, 100 ng/mL Heparin, 10% TeSR-E8) was changed every other day, supplemented with 100 µM sodium butyrate. After four weeks, iPSC colonies formed and were manually passaged into a new Matrigel-coated dish and cultured in E8 medium. The iPSC lines were then enzymatically passaged using dispase once a week. At passage 8, iPSCs were harvested for analysis and cryopreserved in liquid nitrogen.

RT-qPCR:

Total RNA was purified from cells using Trizol/chloroform. Transcriptor High Fidelity cDNA Synthesis Kit (Roche) was used to synthesize cDNA. The transgene-free status was carried out using the SeV primer (**Table 2**). The negative control used was sterile H2O. Quantification of pluripotency markers by multiplex qPCR was performed using the LightCycler® 480 Probes Master kit (Roche) and hydrolysis probes detecting NANOG-FAM (Hs02387400_g1, Thermo Fisher Scientific), OCT4-FAM (Hs00999632_g1, Thermo Fisher Scientific) and DNMT3B (Hs00171876_m1, Thermo Fisher Scientific).

GAPDH-VIC (Hs02758991_g1, Thermo Fisher Scientific) was used as a housekeeping gene. Total RNA purified from fibroblasts was used as a negative control.

Immunofluorescence staining:
iPSCs were fixed with 4% paraformaldehyde in PBS for 15 min and stained using a standard immunofluorescence protocol. The expression of pluripotency markers OCT3/4 and NANOG were visualised using antibodies listed in table 2 together with DAPI nuclear stain. Images were acquired using the Zeiss spinning disk confocal microscope (Carl Zeiss Microimaging GmH).

In vitro differentiation:
The iPSC were plated on matrigel-coated coverslips four days prior to the *in-vitro* differentiation. The ability of the iPSC to differentiate into cell types of the three germ layers was tested using the manufacturer's differentiation protocol (Human Pluripotent Stem Cell Functional Identification Kit, R&D Systems). We confirmed it by ICC using the ectodermal marker Otx2, the mesodermal marker Brachyury and the endodermal marker Sox17. Images were acquired using the Zeiss spinning disk confocal microscope (Carl Zeiss Microimaging GmBH).

Chromosomal analysis:
Molecular karyotyping and identity analysis was performed at Life&Brain GmBH (Bonn) using HumanOmni2.5 Exome-8 DNA Analysis BeadChip.

Mutation analysis:
Genomic DNA was purified from LCSBi001-A iPSC using the QIA Blood and Tissue kit (Qiagen). The exon 15 of *VPS35* was amplified by PCR (**Table 2**) and Sanger sequencing was carried out at Eurofins Genomics Germany GmbH.

References:
Vilariño-Güell, C., Wider, C., Ross, O.A., Dachsel, J.C., Kachergus, J.M., Lincoln, S.J., Soto-Ortolaza, A.I., Cobb, S.A., Wilhoite, G.J., Bacon, J.A., Behrouz, B., Melrose, H.L., Hentati, E., Puschmann, A., Evans, D.M., Conibear, E., Wasserman, W.W., Aasly, J.O., Burkhard, P.R., Djaldetti, R., Ghika, J., Hentati, F., Krygowska-Wajs, A., Lynch, T., Melamed, E., Rajput, A., Rajput, A.H., Solida, A., Wu, R.-M., Uitti, R.J., Wszolek, Z.K., Vingerhoets, F., Farrer, M.J., 2011. VPS35 Mutations in Parkinson Disease. Am. J. Hum. Genet. 89, 162–167. https://doi.org/10.1016/j.ajhg.2011.06.001

Zimprich, A., Benet-Pagès, A., Struhal, W., Graf, E., Eck, S.H., Offman, M.N., Haubenberger, D., Spielberger, S., Schulte, E.C., Lichtner, P., Rossle, S.C., Klopp, N., Wolf, E., Seppi, K., Pirker, W., Presslauer, S., Mollenhauer, B., Katzenschlager, R., Foki, T., Hotzy, C., Reinthaler, E., Harutyunyan, A., Kralovics, R., Peters, A., Zimprich, F., Brücke, T., Poewe, W., Auff, E., Trenkwalder, C., Rost, B., Ransmayr, G., Winkelmann, J., Meitinger, T., Strom, T.M., 2011. A Mutation in VPS35, Encoding a Subunit of the Retromer Complex, Causes Late-Onset Parkinson Disease. Am. J. Hum. Genet. 89, 168–175. https://doi.org/10.1016/j.ajhg.2011.06.008

Table 1: Characterization and validation

Classification	Test	Result	Data
Morphology	Photography	iPSC like morphology	Fig. 1A
Phenotype	Qualitative analysis Immunocytochemistry	Assess staining/expression of pluripotency markers: Oct3/4 and Nanog	Fig. 1E
	Quantitative analysis RT-qPCR	Assess expression of pluripotency markers: Oct3/4, Nanog and DNMT3B	Fig. 1F
Genotype	Genotyping	HumanOmni2.5 Exome-8 DNA Analysis BeadChip	Fig. 1D
Identity	SNP analysis	DNA Profiling: Performed	supplementary file 2
		Matched	submitted in archive with journal
Mutation analysis (IF APPLICABLE)	Sequencing	Heterozygous *VPS35* p.D620N mutation	Fig. 1C
Microbiology and virology	Mycoplasma (PlasmoTest™ Invivogen)	Negative	Supplementary Fig. S1
Differentiation potential	Directed differentiation	Directed differentiation: expression of specific markers for ectodermal (Otx2), mesodermal (Brachyury) and endodermal (SOX17) lineage	Fig. 1G
Donor screening (OPTIONAL)	HIV 1 + 2 Hepatitis B, Hepatitis C	Not performed	N/A
Genotype additional info (OPTIONAL)	Blood group genotyping	Not performed	N/A
	HLA tissue typing	Not performed	N/A

Table 2: Reagents details

Antibodies used for immunocytochemistry			
	Antibody	**Dilution**	**Company Cat # and RRID**
Pluripotency Marker	Mouse anti-OCT3/4	1:1000	Santa Cruz, Cat #: sc-5279; RRID: AB_628051
Pluripotency Marker	Rabbit anti-Nanog	1:500	Abcam, Cat #: ab21624; RRID: AB_446437
Secondary antibody	Alexa Fluor 488 Goat anti-Mouse IgG (H+L)	1:1000	Invitrogen, Cat #: A11029; RRID: AB_138404
Secondary antibody	Alexa Fluor 568 Goat anti-Rabbit IgG (H+L)	1:1000	Invitrogen, Cat #: A11036; RRID: AB_143011
Secondary antibody	Alexa Fluor 647 Donkey α-Goat IgG (H+L)	1:1000	Invitrogen, Cat #: A21447; RRID: AB_141844
Primers			
	Target	**Forward/Reverse primer (5'-3')**	
Sendai virus detection	SeV plasmid (181 bp)	GGATCACTAGGTGATATCGAGC/ACC AGACAAGAGTTTAAGAGATATGTATC	
House-Keeping Gene	*GAPDH* (447 bp)	CAGGGCTGCTTTTAACTC/AAGTTGTCATGGATGACCT TG	
VPS35 exon 15	*VPS35*	AAATGGATATCCTGGAACAAG/ CAAATCTCCTAAGAGTAGGAAGGG	

A

B

Negative control
Sendai virus
GAPDH

500 bp —

C

Heterozygous VPS35 c.1858 G>A (p.D620N)

C A G C R A T T C C
40

D

E

Oct 3/4   Nanog

DAPI   merge

50 µm

F

OCT3/4 relative expression

Fibro   LCSBi001-A

NANOG relative expression

Fibro   LCSBi001-A

DMNT3B relative expression

Fibro   LCSBi001-A

G

Ectoderm   Mesoderm

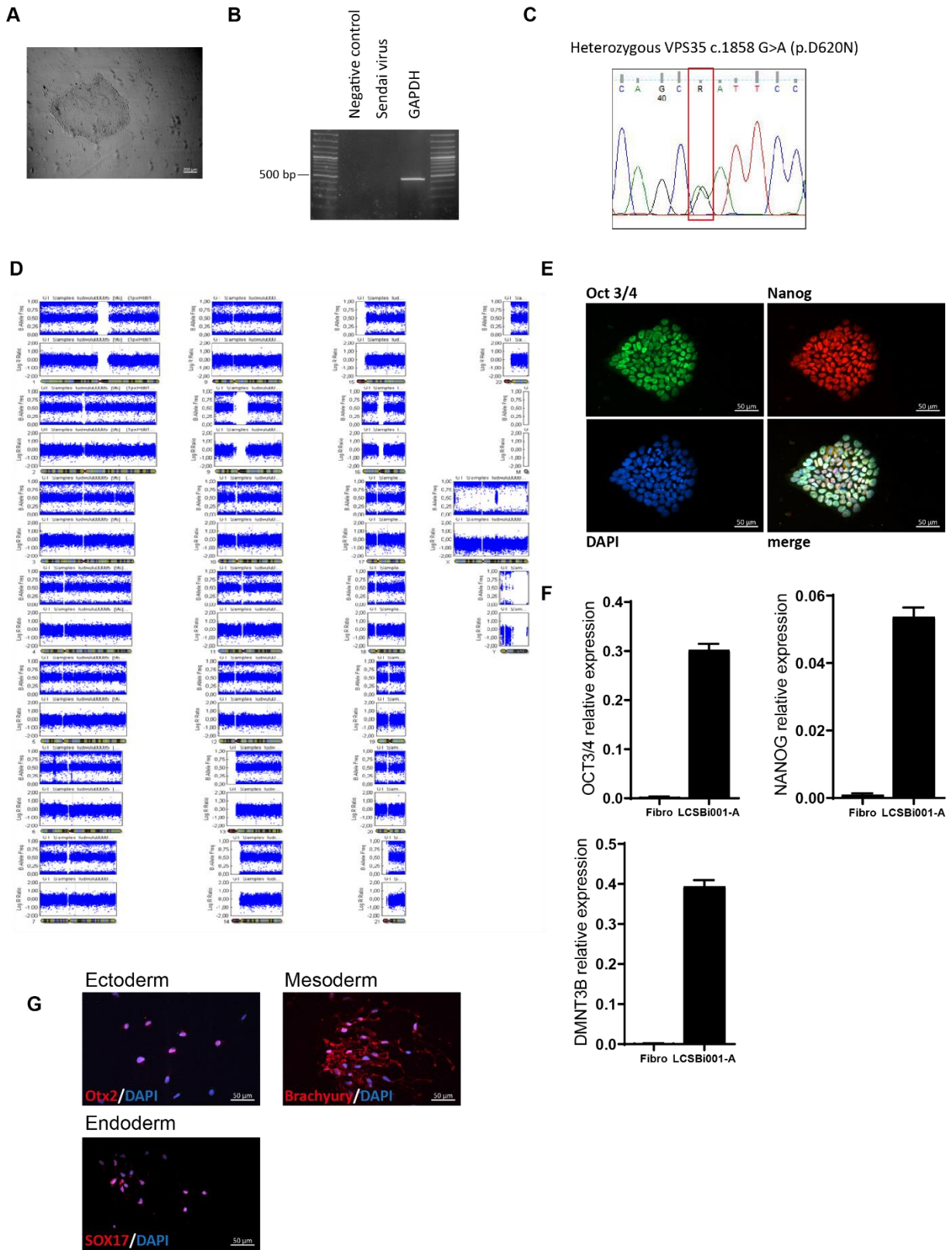Otx2/DAPI   Brachyury/DAPI   50 µm

Endoderm

SOX17/DAPI   50 µm

Figure 1: Characterisation of LCSBi001-A line

PlasmoTest™ - Mycoplasma Detection Kit (Invivogen):

Positive control   Dermal fibroblasts VPS35 p.D620N

Negative control   iPSC VPS35 p.D620N

Figure S1: mycoplasma test of dermal fibroblasts and LCSBi001-A iPSC line (iPSC VPS35 p.D620N)

2.2. Manuscript II

2.2.1. Preface

The second manuscript includes the main findings of my thesis. The patient- and control-derived neurons were characterised and underwent deep phenotyping. We found that the p.D620N mutant neurons displayed smaller mitochondria with less complex network compared to controls. Moreover, mitochondria from p.D620N neurons were functionally impaired with lower respiration and MMP, and increased mitochondrial ROS. Mitochondria in autophagosomes were accumulating after prolonged CCCP treatment showing an impairment of mitochondrial clearance in the patient-derived neurons. A more general clearance impairment was found in the patient-derived neurons with lower autophagic flux and decreased late endosome/lysosomal mass. Furthermore, α-synuclein steady state level was increased under normal culture condition in p.D620N mutant neurons. We tried to pinpoint the mechanism by which VPS35 p.D620N causes mitochondrial impairment and found that α-synuclein was accumulating in the mitochondrial fraction and hypothesised that α-synuclein could be causing this phenotype. We KD α-synuclein in patient neurons to the level of controls, which was not sufficient to rescue the decreased MMP, nor the increased ROS levels. Then, we hypothesised that the over-activation of LRRK2 kinase activity might be causing the mitochondrial impairment. We analysed the steady state level of phosphorylation of one of LRRK2 substrates Rab10 and found that it was not different between the patient and controls derived neurons.

For this manuscript, I designed the experimental plan and did most of the experiments and analysis, except for the following. Dr Paul Antony wrote the script to analyse mitochondrial morphology. Dr Javier Jarazo gene-edited the smNPCs to generate the mitorosella lines and conducted the imaging and analysis of mitophagic events. Zoé Hanss measured α-synuclein protein levels by TR-FRET. George Mellick provided the patient fibroblasts and wrote the clinical phenotype of the patient. I wrote the manuscript and designed the figures. Dr Peter Barbuti and Prof Rejko Krüger reviewed the manuscript.

2.2.2. Manuscript

Patient-derived VPS35 p.D620N neurons display mitochondrial and clearance impairment

Simone B. Larsen[1], Paul Antony[1], Javier Jarazo[1], Zoé Hanss[1], Peter A. Barbuti[1, 2, 5], George D. Mellick[3], Rejko Krüger[1, 4, 5]

[1] Luxembourg Centre for Systems Biomedicine (LCSB), University of Luxembourg, Esch-sur-Alzette, Luxembourg

[2] Department of Pathology and Cell Biology, Columbia University Medical Center, New York, NY, USA

[3] Griffith Institute for Drug Discovery, Griffith University, Nathan, Australia

[4] Parkinson Research Clinic, Centre Hospitalier de Luxembourg (CHL), Luxembourg

[5] Luxembourg Institute of Health (LIH), Strassen, Luxembourg

Abstract:

VPS35 is part of the retromer complex and is responsible for the trafficking of various proteins in the cell. Interestingly, VPS35 has been shown to recycle proteins implicated in autophagy and lysosomal degradation but also takes part in the degradation of mitochondrial proteins via mitochondria derived vesicles. Overall, VPS35, by its central role in endosomal trafficking, regulates cellular and mitochondrial quality control. The p.D620N mutation causes an autosomal-dominant form of PD, highly resembling sporadic PD. The patient and age- and gender-matched controls fibroblasts were reprogrammed into induced pluripotent stem cells (iPSCs). A neuronal culture enriched in dopaminergic neurons (15 to 20%) has been generated from the differentiation of iPSCs and is used to decipher the impact of the p.D620N mutation. A decreased autophagic flux and lysosomal mass was observed in the patient neurons compared to the controls associated with an accumulation of alpha-synuclein. Also, we found that mitochondria were dysfunctional with lower membrane potential (MMP), impaired respiration and increased production of reactive oxygen species compared to controls. We furthered tried to decipher the mechanism underlying mitochondrial dysfunction in iPSC-derived neurons from patient carrying the p.D620N mutation in *VPS35*. Hence, we knocked-down α-synuclein in the differentiated neurons and found that it did not rescue the decreased MMP, nor the increase mitochondrial ROS level. We measured the level of phosphorylated Rab10, a substrate of LRRK2 kinase and found it to be unchanged in patient neurons compared to controls. Here, we show for the first time the impact of p.D620N VPS35 mutant iPSC-derived neurons from patient.

Abbreviations:

CCCP = carbonyl cyanide 3-chlorophenylhydrazone

CIMPR = cation-independent mannose 6-phosphate receptor

CRISPR = clustered regularly interspaced short palindromic repeats

DAT = dopamine transporter

DIV = days in vitro

DRD1 = dopamine receptor D1

Drp1 = dynamin related protein 1

ER = endoplasmic reticulum

HEK293T = human embryonic kidney 293T

iPSC = induced pluripotent stem cell

Lamp = lysosome associated membrane protein

LRRK2 = leucine-rich repeat kinase 2

MAM = mitochondria associated membrane

MAPL = mitochondria associated protein ligase

Mfn2 = mitofusin 2

MMP = mitochondrial membrane potential

MDV = mitochondria derived vesicle

PD = Parkinson's disease

PINK1 = PTEN-induced putative kinase 1

ROS = reactive oxygen species

smNPC = small molecule neuronal precursor cell

TOM = translocase of the outer membrane

TGN = trans-Golgi network

TMRE = Tetramethylrhodamine, ethyl ester

VDAC1 = Voltage-dependent anion-selective channel 1

VPS = vacuolar protein sorting

WB = western blot

Introduction:

Patients with Parkinson's disease (PD) suffer from a progressive motor disorder. They experience a broad range of motor symptoms and non-motor symptoms, highlighting the heterogeneous aspect of the disease. Advances in genetics have broadened the understanding of the underlying mechanisms causing the death of dopaminergic neurons in the *substantia nigra* (Krüger *et al.*, 2017). Different subtypes of PD have been described with the disease heterogeneity depending on the mechanisms driving neurodegeneration. Indeed, mutations in mitochondria associated proteins such as PINK1 (PTEN-induced putative kinase 1), Parkin or DJ-1 have been associated with a severe mitochondrial dysfunction causing neurodegeneration. On the other hand, variants of *LRRK2* (leucine-rich repeat kinase 2), *SNCA*, *DNAJC13* and *VPS35* (vacuolar protein sorting associated protein 35) show an impairment in the endosomal trafficking pathways (Larsen *et al.*, 2018).

The p.D620N mutation in *VPS35* was identified by two independent research groups in 2011 (Vilariño-Güell *et al.*, 2011; Zimprich *et al.*, 2011). It causes a rare autosomal-dominant form of PD, occurring in only 1.3% of familial cases and 0.1% of all PD cases (Deng *et al.*, 2013). The clinical phenotype of patients resembles the one of sporadic PD patients, although the age of onset is earlier (Mohan and Mellick, 2017).

VPS35 is part of the retromer complex, responsible for the recycling of targeted transmembrane proteins from the early endosome back to the plasma membrane and the retrograde transport from the endosomal system towards the trans-Golgi Network (TGN) (Seaman *et al.*, 1998). The retromer is composed of VPS35, VPS29, VPS26A or VPS26B, and various sorting nexins. The pathogenic VPS35 p.D620N does not prevent the formation of the retromer (Zavodszky *et al.*, 2014).

The retromer transports proteins essential to lysosomal clearance, carrying them to the TGN to avoid their degradation. One of the most studied cargo proteins of the retromer is the cation-independent mannose 6-phosphate receptor (CIMPR) (Arighi *et al.*, 2004). CIMPR is an

endosomal protein that transports Pro-Cathepsin D from the endoplasmic reticulum (ER) to the lysosome and is essential for the maturation into the hydrolase Cathepsin D. CIMPR is then recycled via the retromer. In cells with a deficiency in VPS35, either through knock down or by expressing the p.D620N mutant, CIMPR is not properly recycled back to the TGN; this leads to the degradation of the receptor and the subsequent mis-trafficking of Cathepsin D (Follett *et al.*, 2014; McGough *et al.*, 2014; Miura *et al.*, 2014). The retromer also recycles key autophagy proteins: Lamp2a, implicated in chaperone-mediated autophagy; and ATG9, a protein involved in the induction of autophagy. Retromer complexes containing the mutant VPS35 can no longer bind their cargo proteins and, thus, these proteins cannot escape degradation by the lysosome (Zavodszky *et al.*, 2014, Tang *et al.*, 2015*a*). Overall, the retromer is crucial for proper trafficking of lysosomal clearance proteins, and the p.D620N mutation in VPS35 is associated with dysfunctional lysosomal clearance.

Interestingly, studies have identified mitochondrial impairment in rodent dopaminergic neurons containing a *VPS35* p.D620N mutation. It has been reported that VPS35 p.D620N directly interacts with mitochondrial Drp1 (dynamin related protein 1), a key component in mitochondria fission, leading to fragmented mitochondria and cell death (Wang *et al.*, 2016*b*). Moreover in VPS35 deficient mice, mitochondrial fragmentation was observed with reduced level of mitochondrial fusion protein Mfn2 (mitofusin 2) (Tang *et al.*, 2015*b*). Indeed, increased mitochondrial fragmentation, with decreased mitochondrial membrane potential (MMP) and impaired respiration was found in both studies (Tang *et al.*, 2015*b*, Wang *et al.*, 2016*b*) with Zhou and collaborators finding similar results in patient-derived fibroblasts (Zhou *et al.*, 2017).

Most studies with VPS35 deficiency have been conducted in rodent dopaminergic neurons or cell lines overexpressing *VPS35* p.D620N, *VPS35* knock down models or *VPS35* p.D620N patient-derived fibroblasts. To date there have been no studies investigating the effect of *VPS35* p.D620N on mitochondrial phenotype, clearance and protein aggregation in patient-derived neurons. Here, we reprogrammed fibroblasts from one patient carrying the *VPS35* p.D620N mutation and two age- and gender-matched controls into induced pluripotent stem cells (iPSCs). Then, we differentiated iPSCs into small molecule neuronal precursor cells (smNPC) and further into neuronal populations enriched in dopaminergic neurons (Reinhardt *et al.*, 2013).

The patient's clinical examination was followed by a study of cellular processes impaired in PD such as mitochondrial and lysosomal dysfunction. We found that iPSC-derived neurons carrying the p.D620N mutation in VPS35 displayed a severe mitochondrial dysfunction with decreased MMP, increased mitochondrial reactive oxygen species (ROS) level and impaired respiration. In addition, lysosomal clearance of mitochondria was impaired and the autophagic flux was decreased. Furthermore, these patient-derived neurons harbouring the VPS35 p.D620N mutation displayed an accumulation of α-synuclein protein in whole cell, and in both cytosolic and mitochondrial fraction. This suggests that VPS35 p.D620N leads to a profound dysfunction of several cellular processes through its central role in trafficking of proteins.

Material and methods:

Subjects:

We included a male patient carrying the p.D620N mutation in *VPS35*, described previously in (Follett *et al.*, 2014) and two healthy male controls from Tübingen Biobank Control 1 and Control 2. Skin biopsies were taken from each individual at the ages of 73, 72 and 77 respectively.

Ethical approval for the development of and research pertaining to patient-derived cell lines have been given by informed consent for the academic research project (CNER #201411/05): "Disease modelling of Parkinson's disease using patient-derived fibroblasts and induced pluripotent stem cells" (DiMo-PD).

Cell culture reprogramming, differentiation and characterization:

Human dermal fibroblasts from skin biopsies were maintained in Dulbecco's modified Eagle medium (Gibco) supplemented with 10% foetal bovine serum (Gibco) and 1% penicillin/streptomycin (Pen/Strep. Gibco). All fibroblasts were reprogrammed into human iPSCs in our laboratory. Two iPSC clones were derived from the patient's fibroblasts (VPS35 1_1 and 1_2), one iPSC clone was derived from each control (Control 1 and Control 2). iPSCs were maintained on Geltrex (Gibco) in Dulbecco's Modified Eagle Medium/Nutrient Mixture F-12 with HEPES (Gibco) supplemented with 1% Insulin-Transferrin-Selenium (Gibco), 64 mg/L of L-ascorbic acid-2-phosphate magnesium (Sigma), 10 μg/L of FGF-2 (Fibroblasts Growth Factor 2, Peprotech), 2 μg/L of TGF β1 (Transforming growth factor beta 1, Peprotech),

100 ng/mL of Heparin (Sigma) and 10% TeSR-E8 (Stem Cell Technologies). iPSCs were fully characterised and used to generate smNPCs according to Reinhardt *et al.*, 2013. smNPCs were maintained on Geltrex (Gibco) in 1:1 Dulbecco's modified Eagle medium/Nutrient Mixture F-12 (Gibco) and Neurobasal (Gibco) medium supplemented with 1% Pen/Strep (Gibco), 1% GlutaMAX (Gibco), B27 Supplement (Gibco), N2 Supplement (Gibco), 200 mM ascorbic acid (Sigma), 3 mM CHIR 99021 (Axon Medchem) and 0.5 mM purmorphamine (Sigma). All smNPC lines were characterized for the expression of neuronal precursor markers (SOX1, SOX2, NESTIN and MUSASHI) (Fig. S1). smNPCs were further differentiated into a dopaminergic-enriched neuronal culture according to (Reinhardt *et al.*, 2013). Neurons were split at day in vitro 21 (DIV21) in experiment plates coated with Geltrex (Gibco) and cultivated in 1:1 Dulbecco's modified Eagle medium/Nutrient Mixture F-12 (Gibco) and Neurobasal (Gibco) medium supplemented with 1% Pen/Strep (Gibco), 1% GlutaMAX (Gibco), B27 Supplement (Gibco), N2 Supplement (Gibco), 10 ng/mL BDNF (Peprotech), 10 ng/mL GDNF (Peprotech), 1 ng/mL TGF β3 (Peprotech), 500 µM dbcAMP (Applichem), 200 µM ascorbic acid (Sigma). All experiments were performed after DIV30-35.

Compound treatment and viral transduction:

For mitochondrial morphology, membrane potential and ROS assessment, neurons were cultivated in neuronal medium without B27 and ascorbic acid (without antioxidants supplementation) 4 hrs prior to the experiment. All treatments were performed in the neuronal medium without antioxidants. To assess the mitophagic clearance capacity, the edited neurons with the Rosella construct were treated with 10 µM CCCP (Carbonyl cyanide 3 chlorophenylhydrazone) (Abcam) for 24 hrs. For the autophagy experiment, neurons were treated with 100 nM Bafilomycin A1 (Enzo Life Sciences) for 24 hrs. All experiments were repeated three to five times.

The MISSION pLKO.1-puro non-target shRNA and MISSION pLKO.1-puro shRNA against SNCA (TRCN0000003736) were purchased from Sigma. Lentiviral particles were produced in HEK293T in our laboratory. Neurons were transduced at DIV23 with supernatant containing viral particles at a ratio 1:1 in normal neuronal culture medium overnight. A-synuclein protein levels were quantified 7 days post-transduction by western blot analysis. All experiments were repeated three times.

Western blotting:

Cells pellets were extracted using RIPA buffer (50 mM Tris HCl pH 7.4, 150 mM NaCl, 1% Triton X-100, 0.5% sodium deoxylcholate, 0.1% SDS, 1mM EDTA, 50 mM Tris-HCl, 150 mM NaCl, 1 mM proteinase inhibitor cocktail). Gels were blotted by dry transfer onto 0.2 μM nitrocellulose membranes using the iBlot2 device. Isolation of the crude mitochondrial fraction was performed using a differential centrifugation protocol according to (Grünewald *et al.*, 2009). Antibodies used for western blotting (WB) were anti-β-actin (1:20000, Cell Signalling), anti-VPS35 (1:1000, Santa Cruz), anti-VPS29 (1:1000, Santa Cruz), anti-TOM20 (1:1000, Santa Cruz), anti-VDAC1 (1:1000, Millipore), anti-PGC1α (1:1000, Novus Biologicals), anti-p62 (1:1000, BD Biosciences), anti-Lamp1 (1:1000, Santa Cruz), anti-α-synuclein (1:000. BD Biosciences). Secondary antibodies coupled with HRP were purchased from Invitrogen (1:5000 - 1:10 000). Densitometry from western blot were carried out using LI-COR Image Studio Software. All densitometric signals were normalised to β-actin or VDAC1 signals. Densitometry signals were further normalised to the controls where stated in the figure legends.

TR-FRET:

Evaluation of α-synuclein content via TR-FRET was performed using the total α-synuclein kit from Cisbio (6FNSYPEG). Briefly, cells were lysed into the provided lysis buffer by incubation at room temperature under shaking for 30 min. Total protein quantification was performed on each lysate using the Pierce BCA assay (Thermo Fisher Scientific). Lysates at 0.2ng/µl of total protein were incubated in triplicate with both donor cryptate-conjugated antibody and acceptor d2-conjugated antibody overnight at room temperature as recommended by the provider. The TR-FRET signal was measured on a Tecan Genios Pro and the ratio of the signal of the acceptor (665nm) to the donor (620nm) was calculated to evaluate the total α-synuclein content. Results are expressed in ng/ml calculated from a standard curve.

Immunofluorescence staining:

Neurons were fixed at DIV30 in with 4% paraformaldehyde for 15 min, before being permeabilised and blocked in 0.4% Triton-X, 10% goat serum and 2% bovine serum albumin for 1 hr. Immunofluorescence staining was performed with primary antibodies against tyrosine hydroxylase (1:500, Millipore) and Tuj1 (1:500, Covance) and respective secondary antibodies coupled with fluorophore (1:1000, Invitrogen). DAPI (1:50, Thermo Fisher Scientific) was used

to stain nuclei. At least five images per coverslip were acquired using Zeiss spinning disk confocal microscope.

Live cell imaging and analysis:

Mitochondria were visualised using 100 nM MitoTracker Green FM (Invitrogen) in neuronal medium without antioxidants. At least five Z-stack images per well were acquired using Zeiss spinning disk confocal microscope.

To segment mitochondria, the mitochondrial channel was pre-processed with a difference of Gaussians where the foreground image was convolved with a Gaussian of size 11 and standard deviation 1 and the subtracted background image with a Gaussian of size 11 and standard deviation 3 (Mito_DoG). Only pixels above threshold 3000 in Mito_DoG and an intensity above 5000 in the raw mitochondrial channel were considered as foreground pixels. The mitochondrial mask was defined by removing connected components with less than 10 pixels. Mitochondrial morphometrics were quantified as previously described (Baumuratov *et al.*, 2016).

Mitorosella sensor, generation of the lines, image acquisition and analysis:

The generation of the lines carrying the rosella reporter was performed as previously described (Arias-Fuenzalida *et al.*, 2019). Briefly, the tandem fluorescent proteins consisting of pH sensor fluorescent protein pHluorin (F64L, S65T, V193G and H231Q) and DsRed were fused to the entire open reading frame of ATP5C1 serving as a mitochondrial targeting sequence, and placed in between the homology arms targeting the AAV1 safe harbour (Hockemeyer *et al.*, 2009) (Addgene plasmid #22075). A double strand break for triggering homologous recombination was performed with the px330 (Cong *et al.*, 2013) (Addgene plasmid #42230) carrying the sgRNA targeting sequence for the safe harbour as described by (Mali *et al.*, 2013). SmNPCs from patients (VPS35 1_2) and control individuals (Control 1) were nucleofected (P3 Primary Cell 4D-Nucleofector, V4XP-3024, Lonza) with both constructs and expanded before purification by FACS (Aria III, BD).

Images were obtained on an Opera QEHS confocal spinning disk microscope (Perkin Elmer) with a 60x water immersion objective (NA = 1.2). pHluorin was excited with a 488 nm laser and detected on camera 1 behind a 520/35 bandpass filter. While DsRed was excited with a 561 nm laser and detected on camera 2 behind a 600/40 bandpass filter. A 568 dichroic mirror split the light towards the corresponding cameras. Both fluorescent channels were acquired

simultaneously with a binning setting of 2. One plane and 15 fields per well were acquired. One pixel corresponds to 0.2152 µm. Differentiated neurons were maintained under normal incubation conditions (37°C, 5% CO_2, and 80% humidity) within the microscope in between and during the different acquisition time points.

The automated image analysis was performed through a series of pre-processing and thresholds in MATLAB (The MathWorks, Inc.) as previously described (Arias-Fuenzalida *et al.*, 2019). Briefly, a difference of Gaussian of convoluted foreground and background images was used for detecting all the events in the field. For classifying the events either as mitochondria or mitophagic event, a combination of green to red fluorescence ratio analysis and morphological filtering based on difference of Gaussians thresholding was used. Those presenting a mean ratio value below 0.6 were classified as mitophagic events.

Flow cytometry:

Neurons were detached with accutase (Sigma) and centrifuged at 300g for 3 min. 200 000 cells were then incubated in the dye or in the buffer (unstained). MMP was assessed with 200 nM tetramethylrhodamine, ethyl ester (TMRE, Invitrogen). To correct for mitochondrial mass, Mitotracker Green FM (Invitrogen) was used as a counterstaining. For mitochondrial ROS, 2 µM of MitoSox Red (Invitrogen) was used. Cells were analysed with the Fortessa flow cytometry analyser. Mean fluorescence of the unstained cells was subtracted to account for autofluorescence.

Oxygen consumption rate measurement:

Oxygen consumption rates were measured in whole cells using the Seahorse XFe96 Cell Metabolism Analyser (Agilent). Neurons were plated in the Seahorse XFe96 well plates 24hrs prior to measuring at a density of 80 000 cells per well. The concentrations of mitochondrial toxins used were optimized for neurons according to the manufacturer's recommendations. The final concentration of toxin used are the following: oligomycin (oligo) - 2 µM; FCCP - 250 nM; antimycin A (AA) and rotenone (rot) - 5 µM. The cells of each well were lysed with RIPA buffer after the experiment and the OCR of each well was corrected for protein amount.

Statistics:

Statistical analyses were performed with GraphPad Prism. The statistical analyses performed and the P-value of each experiment can be found in the legend of the figures.

Data availability:

The authors confirm that the data supporting the findings of this study are available within the article and its Supplementary material.

Results

Clinical phenotype of VPS35 p.D620N patient:

The male patient donor case #2610 comes from a multi-incident family #445 reported previously from the Queensland Parkinson's Project (Bentley *et al.*, 2018), that immigrated from Western Europe. Besides the index patient, the diagnosis of PD was made in his mother and maternal grandfather but no additional family members are known to be affected. He was born in 1940 and worked as a sugar cane farmer. The diagnosis of PD was made by a Movement Disorders Neurologist after around one year complaining of muscular skeletal symptoms (rigidity) and tremor, which were his predominant presenting symptoms. The PD related motor symptoms responded well to levodopa therapy. The index patient underwent deep brain stimulation for his Parkinson's symptoms six years after diagnosis with good symptomatic response.

VPS35 and VPS29 levels are unchanged in VPS35 p.D620N patient-derived neurons:

Previous studies have reported that VPS35 protein levels did not change in cells carrying mutant VPS35 (Zavodszky *et al.*, 2014). The p.D620N mutation in VPS35 has been shown not to impair its binding to the other components of the retromer (Follett *et al.*, 2014). To confirm this in our patient-derived cells, we generated iPSC from one patient (VPS35 1_1 and 1_2) and two age- and gender-matched controls (Control 1 and 2) that were further differentiated into smNPC. smNPCs were fully characterised (Fig. S1). We successfully generated from the smNPC a neuronal culture expressing the neuronal marker Tuj1 (Tubulin β3), enriched in dopaminergic neurons expressing Tyrosine Hydroxylase (TH) (Fig. 1A) after 30 days of differentiation *in vitro*. WB against VPS35 and VPS29 revealed that the protein level of both retromer components is unchanged between both controls and mutant clones (Fig. 1B and C).
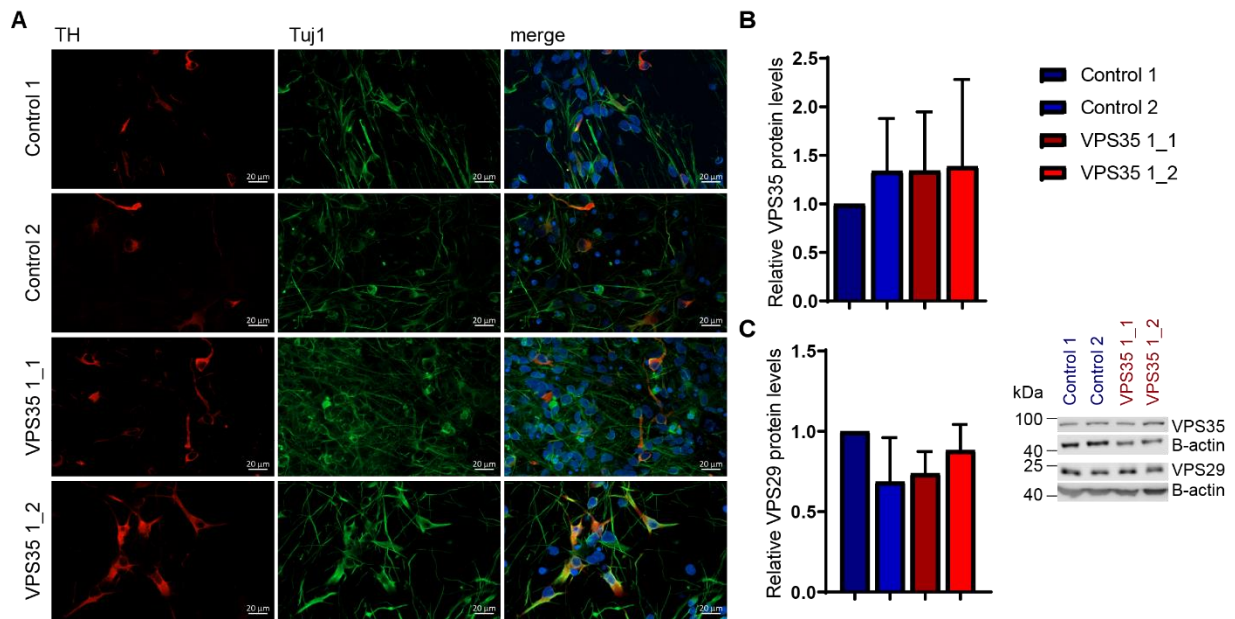
Figure 1: **No difference in retromer components protein expression in iPSC-derived neurons**. (**A**) Immunofluorescence staining shows expression of tyrosine hydroxylase (TH), class III β-tubulin (Tuj1), and nuclear DAPI in iPSC-derived neurons. (**B-C**) Western blot analysis of VPS35 (**B**), VPS29 (**C**) and β-actin (loading control) from three independent differentiations of control (Control 1 and 2) and VPS35 p.D620N mutant (VPS35 clones 1_1 and 1_2) neurons under basal culture condition.

Fragmented mitochondria with decreased MMP, increased mitochondrial ROS and impaired respiration in VPS35 p.D620N patient-derived neurons:

Here we characterized, for the first time, human neurons derived from iPSCs of a p.D620N VPS35 carrier. We analysed z-stack images from two controls and two clones of patient-derived neurons (Fig. 2A). Computational analyses revealed a decrease in mitochondrial size, representative of fragmentation (Fig. 2B). Moreover, mitochondrial branching as a readout for connectivity within the mitochondrial network was also impaired with a decreased average number of links (Fig. 2C) and nodes (Fig. 2D).

The identification of these morphological alterations observed in patient-derived cells led us to assess the mitochondrial function. We measured MMP and found a decrease in patient-derived neurons compared to controls (Fig. 2E). The reduced MMP was accompanied by a significant increase of intra-mitochondrial ROS compared to controls (Fig. 2F). Mitochondrial respiration was assessed by recording the oxygen consumption rate while we applied mitochondrial stress such as oligomycin, FCCP, antimycin A and rotenone to measure different respiratory

parameters (Fig. 2G). We found that neurons carrying the p.D620N mutation displayed a reduced basal and maximal respiration, reduced spare respiratory capacity, and non-mitochondrial oxygen consumption (Fig. 2H). This was associated with a significantly reduced ATP production in patient cells compared to controls.
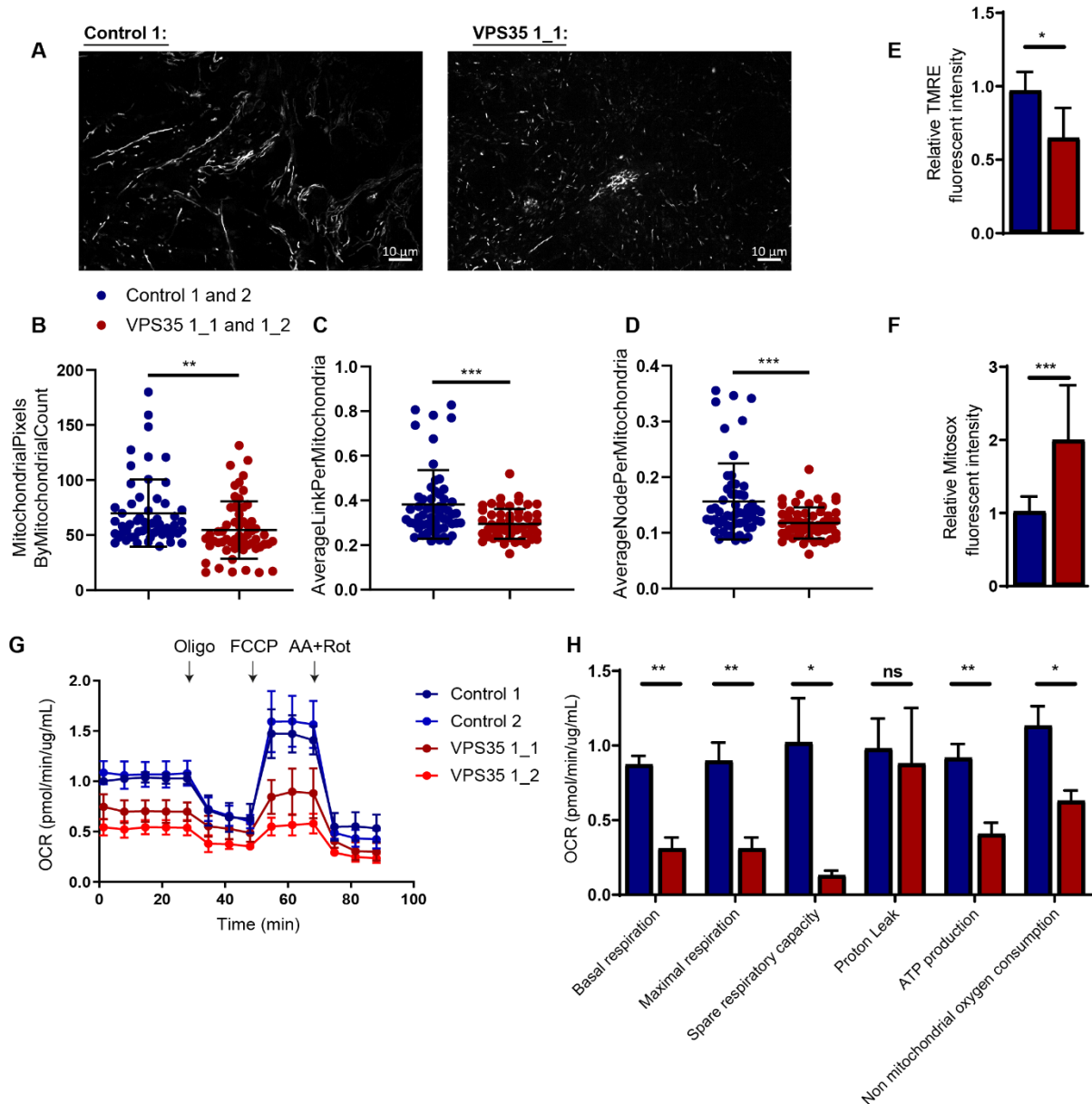

Figure 2: Mitochondrial fragmentation and dysfunction in VPS35 mutant iPSC-derived neurons. (**A**) Representative image of mitochondria stained with Mitotracker green FM and calculated mitochondrial size (**B**), average links per mitochondrion (**C**) and average nodes per mitochondrion (**D**) from four independent differentiations of control (Control 1 and 2) and VPS35 D620N mutant (VPS35 clones 1_1 and 1_2) neurons in culture medium without antioxidants (without B27 and ascorbic acid) for 24 hrs. (**E**) Mitochondrial membrane potential

54

measured by TMRE mean fluorescence intensity and (**F**) mitochondrial reactive oxygen species measured by Mitosox mean fluorescence intensity by flow cytometry from four independent differentiations of control (Control 1 and 2) and VPS35 D620N mutant (VPS35 clones 1_1 and 1_2) neurons in culture medium without antioxidants (without B27 and ascorbic acid) for 4 hrs. (**G**) Mean average OCR of four independent differentiations of control (Control 1 and 2) and VPS35 D620N mutant (VPS35 clones 1_1 and 1_2) neurons over a time course. Measurement of basal OCR is followed by the addition of oligomycin (oligo) 2 µM final concentration, FCCP 250 nM final concentration and antimycin A (AA) 5 µM final concentration and rotenone (rot) 5 µM final concentration (left side). Calculated basal respiration, maximal respiration, spare respiratory capacity, proton leak, ATP production and non-mitochondrial oxygen consumption (right side). All statistical tests were Mann-Whitney tests to compare groups. Error bars show standard deviation and ns $p>0.05$; *$p<0.05$; **$p<0.01$; ***$p<0.001$

<u>VPS35 p.D620N patient-derived neurons show an impaired mitochondrial clearance:</u>

As patient neurons present morphologically and functionally altered mitochondria, we hypothesised that mitochondrial mass, biogenesis and clearance, i.e. mitophagy, might be dysregulated. We found no differences in mitochondrial mass between patient and control neurons as defined by WB against TOM20 (Fig. 3A) and VDAC1 (Fig. 3B). Moreover, protein expression levels of PGC1α (Fig. 3C), the master regulator of mitochondrial biogenesis, were unchanged in patient derived neurons under basal conditions.

In order to study mitophagy, control 1 and VPS35 1_2 smNPCs were edited using CRISPR-Cas9 technology to express a fusion mitochondrial protein: ATP5C1-DsRed-pHluorin. Briefly, when mitochondria are in the cytoplasm, both fluorophores are functional. Once mitochondria are exposed to an acidic environment inside the autophagosome (mitophagic event), the green fluorescence will be quenched (Fig. 3D). We treated the gene edited neurons with CCCP and acquired images from the same field of view at different time points: t=0 hr, 3 hrs, 8 hrs and 24 hrs. In control neurons (Fig. 3E), the number of mitochondria inside autophagosomes increased significantly after 3 hrs CCCP treatment. After 8 hrs and further after 24 hrs of CCCP treatment, the number of mitochondria inside autophagosomes were decreasing showing an efficient clearance. In the patient-derived neurons harbouring the *VPS35* p.D620N (Fig. 3F), the number of mitochondria inside autophagosome also increased significantly after 3 hrs of CCCP treatment. After 8 hrs and 24 hrs, the number of mitochondria inside autophagosome failed to decrease and stayed elevated, indicating a deficient clearance (Fig. 3G). Under basal conditions (t=0), we see no significant differences in the number of mitochondria inside autophagosome

between patient and control neurons. In addition, after 3 hrs of CCCP treatment there was no difference in the number of mitochondria inside autophagosome between patients and controls (Fig. 3G), indicating that the induction of mitophagy was not impaired in patient neurons. However, the difference between patient and control cells becomes significant at 8 hrs and 24 hrs, as the number of mitochondria inside autophagosome decreased in control-derived and stayed elevated in patient-derived neurons.
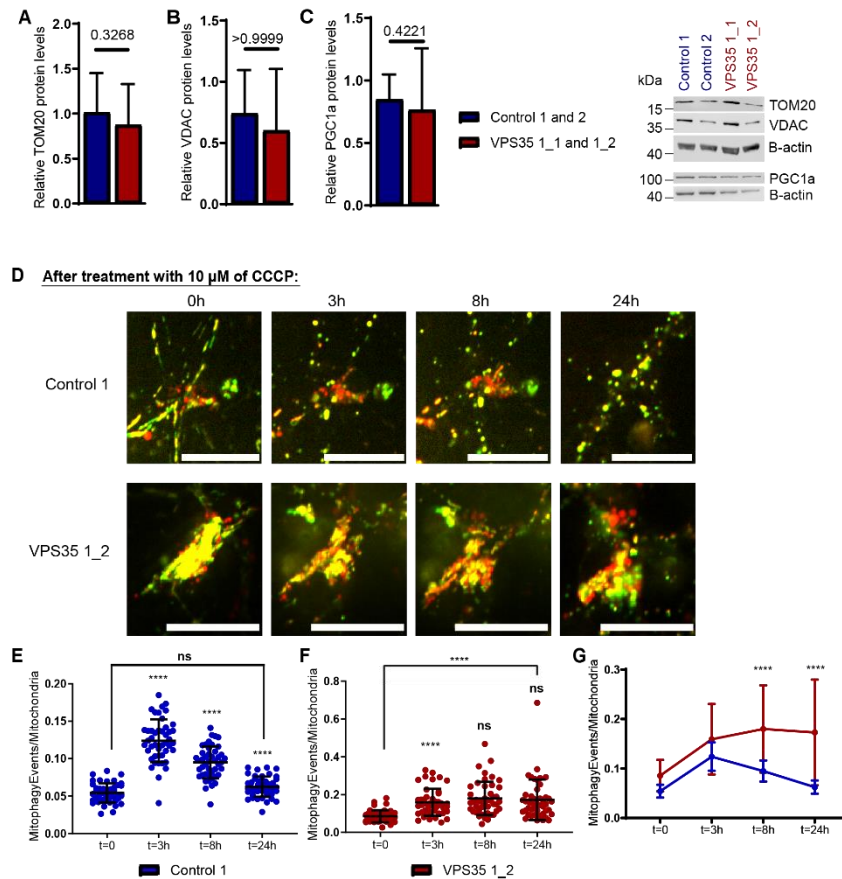

Figure 3: Mitophagy clearance impairment in VPS35 mutant iPSC-derived neurons after CCCP treatment. (**A**, **B**, **C**) Western blot analysis of TOM20 (**A**), VDAC (**B**), PGC1α (**C**) and β-actin (loading control) from four independent differentiations of control (Control 1 and 2) and VPS35 D620N mutant (VPS35 clones 1_1 and 1_2) neurons under basal culture condition. (**D**) Representative image of mitochondria and mitophagy events under CCCP treatment over a time course. The scale bar represents 20 μm. Calculated mitophagic events by mitochondria count in Control 1 (**E**) and mutant VPS35 1_2 (**F**) from three independent differentiations of control (Control 1) and VPS35 D620N mutant (VPS35 clone 1_2) neurons expressing ATP5C1-RFP-pHluorin protein in culture medium without antioxidants (without B27 and ascorbic acid) and treated with CCCP 10 μM for 0, 3, 8 and 24 hrs. Each time point is compared with the previous

one. (**G**) Comparison of both lines. All statistical tests were Mann-Whitney tests or One-way Anova followed by Sidak's multiple comparisons tests to compare groups and conditions. Error bars show standard deviation and ns p>0.05; *p<0.05; **p<0.01; ***p<0.001; ****p<0.0001.

<u>Lysosomal clearance dysfunction and α-synuclein accumulation in VPS35 p.D620N patient-derived neurons:</u>

The link between the retromer and macroautophagy has been identified by the sorting of ATG9, a protein important for the induction of autophagy with the retromer (Popovic and Dikic, 2014). Additionally, in cells overexpressing the mutant p.D620N VPS35, ATG9 was missorted which is thought to lead to impaired autophagy (Zavodszky *et al.*, 2014). Here, we measured the steady state level of the autophagy protein p62 (Fig. 4A) which was not different between patient and controls. Upon Bafilomycin A1 treatment, p62 was accumulating in the controls, as shown by a significant increase compared to the untreated state. However, p62 did not significantly increase in the patient neurons after Bafilomycin A1 treatment, showing an impaired autophagic flux. Moreover, compared to control-derived neurons, we found a significantly reduced Lamp1 steady state protein level in the patient neurons (Fig. 4B), suggesting a lower late-endosome/lysosome mass compared to controls.

The impaired lysosomal clearance was accompanied by an increase of α-synuclein in patient-derived neurons as shown by WB (Fig. 4C) and TR-FRET against α-synuclein (Fig. 4D).
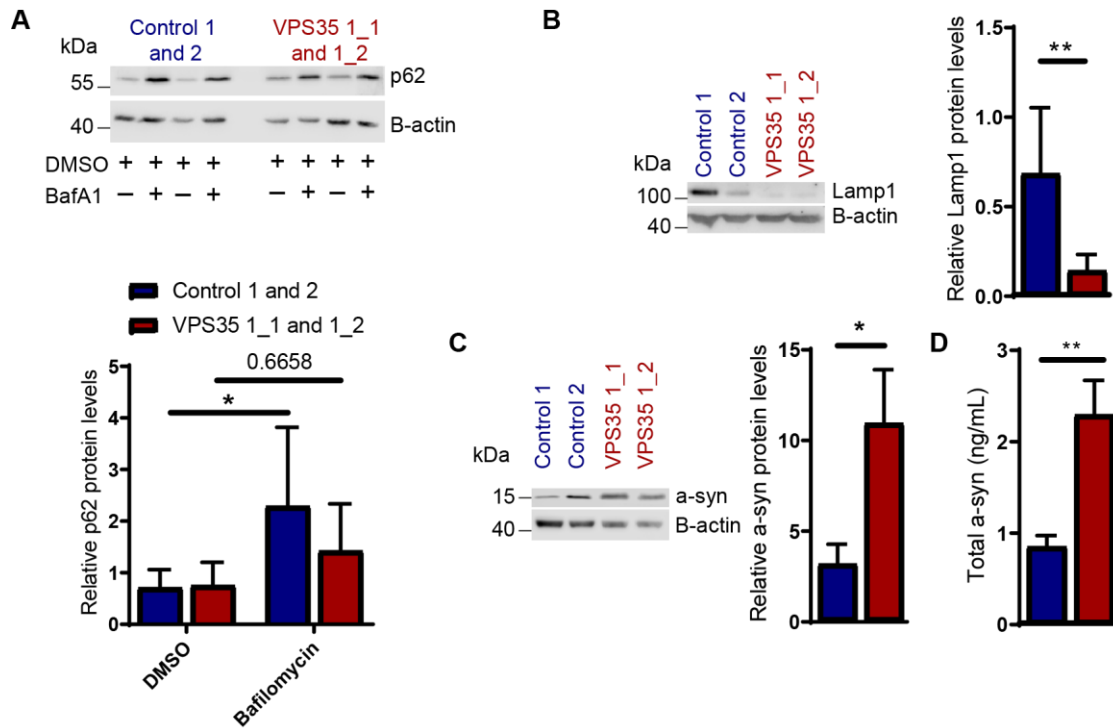
Figure 4: Impaired lysosomal clearance and α-synuclein accumulation in VPS35 mutant iPSC-derived neurons. (**A**) Western blot analysis of p62 and β-actin (loading control) from five independent differentiations of control (Control 1 and 2) and VPS35 D620N mutant (VPS35 clones 1_1 and 1_2) neurons under basal culture condition and Bafilomycin A1 (BafA1) 100 nM treatment for 24 hrs. (B, C) Western blot analysis of Lamp1 (**B**), α-synuclein (α-syn) (**C**) and β-actin (loading control) from four independent differentiations of control (Control 1 and 2) and VPS35 D620N mutant (VPS35 clones 1_1 and 1_2) neurons under basal culture condition. (**D**) TR-FRET measurement of total α-synuclein (α-syn) amount from four independent differentiations of control (Control 1 and 2) and VPS35 D620N mutant (VPS35 clones 1_1 and 1_2) neurons under basal culture condition. All statistical tests were Mann-Whitney tests or One-way Anova followed by Sidak's multiple comparisons tests to compare groups and conditions. Error bars show standard deviation and $*p<0.05$; $**p<0.01$.

Accumulation of α-synuclein at the mitochondria in patient-derived neurons:

The subcellular localization of α-synuclein has been debated, with initial description at the synapses and within the nucleus (Burré *et al.*, 2018). A mitochondrial association has been further debated, from entering the mitochondria via Tom40 (Devi *et al.*, 2008) to being located within the mitochondria-associated ER membranes (MAMs) (Guardia-Laguarta *et al.*, 2014). In SH-SY5Y cell lines overexpressing α-synuclein, the co-localisation between α-synuclein and the mitochondrial membrane is increased (Parihar *et al.*, 2008). In patient-derived neurons carrying a triplication of the *SNCA* gene locus extensive mitochondrial defects are found (Little

et al., 2018; Zambon *et al.*, 2019). The cellular phenotypes that we have identified in our patient-derived neurons, i.e. (i) increased mitochondrial fragmentation, (ii) decreased MMP, (iii) increased ROS and (iv) impaired respiration, coincides with the accumulation of α-synuclein in the patient-derived neurons harbouring the VPS35 p.D620N mutation. Consequently, we hypothesised that the mitochondrial impairment seen in our patient-derived neurons could be due to α-synuclein accumulation at or in the mitochondria. To explore this, we performed a mitochondrial fractionation (Fig. 5). Here, α-synuclein protein levels were significantly increased in both cytosolic and mitochondrial fractions with a two to three-fold increase in patient-derived neurons compared to controls. Our data shows that there is indeed an accumulation of α-synuclein at or in the mitochondria.
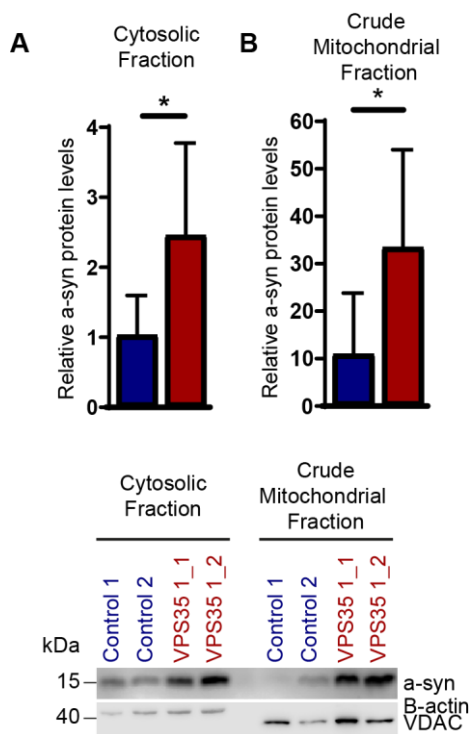

Figure 5: α-synuclein accumulation at the mitochondria in patient-derived neurons. Western blot analysis of α-synuclein (α-syn) and β-actin (loading control) in the cytosolic (**A**) and in the crude mitochondrial (**B**) fraction from three independent differentiations of control (Control 1 and 2) and VPS35 D620N mutant (VPS35 clones 1_1 and 1_2) neurons under basal culture condition. All statistical tests were Mann-Whitney tests to compare groups. Error bars show standard deviation and *$p < 0.05$.

Reduction of α-synuclein protein level does not rescue mitochondrial impairment in p.D620N VPS35 patient-derived neurons:

To test whether α-synuclein accumulation at or in the mitochondria can be the cause of the observed mitochondrial dysfunction, we decided to rescue the levels of α-synuclein and study MMP and mitochondrial ROS levels.

We knocked-down α-synuclein in both controls and patient-derived neurons with shRNA against *SNCA* (Mazzulli *et al.*, 2016). We transduced neurons at DIV23 and analysed α-synuclein protein levels 7 days post-transduction. Using WB we detected a reduction of the levels of α-synuclein in the patient-derived neurons to the physiological levels of α-synuclein in controls-derived neurons transduced with scrambled shRNA (Fig. 6A). We measured MMP and mitochondrial ROS using the same technique as previously and found that the reduction of α-synuclein protein levels did not rescue the loss of MMP (Fig. 6B) nor the increased ROS level (Fig. 6C).
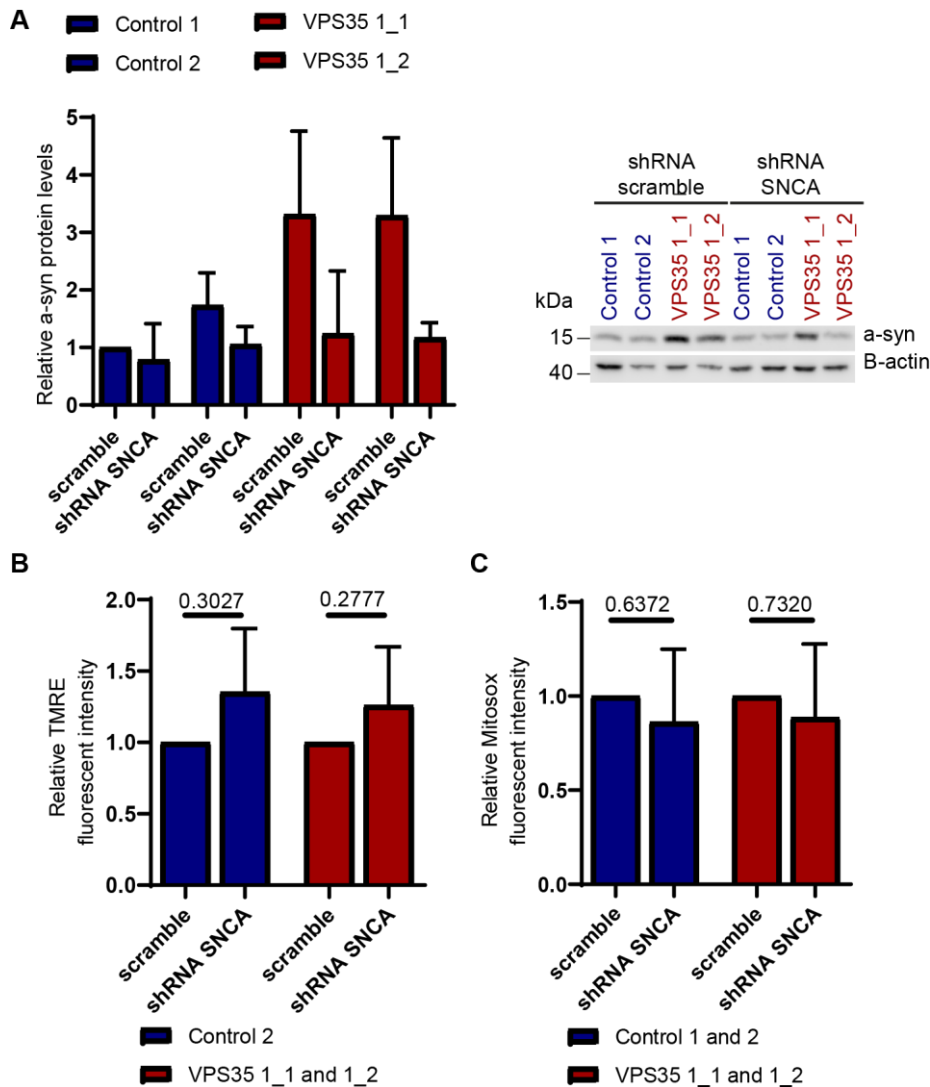

Figure 6: Rescue of α-synuclein level does not rescue mitochondrial impairment. (A) Western blot analysis of α-synuclein (α-syn) and β-actin (loading control) from three independent differentiations of control (Control 1 and 2) and VPS35 D620N mutant (VPS35

clones 1_1 and 1_2) neurons transduced with scramble shRNA and shRNA against α-synuclein. (**B**) Mitochondrial membrane potential measured by TMRE mean fluorescence intensity and (**C**) mitochondrial reactive oxygen species measured by Mitosox mean fluorescence intensity by flow cytometry from three independent differentiations of control (Control 1 and 2) and VPS35 D620N mutant (VPS35 clones 1_1 and 1_2) neurons transduced with scramble shRNA and shRNA against α-synuclein and in culture medium without antioxidants (without B27 and ascorbic acid) for 4 hrs. All statistical tests One-way Anova followed by Sidak's multiple comparisons tests to compare groups and conditions. Error bars show standard deviation.

LRRK2 kinase activity is not increased in patient-derived neurons:

Overactivation of LRRK2 kinase activity has been shown in p.D620N VPS35 knock-in mouse embryonic fibroblasts and in patient neutrophils carrying the mutant VPS35 (Mir *et al.*, 2018). Furthermore, a similar mitochondrial phenotype with reduced MMP, increased ROS and impaired respiration were found in LRRK2 p.G2019S mutant cells, reviewed in (Larsen *et al.*, 2018). The p.G2019S mutation leads to an overactivation of the kinase activity of LRRK2, and consequently to increased phosphorylation of LRRK2 targets, such as Rab10 (Seol *et al.*, 2019). Therefore, we hypothesised that the mitochondrial phenotype seen in our model could originate from an overactivation of LRRK2 kinase activity. We measured by WB the steady state ratio between phosphorylated pT73 Rab10 and Rab10 and found no difference between patients and controls (Fig. 7).
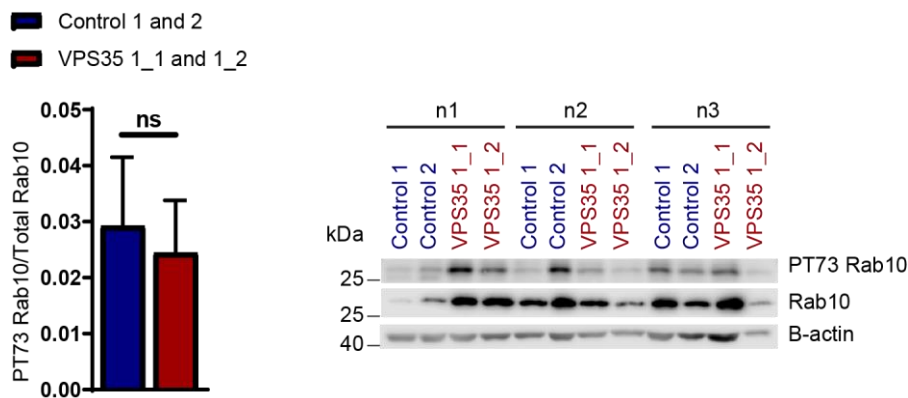

Figure 7: No difference in LRRK2 kinase activity on Rab10 phosphorylation between patient and controls derived neurons. Western blot analysis of Rab10, pT73 Rab10 and β-actin (loading control) from three independent differentiations of control (Control 1 and 2) and VPS35 p.D620N mutant (VPS35 clones 1_1 and 1_2) neurons under baseline conditions. Graph shows the ratio between pT73 and total Rab10. Statistical test was Mann-Whitney test to compare groups. Error bars show standard deviation and ns $p > 0.05$.

Discussion:

The increasing importance of endosomal trafficking pathways in PD pathogenesis has been widely recognized with their implication in many other established pathways such as mitochondrial impairment, lysosomal dysfunction, protein aggregation and synaptic dysfunction (Perrett *et al.*, 2015). Indeed, numerous *PARK* genes (*DNAJC13*, *LRRK2* and *SNCA*) are implicated in this pathway and there is a growing interest in finding other disease-relevant endosomal trafficking genes (Bandres-Ciga *et al.*, 2019).

In this study, we found that the PD-causing mutation in *VPS35* leads to fragmented and impaired mitochondria with decreased size and branching, decreased membrane potential, increased mitochondrial ROS and dysfunctional respiration. VPS35 deficiency has already been linked to mitochondrial impairment in multiple cellular models such as dopaminergic neurons from mice carrying a heterozygous loss of VPS35, rat cortical neurons overexpressing p.D620N VPS35 and patient fibroblasts carrying the p.D620N VPS35 mutation. These studies consistently report fragmented mitochondria with decreased MMP and impaired respiration (Tang *et al.*, 2015*c*; Wang *et al.*, 2015; Zhou *et al.*, 2017). Here we confirm these findings for the first time in iPSC-derived neurons from patients.

Furthermore, clearance is impacted with accumulation of mitophagic events under mitochondrial stress, decreased autophagic flux and decreased late-endosome/lysosome mass. The decreased autophagic flux together with impaired Cathepsin-D and Lamp2a trafficking previously described (Mohan and Mellick, 2017), leads to an accumulation of α-synuclein in the whole cell, and at the same ratio in the cytosol and at or in mitochondria.

The observation that similar mitochondrial defects were found in patient-derived neurons carrying a triplication in *SNCA* gene (Little *et al.*, 2018; Zambon *et al.*, 2019) led us to hypothesize that α-synuclein accumulation at or in mitochondria might be involved. However, reducing the protein level of α-synuclein did not rescue the loss of MMP nor the increased ROS levels. α-synuclein accumulation does not seem to be the primary cause of mitochondrial impairment observed in our model.

Impaired mitochondrial morphology and function have also been reported in patient-derived neurons carrying the p.G2019S mutation in LRRK2 (Walter *et al.*, 2019; Weykopf *et al.*, 2019). Furthermore, increased phosphorylation of LRRK2 and its substrate Rab10 has been shown in

homozygous p.D620N *VPS35* knock-in mice embryonic fibroblasts and mouse brain, and heterozygous *VPS35* p.D620N patients neutrophils and monocytes, which was decreased after LRRK2 kinase inhibitor treatment (Mir *et al.*, 2018). That study revealed a strong link between *VPS35* and *LRRK2*, both genes responsible for autosomal-dominantly inherited PD and both involved in endosomal trafficking. Here we found no evidence of overactivation of LRRK2 kinase activity in patient-derived neurons. However, the study of (Mir *et al.*, 2018) only reported an overactivation of LRRK2 kinase activity in the homozygous knock-in mouse brain; therefore it remains to be determined, whether the heterozygous state is sufficient to cause overactivation of LRRK2. On the other hand, a recently published study showed that the recruitment of Rab10 to depolarised mitochondria triggered mitophagy in human-derived fibroblasts. Upon phosphorylation, Rab10 was not recruited to depolarised mitochondria anymore and mitophagy was impaired in PD patient-derived fibroblasts carrying the *LRRK2* p.G2019S mutation (Wauters *et al.*, 2019). Thus, we cannot exclude changes of phospho-Rab10 levels specifically in the mitochondrial fraction of patient-derived neurons carrying the heterozygous p.D620N VPS35 mutation.

Some studies have reported that VPS35 and the retromer might be involved in mitochondria-derived vesicles (MDVs), a form of mitochondrial quality control (Braschi *et al.*, 2009). Two cargos have been identified trafficking towards the lysosome or the peroxisome for degradation, Drp1 (Wang *et al.*, 2016*b*) and MAPL (mitochondrial associated protein ligase) or Mul1 (Braschi *et al.*, 2009, Tang *et al.*, 2015*b*). MAPL or Mul1 is known to stabilize Drp1, a mitochondrial fission protein and degrade Mfn2, a mitochondrial fusion protein. By trafficking both proteins, VPS35 seems to stabilise mitochondrial network in a fused state. In cells overexpressing VPS35 p.D620N, the retromer does not correctly transport Drp1 and MAPL, which leads to an increase of MAPL and Drp1 protein level and a decreased Mfn2 protein level. This subsequently leads to a fragmented mitochondrial network (Tang *et al.*, 2015*b*, Wang *et al.*, 2016*b*), also observed in patient-derived neurons in our study. Interestingly, treatment of cells overexpressing VPS35 p.D620N and patient fibroblasts carrying the VPS35 p.D620N variant with Mdivi1, a Drp1 inhibitor, rescues the mitochondrial functional impairment (Wang *et al.*, 2016*b*; Zhou *et al.*, 2017). This shows that mitochondrial functional impairment is at least in part caused by the mistrafficking of Drp1 and MAPL by the retromer containing mutant VPS35 p.D620N.

Although Mdivi1 treatment is promising to rescue mitochondrial deficits, this only resolves one aspect of the disease. Indeed, VPS35 and the retromer also interact with essential proteins of the lysosomal clearance pathway and some studies show that the retromer is implicated in the recycling of neurotransmitter receptors. Wang and collaborators (Wang *et al.*, 2016*a*) show that VPS35 interacts with the post-synaptic dopamine receptor D1 (DRD1) and is responsible for its recycling back to the plasma membrane after clathrin-mediated endocytosis. The downregulation of VPS35 or the overexpression of mutant D620N led to a decrease of DRD1 recycling. Others have shown that VPS35 interacts with the pre-synaptic dopamine transporter (DAT) (Wu *et al.*, 2017). Whether the p.D620N mutant still binds to DAT remains to be explored. Furthermore, overexpression of VPS35 p.D620N in rat *substantia nigra* leads to dopaminergic neurodegeneration (Tsika *et al.*, 2014).

Overall, the retromer and VPS35 seem to play a central role in the cell with regulation of mitochondrial dynamics, lysosomal clearance and dopaminergic transmission. The autosomal-dominant mutation in VPS35 shows that the retromer and endosomal trafficking deficiency might be the cause of underlying impaired cellular mechanisms in PD. Therefore, one might consider targeting the retromer complex for future therapy. In Alzheimer's disease, the use of chaperones to stabilize the retromer has already shown promises (Mecozzi *et al.*, 2014; Berman *et al.*, 2015; Chu and Praticò, 2017).

like to thank Prof. T. Graham and A. Sargsyan from the University of Utah for kindly providing us with the pHluorin construct.

Competing interests:

The authors report no competing interests.

References:

Arias-Fuenzalida J, Jarazo J, Walter J, Gomez-Giro G, Forster JI, Krueger R, et al. Automated high-throughput high-content autophagy and mitophagy analysis platform. Sci Rep 2019; 9: 9455.

Arighi CN, Hartnell LM, Aguilar RC, Haft CR, Bonifacino JS. Role of the mammalian retromer in sorting of the cation-independent mannose 6-phosphate receptor. J Cell Biol 2004; 165: 123–133.

Bandres-Ciga S, Saez-Atienzar S, Bonet-Ponce L, Billingsley K, Vitale D, Blauwendraat C, et al. The endocytic membrane trafficking pathway plays a major role in the risk of Parkinson's disease. Mov Disord 2019; 34: 460–468.

Baumuratov AS, Antony PMA, Ostaszewski M, He F, Salamanca L, Antunes L, et al. Enteric neurons from Parkinson's disease patients display ex vivo aberrations in mitochondrial

structure. Sci Rep 2016; 6: 33117.

Bentley SR, Bortnick S, Guella I, Fowdar JY, Silburn PA, Wood SA, et al. Pipeline to gene discovery - Analysing familial Parkinsonism in the Queensland Parkinson's Project. Parkinsonism Relat Disord 2018; 49: 34–41.

Berman DE, Ringe D, Petsko GA, Small SA. The Use of Pharmacological Retromer Chaperones in Alzheimer's Disease and other Endosomal-related Disorders. Neurotherapeutics 2015; 12: 12–18.

Braschi E, Zunino R, McBride HM. MAPL is a new mitochondrial SUMO E3 ligase that regulates mitochondrial fission. EMBO Rep 2009; 10: 748–754.

Burré J, Sharma M, Südhof TC. Cell Biology and Pathophysiology of α-Synuclein. Cold Spring Harb Perspect Med 2018; 8: a024091.

Chu J, Praticò D. The retromer complex system in a transgenic mouse model of AD: influence of age. Neurobiol Aging 2017; 52: 32–38.

Cong L, Ran FA, Cox D, Lin S, Barretto R, Habib N, et al. Multiplex Genome Engineering Using CRISPR/Cas Systems. Science (80-) 2013; 339: 819–823.

Deng H, Gao K, Jankovic J. The VPS35 gene and Parkinson's disease. Mov Disord 2013; 28: 569–575.

Devi L, Raghavendran V, Prabhu BM, Avadhani NG, Anandatheerthavarada HK. Mitochondrial Import and Accumulation of α-Synuclein Impair Complex I in Human Dopaminergic Neuronal Cultures and Parkinson Disease Brain. J Biol Chem 2008; 283: 9089–9100.

Follett J, Norwood SJ, Hamilton NA, Mohan M, Kovtun O, Tay S, et al. The Vps35 D620N Mutation Linked to Parkinson's Disease Disrupts the Cargo Sorting Function of Retromer. Traffic 2014; 15: 230–244.

Grünewald A, Gegg ME, Taanman J-W, King RH, Kock N, Klein C, et al. Differential effects of PINK1 nonsense and missense mutations on mitochondrial function and morphology. Exp Neurol 2009; 219: 266–273.

Guardia-Laguarta C, Area-Gomez E, Rub C, Liu Y, Magrane J, Becker D, et al. -Synuclein Is Localized to Mitochondria-Associated ER Membranes. J Neurosci 2014; 34: 249–259.

Hockemeyer D, Soldner F, Beard C, Gao Q, Mitalipova M, DeKelver RC, et al. Efficient targeting of expressed and silent genes in human ESCs and iPSCs using zinc-finger nucleases. Nat Biotechnol 2009; 27: 851–857.

Krüger R, Klucken J, Weiss D, Tönges L, Kolber P, Unterecker S, et al. Classification of advanced stages of Parkinson's disease: translation into stratified treatments. J Neural Transm 2017; 124: 1015–1027.

Larsen SB, Hanss Z, Krüger R. The genetic architecture of mitochondrial dysfunction in Parkinson's disease. Cell Tissue Res 2018; 373: 21–37.

Little D, Luft C, Mosaku O, Lorvellec M, Yao Z, Paillusson S, et al. A single cell high content assay detects mitochondrial dysfunction in iPSC-derived neurons with mutations in SNCA. Sci Rep 2018; 8: 9033.

Mali P, Yang L, Esvelt KM, Aach J, Guell M, DiCarlo JE, et al. RNA-Guided Human Genome Engineering via Cas9. Science (80-) 2013; 339: 823–826.

Mazzulli JR, Zunke F, Isacson O, Studer L, Krainc D. α-Synuclein–induced lysosomal dysfunction occurs through disruptions in protein trafficking in human midbrain synucleinopathy models. Proc Natl Acad Sci 2016; 113: 1931–1936.

McGough IJ, Steinberg F, Jia D, Barbuti PA, McMillan KJ, Heesom KJ, et al. Retromer Binding to FAM21 and the WASH Complex Is Perturbed by the Parkinson Disease-Linked VPS35(D620N) Mutation. Curr Biol 2014; 24: 1670–1676.

Mecozzi VJ, Berman DE, Simoes S, Vetanovetz C, Awal MR, Patel VM, et al. Pharmacological chaperones stabilize retromer to limit APP processing. Nat Chem Biol 2014; 10: 443–449.

Mir R, Tonelli F, Lis P, Macartney T, Polinski NK, Martinez TN, et al. The Parkinson's disease VPS35[D620N] mutation enhances LRRK2-mediated Rab protein phosphorylation in mouse and human. Biochem J 2018; 475: 1861–1883.

Miura E, Hasegawa T, Konno M, Suzuki M, Sugeno N, Fujikake N, et al. VPS35 dysfunction impairs lysosomal degradation of α-synuclein and exacerbates neurotoxicity in a Drosophila model of Parkinson's disease. Neurobiol Dis 2014; 71: 1–13.

Mohan M, Mellick GD. Role of the VPS35 D620N mutation in Parkinson's disease. Parkinsonism Relat Disord 2017; 36: 10–18.

Parihar MS, Parihar A, Fujita M, Hashimoto M, Ghafourifar P. Mitochondrial association of alpha-synuclein causes oxidative stress. Cell Mol Life Sci 2008; 65: 1272–1284.

Perrett RM, Alexopoulou Z, Tofaris GK. The endosomal pathway in Parkinson's disease. Mol Cell Neurosci 2015; 66: 21–28.

Popovic D, Dikic I. TBC1D5 and the AP2 complex regulate ATG9 trafficking and initiation of autophagy. EMBO Rep 2014; 15: 392–401.

Reinhardt P, Glatza M, Hemmer K, Tsytsyura Y, Thiel CS, Höing S, et al. Derivation and Expansion Using Only Small Molecules of Human Neural Progenitors for Neurodegenerative Disease Modeling. PLoS One 2013; 8: e59252.

Seaman MNJ, Michael McCaffery J, Emr SD. A Membrane Coat Complex Essential for Endosome-to-Golgi Retrograde Transport in Yeast. J Cell Biol 1998; 142: 665–681.

Seol W, Nam D, Son I. Rab GTPases as Physiological Substrates of LRRK2 Kinase. Exp Neurobiol 2019; 28: 134.

Tang F-L, Erion JR, Tian Y, Liu W, Yin D-M, Ye J, et al. VPS35 in Dopamine Neurons Is Required for Endosome-to-Golgi Retrieval of Lamp2a, a Receptor of Chaperone-Mediated Autophagy That Is Critical for -Synuclein Degradation and Prevention of Pathogenesis of Parkinson's Disease. J Neurosci 2015; 35: 10613–10628.

Tang F-L, Liu W, Hu J-X, Erion JR, Ye J, Mei L, et al. VPS35 Deficiency or Mutation Causes Dopaminergic Neuronal Loss by Impairing Mitochondrial Fusion and Function. Cell Rep 2015; 12: 1631–1643.

Tang FL, Liu W, Hu JX, Erion JR, Ye J, Mei L, et al. VPS35 Deficiency or Mutation Causes Dopaminergic Neuronal Loss by Impairing Mitochondrial Fusion and Function. Cell Rep

2015; 12: 1631–1643.

Tsika E, Glauser L, Moser R, Fiser A, Daniel G, Sheerin U-M, et al. Parkinson's disease-linked mutations in VPS35 induce dopaminergic neurodegeneration. Hum Mol Genet 2014; 23: 4621–4638.

Vilariño-Güell C, Wider C, Ross OA, Dachsel JC, Kachergus JM, Lincoln SJ, et al. VPS35 Mutations in Parkinson Disease. Am J Hum Genet 2011; 89: 162–167.

Walter J, Bolognin S, Antony PMA, Nickels SL, Poovathingal SK, Salamanca L, et al. Neural Stem Cells of Parkinson's Disease Patients Exhibit Aberrant Mitochondrial Morphology and Functionality. Stem Cell Reports 2019; 12: 878–889.

Wang C, Niu M, Zhou Z, Zheng X, Zhang L, Tian Y, et al. VPS35 regulates cell surface recycling and signaling of dopamine receptor D1. Neurobiol Aging 2016; 46: 22–31.

Wang W, Wang X, Fujioka H, Hoppel C, Whone AL, Caldwell MA, et al. Parkinson's disease–associated mutant VPS35 causes mitochondrial dysfunction by recycling DLP1 complexes. Nat Med 2015; 22: 54–63.

Wang W, Wang X, Fujioka H, Hoppel C, Whone AL, Caldwell MA, et al. Parkinson's disease–associated mutant VPS35 causes mitochondrial dysfunction by recycling DLP1 complexes. Nat Med 2016; 22: 54–63.

Wauters F, Cornelissen T, Imberechts D, Martin S, Koentjoro B, Sue C, et al. LRRK2 mutations impair depolarization-induced mitophagy through inhibition of mitochondrial accumulation of RAB10. Autophagy 2019: 1–20.

Weykopf B, Haupt S, Jungverdorben J, Flitsch LJ, Hebisch M, Liu G-H, et al. Induced pluripotent stem cell-based modeling of mutant LRRK2-associated Parkinson's disease. Eur J Neurosci 2019; 49: 561–589.

Wu S, Fagan RR, Uttamapinant C, Lifshitz LM, Fogarty KE, Ting AY, et al. The Dopamine Transporter Recycles via a Retromer-Dependent Postendocytic Mechanism: Tracking Studies Using a Novel Fluorophore-Coupling Approach. J Neurosci 2017; 37: 9438–9452.

Zambon F, Cherubini M, Fernandes HJR, Lang C, Ryan BJ, Volpato V, et al. Cellular α-

synuclein pathology is associated with bioenergetic dysfunction in Parkinson's iPSC-derived dopamine neurons. Hum Mol Genet 2019; 28: 2001–2013.

Zavodszky E, Seaman MNJ, Moreau K, Jimenez-Sanchez M, Breusegem SY, Harbour ME, et al. Mutation in VPS35 associated with Parkinson's disease impairs WASH complex association and inhibits autophagy. Nat Commun 2014; 5: 3828.

Zhou L, Wang W, Hoppel C, Liu J, Zhu X. Parkinson's disease-associated pathogenic VPS35 mutation causes complex I deficits. Biochim Biophys Acta - Mol Basis Dis 2017; 1863: 2791–2795.

Zimprich A, Benet-Pagès A, Struhal W, Graf E, Eck SH, Offman MN, et al. A Mutation in VPS35, Encoding a Subunit of the Retromer Complex, Causes Late-Onset Parkinson Disease. Am J Hum Genet 2011; 89: 168–175.

Supplemental Methods:

Immunofluorescence staining:

iPSCs and smNPCs were fixed on coverslips with 4% paraformaldehyde for 15 min, before being permeabilised and blocked in 0.4% Triton-X, 10% goat serum and 2% bovine serum albumin for 1 hr. Immunofluorescence staining was performed with primary antibodies against Nanog (1:500, Abcam), Oct3/4 (1:1000, Santa Cruz), Nestin (1:250. R&D Systems), Musashi-1 (1:250, Abcam), Sox1 (1:250, R&D Systems) and Sox2 (1:250, Santa Cruz) and respective secondary antibodies coupled with fluorophore (1:1000, Invitrogen). DAPI (1:50, Thermo Fisher Scientific) was used to stain nuclei. At least five images per coverslip were acquired using Zeiss spinning disk confocal microscope.

Flow cytometry staining:

200 000 smNPCs were harvested and fixed with 4% paraformaldehyde 15 min and permeabilised in water with 0.05% Saponin and 1% BSA for 20 min. Immunofluorescence staining was performed with primary antibodies against (1:250. R&D Systems), Musashi-1 (1:250, Abcam), Sox1 (1:250, R&D Systems) and Sox2 (1:250, Santa Cruz) and respective secondary antibodies coupled with fluorophore (1:1000, Invitrogen). smNPCs were resuspended in 300 µL of PBS and 10 000 events were measured using the BD LSRFortessa (Becton). Data were analysed using the Flowjo LLC software.

RT-qPCR:

Total RNA was purified from iPSCs using Trizol/chloroform. Transcriptor High Fidelity cDNA Synthesis Kit (Roche) was used to synthesize cDNA. Quantification of pluripotency markers by multiplex qPCR was performed using the LightCycler® 480 Probes Master kit (Roche) and hydrolysis probes detecting NANOG-FAM (Hs02387400_g1, Thermo Fisher Scientific), OCT4-FAM (Hs00999632_g1, Thermo Fisher Scientific) and DNMT3B (Hs00171876_m1, Thermo Fisher Scientific). GAPDH-VIC (Hs02758991_g1, Thermo Fisher Scientific) was used as a housekeeping gene. Total RNA purified from fibroblasts was used as a negative control.

A

B
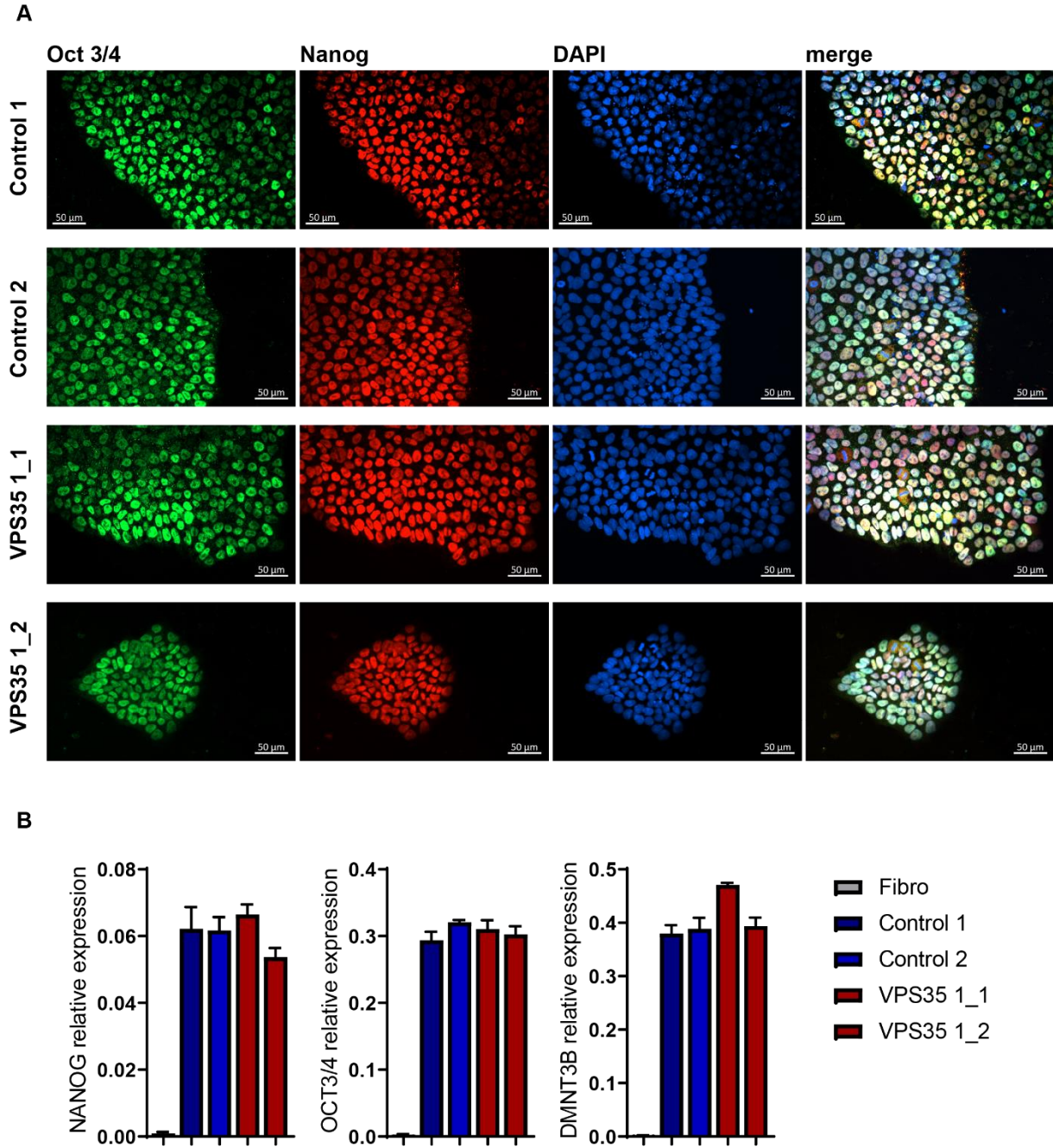
Figure S1: All iPSC clones express the pluripotency markers. (**A**) Immunofluorescence staining shows expression of Oct3/4, Nanog and DAPI. (**B**) Relative expression of Oct3/4, Nanog and DMNT3B transcript of three technical replicates of iPSC clones and patient fibroblasts with GAPDH as housekeeping gene. Error bar shows standard deviation.
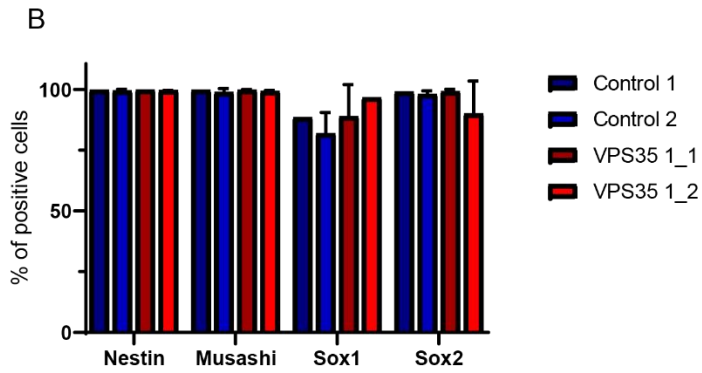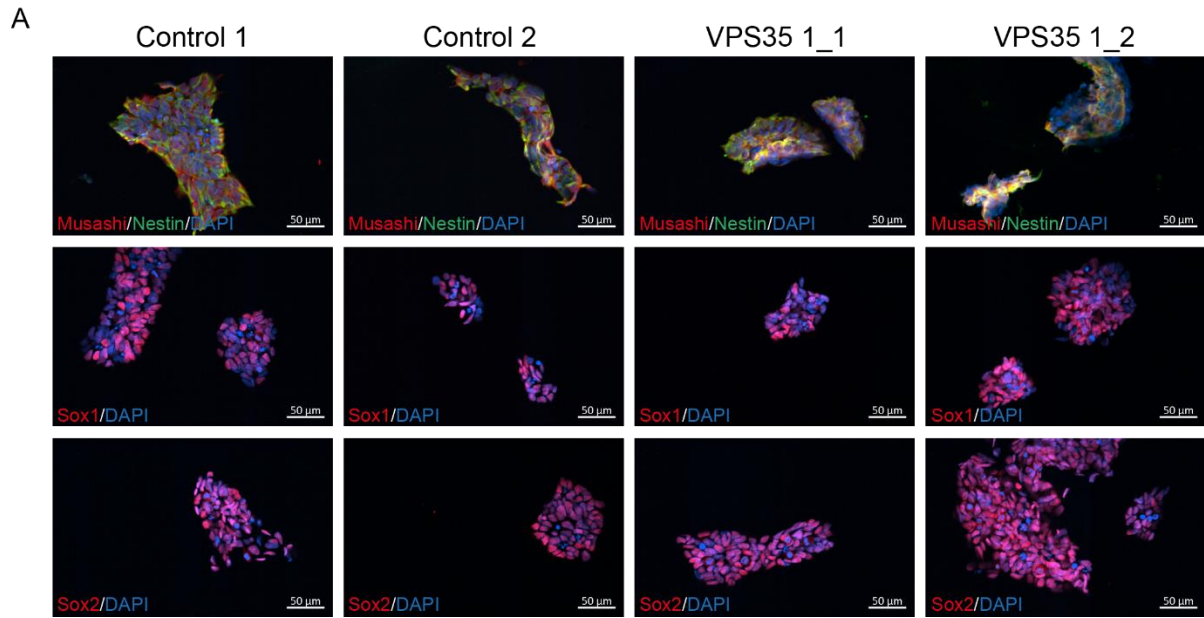
Figure S2: All smNPC clones express the neuronal precursor markers. (**A**) Immunofluorescence staining shows expression of Musashi, Nestin, Sox1, Sox2 and DAPI. (**B**) Percentage (%) of Nestin, Musashi, Sox1 and Sox2 positive cells measured by flow cytometry. Error bar shows standard deviation.

3. Discussion and perspectives

So far, no group has studied the impact of the *VPS35* p.D620N mutation on mitochondria and autophagy in iPSC-derived models from patient. Here, we found that iPSC-derived neurons from patient carrying *VPS35* p.D620N mutation displayed fragmented mitochondria with decreased MMP, increased ROS and impaired respiration. In addition, mitophagy clearance is impaired which is accompanied by a decreased autophagic flux and late endosome-lysosomal mass. Furthermore, α-synuclein protein is accumulating in the whole cell, the cytosolic compartment and the mitochondria.

Firstly, by using fibroblasts from patient and healthy controls we found that the VPS35 p.D620N mutant protein caused a decrease of MMP without significant changes of the mitochondrial morphology (Figure S1, Appendix). The observed decrease of MMP confirmed previous findings in patient-derived fibroblasts carrying the p.D620N mutation, concomitantly with a fragmented mitochondrial network (Wang *et al.*, 2016*c*). However, we did not find fragmented mitochondria in the patient-derived fibroblasts. This may be due to differences of the cell culture conditions prior to the experiment. We cultured the fibroblasts in DMEM + 1% P/S only for 4 hrs, whereas in the previous publication the cells starved longer before the experiments. PD being a disease of the brain, we decided to study the impact of p.D620N mutation in a more disease-relevant setting.

Therefore, we reprogrammed the fibroblasts into iPSCs. These iPSCs were fully characterised (Manuscript I) and we showed they were expressing the pluripotency markers and could differentiate in the three germ layer cell types. The advantage of iPSCs is that they can be differentiated into any cell type of the organism. Several studies have already used these cells to study neurodegenerative diseases (Amin *et al.*, 2019). Monogenic forms of PD as well as sporadic have been investigated in iPSC-derived models (Cobb *et al.*, 2018). iPSCs represent a scalable and screenable model to study disease phenotype in a relevant cell type (Cobb *et al.*, 2018). So far, Munsie and collaborators were the only ones to show the impact of VPS35 p.D620N in iPSC-derived neurons from patient and found an impaired recycling of the GluR1 subunits of AMPA receptors (Munsie *et al.*, 2015).

We differentiated the iPSCs into smNPCs (Reinhardt *et al.*, 2013) and fully characterised them to confirm the expression of the neuronal precursor markers Sox2, Nestin and Musashi (Figure S1, manuscript II). smNPCs are already specified towards neuronal lineage and are highly scalable and screenable. We found that the VPS35 p.D620N mutant smNPCs did not recapitulate the decreased MMP shown in patient-derived fibroblasts (Figure S2, Appendix).

This could be explained by the fact that smNPCs are transient and highly proliferative cells with very small cytoplasmic compartment. We further decipher the cellular phenotype of patient smNPCs by measuring the autophagy-linked protein p62 before and after Bafilomycin A1 treatment. p62 steady state protein level did not differ between patient and control cells. However, p62 protein failed to accumulate after Bafilomycin A1 treatment in the patient-derived smNPCs compared to the control, indicating that the autophagic flux was decreased. We further measured the lysosomal hydrolase Cathepsin D protein expression and found it reduced in smNPCs carrying VPS35 p.D620N mutation. This finding is in line with previous studies showing a mistrafficking of Pro-Cathepsin D in the lysosomal compartment, resulting in the decrease of its protein level in patient-derived fibroblasts and in cells overexpressing p.D620N mutant (Follett *et al.*, 2014; McGough *et al.*, 2014). Lysosomal degradation of α-synuclein depends on hydrolases such as Cathepsin D and autophagy (Qiao *et al.*, 2008; Ebrahimi-Fakhari *et al.*, 2011). However, the lysosomal clearance deficiency observed in VPS35 p.D620N mutant smNPCs did not lead to the expected accumulation of α-synuclein. The levels of α-synuclein have been previously shown in the lab to be very low in smNPCs compared to neurons, which could explain this finding.

The smNPCs failed to reproduce the mitochondrial impairment but revealed a deficit in lysosomal clearance with reduced autophagic flux and Cathepsin-D protein levels in cells expressing p.D620N mutant VPS35.

To further decipher the impact of VPS35 p.D620N in patient-derived cells, we differentiated the smNPCs in neuronal culture enriched in midbrain DA neurons (Reinhardt *et al.*, 2013). This protocol enables to obtain between 10 and 20% midbrain DA neurons. We confirmed the presence of midbrain-specific DA neurons in our cultures and measured the levels of retromer component VPS35 and VPS29. Both proteins were expressed in a similar level between patient-derived neurons carrying the D620N mutation and controls, as expected from previous studies (Follett *et al.*, 2014).

Here, we showed that iPSC-derived neurons carrying the p.D620N mutation display fragmented mitochondrial network compared to control neurons. This finding contrasts with the intact mitochondrial network previously found in patient-derived fibroblasts. One could explain this discrepancy by the fact that neuronal function highly depends on oxidative energy produced by mitochondria for signal transport along neurites whereas fibroblasts are less energy demanding. In addition, the fragmentation found in patient neurons is in line with previous studies in rat primary neurons *in vitro* and rat *substantia nigra* DA neurons *in vivo*

overexpressing p.D620N VPS35 where aspect ratio was decreased (Wang *et al.*, 2015). VPS35 deficiency in mice *substantia nigra* also leads to fragmentation of mitochondrial network (Tang *et al.*, 2015*c*). The fragmentation was rescued by overexpressing WT VPS35 but not VPS35 p.D620N. This finding suggests that the p.D620N mutant lacks an important function of the physiological protein and contributes to the mitochondrial morphology phenotype via haploinsufficiency.

It has been shown that the retromer is a regulator of mitochondrial dynamics with a direct interaction with Drp1 and MAPL (mitochondria-associated protein ligase) (Braschi *et al.*, 2010, Tang *et al.*, 2015*c*; Wang *et al.*, 2015). Indeed, the retromer has been linked to a form of mitochondrial quality control through MDVs (Braschi *et al.*, 2010). The only two cargos found so far are Drp1 and MAPL. MAPL is responsible for the stabilization of Drp1, the fission protein, in mitochondrial membranes and for the degradation of Mfn2, the fusion protein. In *VPS35* deficient cells, MAPL colocalisation with mitochondria is increased which leads to a fragmented phenotype (Braschi *et al.*, 2010). VPS35 is responsible for the identification of cargo but is not essential for the formation of MDVs. Indeed, when VPS35 was KD in HEK293T cells, MDVs were still formed. VPS35+/MAPL+ vesicles are directed towards the peroxisomes or lysosomes for degradation of MAPL (Braschi *et al.*, 2010, Tang *et al.*, 2015*c*). VPS35 also directly interacts with Drp1 complexes on mitochondrial membranes. Indeed, VPS35 was described to be responsible for the targeting of Drp1 inactivated complexes and the MDVs are transported to lysosomes for degradation (Wang *et al.*, 2015). This removal of inactivated Drp1 complexes enables newly synthesized Drp1 to be redirected towards mitochondria to exert their fission function. The interaction between Drp1 and VPS35 p.D620N seemed to be increased in rat cortical neurons overexpressing the mutant protein suggesting an increased turnover of Drp1 on mitochondrial membranes (Wang *et al.*, 2015). Interestingly, Wang and collaborators also found increased Drp1-VPS35 interaction in *post-mortem* brain samples from individuals with sporadic PD. Furthermore, by analyzing the peptide sequence of Drp1 they found a FLV sorting motif in the C-terminus end of the protein, similar to the one found on Sortilin1, a known retromer cargo (Wang *et al.*, 2016*b*). This FLV motif is essential for retromer recognition of Drp1 and treatment of M17 cells overexpressing p.D620N mutant with a peptide mimicking the FLV sorting motif could rescue mitochondrial morphology and function.

In our study, mitochondrial fragmentation was concomitant with a decrease of MMP, an increase of mitochondrial ROS and an impairment of mitochondrial respiration in iPSC-derived neurons expressing VPS35 p.D620N compared to controls. This mitochondrial dysfunction was

previously described in patient-derived fibroblasts (Wang *et al.*, 2015, 2016*b*) and in cells overexpressing VPS35 p.D620N or deficient for VPS35 (Tang *et al.*, 2015*c*; Wang *et al.*, 2015, 2016*b*). Furthermore, Zhou and collaborators showed that patient-derived fibroblasts expressing VPS35 p.D620N have a decreased activity of complex I and complex II of the ETC (Zhou *et al.*, 2017) using an enzymatic assay. Interestingly, in several studies, the mitochondrial impairment caused by VPS35 p.D620N was rescued in part by treatment with Drp1 inhibitor Mdivi-1. The treatment rescued the mitochondrial morphology and function in VPS35 p.D620N overexpressing cells and patient-derived fibroblasts, suggesting that mitochondrial functional impairment is caused by Drp1 dysregulation. This stresses the importance of VPS35 and the retromer in regulating mitochondrial dynamics and thereby, function (Wang *et al.*, 2015; Zhou *et al.*, 2017).

Fragmented and depolarized mitochondria usually activate mitochondrial clearance via mitophagy. To decipher whether VPS35 p.D620N had an impact on mitophagy, we generated CRISPR-Cas9 edited smNPCs expressing the fusion mitochondrial protein ATP5C1-pHluorin-DsRed from one clone of the patient and one of the controls. This allowed us to study mitophagy in living cells without interfering with the cells by transfection or transduction. At baseline, there was no difference in the number of mitochondria in autophagosome (mitophagic events) between iPSC-derived neurons expressing VPS35 p.D620N and control neurons. We treated the neurons with CCCP and visualized the same number of mitochondria inside autophagosome in patient and control neurons 3 hrs post treatment, suggesting that the induction of mitophagy is not impaired by VPS35 p.D620N. After 3 hrs, the number of mitophadria inside autophagosome decreased until baseline after 24 hrs of treatment in control neurons showing efficient clearance whereas in patient neurons the number of mitochondria in autophagosome stayed elevated. This suggests that the patient neurons carrying the p.D620N *VPS35* mutation were unable to clear the dysfunctional mitochondria. Giving that the induction of mitophagy does not seem to be impaired in mutant neurons, we can hypothesize that VPS35 is not implicated in the induction of mitophagy but rather that the p.D620N mutation causes a deficit of lysosomal clearance.

Further investigations showed that patient-derived neurons failed to accumulate autophagic marker p62 after Bafilomycin A1 treatment compared to controls, suggesting an impaired general autophagy with decreased autophagic flux. The retromer mediates the trafficking of ATG9A from the TGN to the early autophagosome. ATG9A is thought to be implicated in the transport of membranes to the autophagosome and is thus important for the induction of

autophagy. In cells overexpressing VPS35 p.D620N, upon induction of autophagy, ATG9A was significantly less recruited to autophagosome than in cells overexpressing WT VPS35 (Zavodszky *et al.*, 2014), leading to a decrease of autophagic events. This would rather suggest that the induction of autophagy is impaired, thus leading to a decrease of the autophagic flux. Furthermore, we found a significant decrease of late-endosome/early lysosome protein Lamp1 level in patient-derived neurons. Others have reported an increase of the size of Lamp1 positive vesicles in mice midbrain DA neurons VPS35 +/-, suggesting that the late endosome/lysosome pathway might be altered due to VPS35 deficiency (Tang *et al.*, 2015*a*). One could hypothesise that the lysosomal dysfunction comes from a deficit in maturation of late endosomal vesicles. Indeed, G2019S mutation in *LRRK2* also leads to an impairment of lysosomal maturation, as shown by the presence of enlarged and perinuclear lysosomes in mutant drosophila (Dodson *et al.*, 2012).

Furthermore, we found a significant three-fold increase in α-synuclein protein level in iPSC-derived neurons carrying the *VPS35* p.D620N mutation compared to controls. Aggregation of high molecular weight α-synuclein and phosphorylated α-synuclein has previously been observed in ventral midbrain of VPS35 +/- mice, in mice overexpressing VPS35 p.D620N (Tang et al., 2015a) and in Drosophila VPS35 +/- expressing human α-synuclein (Miura et al., 2014). However, some studies failed to see this accumulation of α-synuclein in VPS35 p.D620N KI mice models (Ishizu et al., 2016; Chen et al., 2019). These results suggest that the autophagy impairment and decreased late endosome/lysosome mass are in part responsible for α-synuclein accumulation.

In addition, the retromer mediates the trafficking of CIMPR, a receptor essential for the lysosomal hydrolase Cathepsin D processing in the endosomal/lysosomal pathway. In cancer cell lines, VPS35 deficiency and overexpressing the p.D620N mutant lead to a mistrafficking of CIMPR, resulting in a more diffuse expression in the cell instead of localising mainly at the TGN (Follett *et al.*, 2014; McGough *et al.*, 2014). CIMPR binds to Pro-Cathepsin D at the TGN and transports it in the endosomal pathway where it is cleaved into mature Cathepsin D in the lysosome. As CIMPR is not recycled back to the TGN properly anymore, it leads to an increase of Pro-Cathepsin D levels in the TGN and a decrease of Cathepsin D levels in the lysosome (Follett *et al.*, 2014; McGough *et al.*, 2014). In addition, one study showed that the retromer regulates chaperone-mediated autophagy (CMA) by recycling LAMP2a. In VPS35 deficient mice, the number of LAMP2a positive vesicles are decreased (Tang *et al.*, 2015*a*).

Overall, retromer function is essential for regulating lysosomal degradation. Indeed, lysosomal dysfunction will most likely lead to α-synuclein accumulation, one of the hallmarks of PD.

In turn, the increase of α-synuclein could lead to lysosomal dysfunction and maturation impairment. Indeed, accumulation of α-synuclein inhibits the trafficking of GCase from the ER to the Golgi (Mazzulli *et al.*, 2011). GCase accumulates in the ER and is not directed towards the lysosome where it is mature and exert its proper function. GCase deficiency in mice primary neurons leads to α-synuclein accumulation, creating a deleterious feedback loop. We measured GCase activity in the iPSC-derived neurons from the VPS35 p.D620N patient and controls and found no differences. However, we measured the activity in whole cell, whereas Mazzulli and collaborators show the GCase decrease in activity specifically in the lysosomal compartment (Mazzulli *et al.*, 2016). Further investigations are needed to decipher whether α-synuclein could lead to lysosomal maturation impairment in patient-derived neurons carrying the VPS35 p.D620N mutation.

Interestingly, the increase of α-synuclein in whole cell lysate was accompanied by an increase of α-synuclein in the mitochondrial fraction of patient-derived neurons compared to controls. A mitochondrial association of α-synuclein has been described in several studies overexpressing WT *SNCA* with a debate in sublocalisation within the mitochondria (Parihar *et al.*, 2008). It has been hypothesised that α-synuclein enters in the mitochondrion via TOM40 (Devi *et al.*, 2008) or that it is localised within MAMs (Guardia-Laguarta *et al.*, 2014). iPSC-derived neurons from a patient carrying a triplication of the *SNCA* locus displayed similar mitochondrial deficits as the ones described here with fragmented mitochondrial network, decreased MMP and impaired respiration (Little *et al.,* 2018; Zambon *et al.*, 2019). This observation led us to hypothesise that the mitochondrial impairment in VPS35 p.D620N iPSC-derived neurons could be the consequence of α-synuclein accumulation. Thus, we rescued the increased levels of α-synuclein in patient-derived neurons to the level of the controls by using lentivirus delivered shRNA against *SNCA*. Seven days after transduction, we assessed MMP and mitochondrial ROS level and found it unchanged compared to the scramble condition. This result led us to consider that the mitochondrial impairment observed in VPS35 p.D620N mutant iPSC-derived neurons is independent of the observed α-synuclein accumulation. We cannot exclude that α-synuclein plays a role in the pathogenic phenotype but it does not seem to be the primary cause of mitochondrial dysfunction.

Recently, VPS35 has been linked to LRRK2, another protein found to be mutated in PD. The first evidence came from a genetic study in drosophila where the overexpression of *VPS35*

rescued the locomotor impairment of overexpressing *LRRK2* G2019S drosophila (Linhart *et al.*, 2014). VPS35 and LRRK2 are both found in the endosomal compartment and mutations in these genes both lead to autosomal-dominant forms of familial PD. In addition, both are associated with synaptic vesicle recycling (Inoshita *et al.*, 2017) and VPS35 protein level is reduced in the frontal cortex of *LRRK2* mutation carriers in *post-mortem* brains. Interestingly, LRRK2 kinase activity has been found to be increased in VPS35 p.D620N KI mice and neutrophils and monocytes of human carriers of the p.D620N mutation (Mir *et al.*, 2018). These authors investigated the phosphorylation status of Rab10 on the residue Ser73, one of the known substrate of LRRK2 kinase activity. They found elevated pT73 Rab10 as well as autophosphorylation of LRRK2 at the residue Ser1292 in heterozygous and homozygous VPS35 p.D620N KI mouse embryonic fibroblasts (MEFs) and brain. The same result was found in neutrophils and monocytes from three VPS35 p.D620N patients where the phosphorylation of Rab10 was three fold higher than in idiopathic PD patients cells. In addition, in VPS35 KO cell lines, Rab10 phosphorylation was reduced 4-5 fold suggesting that VPS35 regulates LRRK2 kinase activity. VPS35 p.D620N would exacerbate the LRRK2 kinase activity in a gain of function manner (Mir *et al.*, 2018). Interestingly, LRRK2 also mediates phosphorylation of Drp1 and thus, regulates mitochondrial fission. The LRRK2 p.G2019S mutation leads to increased kinase activity and – via increased levels of phosphorylated Drp1 - to mitochondrial fragmentation in cell lines and patient fibroblasts (Su and Qi, 2013). Furthermore, similar mitochondrial impairment with decreased MMP and mitochondrial respiration have been described in iPSC-derived neurons of individuals carrying *LRRK2* p.G2019S mutation (Weykopf *et al.*, 2019). These observations led us to hypothesise that mitochondrial impairment seen in VPS35 p.D620N iPSC-derived neurons were due to overactivation of LRRK2 kinase activity. Thus, we measured the phosphorylation of Rab10 at the residue T73 in whole cell lysates from neurons of the human carrier. However, we did not find any difference in the phosphorylation status of Rab10 in patient-derived neurons, although the results were highly variable. We further analysed the presence of Rab10 in the mitochondrial fraction versus cytosolic fraction. Indeed, a study recently showed that Rab10 was recruited to depolarised mitochondria, which triggered mitophagy in human-derived fibroblasts (Wauters *et al.*, 2019). In LRRK2 p.G2019S mutant fibroblasts, Rab10 was phosphorylated and thus not recruited to depolarised mitochondria which decrease mitophagy. LRRK2 could directly regulate mitochondrial clearance through phosphorylation of Rab10.

In our study, VPS35 p.D620N does not seem to induce mitochondrial impairment through increased α-synuclein at the mitochondria, nor by overactivation of LRRK2 kinase activity.

Considering that the retromer has been shown to regulate Drp1 and MFN2 protein levels (Tang *et al.*, 2015*c*; Wang *et al.*, 2015), VPS35 p.D620N most likely causes mitochondrial impairment through the regulation of mitochondrial dynamics. Indeed, the fact that mitochondrial defect can be rescued by Mdivi1 treatment would confirm this hypothesis. However, we cannot exclude that VPS35 regulates mitochondrial dynamics concomitantly with LRRK2 and α-synuclein. Indeed, as discussed above, LRRK2 directly regulates mitochondrial fission by phosphorylation of Drp1. On the other hand, α-synuclein has been shown to be present in MAM (Guardia-Laguarta *et al.*, 2014), which is also the site where mitochondrial fission occurs (Friedman *et al.*, 2011). The observation that increased α-synuclein levels lead to increased fission might suggest that α-synuclein regulates Drp1 in some way. Kamp and collaborators suggested that α-synuclein does not interact directly with Drp1 but rather regulates mitochondrial dynamics via membrane lipids, inhibiting the formation of the fusion stalk (Kamp *et al.*, 2010). The effect of the three proteins could converge on mitochondrial dynamics, which further leads to mitochondrial impairment. Interestingly, a recent study has shown that VPS35 could be ubiquitinated by Parkin in drosophila, suggesting that Parkin might regulate the retromer function (Martinez *et al.*, 2017). This finding was confirmed in mammalian cells in the same study.

In addition, Mdivi1 treatment rescues neuronal spine loss observed in primary cortical neurons overexpressing VPS35 p.D620N and neuronal death *in vivo* (Wang *et al.*, 2015). Although this treatment strategy seems to efficiently rescue not only mitochondrial impairment but also neuronal death, no one showed the impact on lysosomal dysfunction and α-synuclein accumulation. In order to rescue all the pathological phenotypes caused by VPS35 p.D620N, one strategy could be to increase the activity of the WT retromer complex. In this regard, there is a lot to learn from other neurodegenerative diseases. Indeed, VPS35 and VPS26 protein levels have been found to be decreased in AD patient brains (Small *et al.*, 2005). Studies in AD have already shown the benefit of a retromer chaperone which stabilises the complex assembly and increases the expression of VPS35, VPS26 and VPS29 (Mecozzi *et al.*, 2014). The retromer complex mediates the sorting of Sortilin A, a transmembrane receptor, responsible for the trafficking of APP (Berman *et al.*, 2015). In *VPS35* deficient cells, APP resides longer in the endosomal compartment together with β-secretase which increases the amyloidogenic cleavage of APP, leading to β-amyloid accumulation (Andersen *et al.*, 2005). The chaperone binds to VPS35 and VPS29, increasing the binding stability between these proteins, thus increasing protein level in mice hippocampal neurons (Mecozzi *et al.*, 2014). APP and Sortilin A were significantly less localised to endosome, suggesting an increased

recycling of Sortilin A by the retromer. This led to a decreased cleavage by β-secretase, resulting in a reduction of β-amyloid protein level (Mecozzi *et al.*, 2014). The chaperone treatment seems to be a good candidate for further testing. However, we do not know whether it affects the trafficking of other binding cargos such as the ones involved in lysosomal clearance. In addition, if considering the fact that the p.D620N mutant has an increased binding to Drp1, leading to an increased turnover of the protein and thus to mitochondrial fragmentation (Wang *et al.*, 2016*c*), increasing the levels of retromer might not be a good solution.

Some studies report that the mutant p.D620N VPS35 results in a gain of toxic function for certain phenotypes. Indeed, they show that overexpression of WT VPS35 also increases mitochondrial fragmentation, even though overexpression of VPS35 p.D620N had worse effects (Wang *et al.*, 2016*c*). Another study has described that overexpression of VPS35 and VPS35 p.D620N caused a decrease of neurite length in primary cortical neurons and an increase of nigral dopaminergic neurons loss in rats *in vivo* (Tsika *et al.*, 2014). Again, the authors suggested that VPS35 p.D620N mutant works as a toxic gain-of-function. However, most studies show a loss of VPS35 function due to the p.D620N mutation and one can argue that overexpressing WT or mutant VPS35 leads to an imbalance in stoichiometry between the retromer complex components, explaining the toxic gain of function. This could have a detrimental effect in itself, leading to the observed phenotype. By using the chaperone treatment, all components of the retromer are increased in a proportional way, which might be protective. In this context, it could increase the WT retromer levels, thus restoring the trafficking of key components of the lysosomal degradation pathway such as CIMPR, LAMP2A and ATG9A. This would ultimately rescue the levels of α-synuclein.

The retromer has also been studied in the context of neurotransmitter receptor recycling from the early endosome back to the plasma membrane. The first receptor showed to be recycled by retromer is β2 adrenergic receptors (β2AR) in HEK 293 cells (Temkin *et al.*, 2011) and in primary neurons (Choy *et al.*, 2014), both stably expressing tagged β2AR. They showed that retromer allowed a fast recycling of receptors, without passing through the TGN. Upon KD of VPS35, β2AR is still endocytosed but is not recycled back to the membrane, instead it is redirected towards the lysosomal compartment (Temkin *et al.*, 2011). Other neurotransmitter receptors are recycled by the retromer such as NMDAR and AMPAR. Indeed, in VPS35 KD hippocampal slices, synaptic AMPA and NMDA excitatory post synaptic currents were decreased, however GABA inhibitory postsynaptic currents seemed not to be affected (Choy *et al.*, 2014). Surface GluA1 (AMPAR) expression was showed to be increased after long term

potential (LTP) in CA1 pyramidal cells, which was retromer dependent. Indeed, this increase of surface GluA1 expression was not observed in VPS35 KD mice, nor was the LTP, but was rescued by overexpression of VPS35 WT but not the p.D620N mutant (Temkin *et al.*, 2017). In addition, in primary cortical neurons, overexpression of mutant p.D620N led to an increase of AMPAR surface localisation in synapses, which was reproduced in patient iPSC-derived dopaminergic neurons (Munsie *et al.*, 2015). Here, it seems that the retromer is needed for the endocytosis of the receptors, not only for the transport from the endosome to the plasma membrane. This function of the retromer was inhibited with mutant p.D620N VPS35, working here as a loss of function mutation.

Recently, the retromer has been linked to dopaminergic neural transmission. The retromer is responsible for the recycling of dopamine receptor D1 (DRD1) in a concentration dependent manner in N2A cells and in HEK297 cells expressing tagged DRD1 and VPS35 (Wang *et al.*, 2016*a*). Indeed, when VPS35 is overexpressed, surface DRD1 levels increases, whereas when VPS35 is KD, surface DRD1 decreases (Wang *et al.*, 2016*a*), suggesting that the retromer does not affect the endocytosis but rather the cell surface recycling. On the other hand, VPS35 p.D620N seems to still be able to interact with DRD1 but cannot increase the surface level when overexpressed. Again, VPS35 p.D620N seems to be working as a loss of function mutation. Interestingly, dopamine transporter DAT colocalises with retromer in endosomal vesicles in rat mesencephalic cell lines (Wu *et al.*, 2017). When VPS35 is KD, the recycling of DAT decreases with reduced levels of surface DAT levels and total DAT, suggesting that DAT gets degraded. Retromer seems to be responsible for the recycling of DAT but not the endocytosis itself. Furthermore, VPS35 p.D620N KI mice display lower levels of striatum DAT, while levels of VMAT2 are increased, most likely as a compensation mechanism (Cataldi *et al.*, 2018). They also report increased dopamine turnover in homozygous p.D620N KI mice. In addition, in VPS35 deficient drosophila, a decreased number of synaptic vesicles and increased size of synaptic boutons were observed in dopaminergic neurons. This deficit was rescued by the introduction of WT VPS35 but not mutant p.D620N (Inoshita *et al.*, 2017). The authors suggest a loss of function of p.D620N mutant in synaptic vesicles regeneration. Interestingly, the synaptic bouton morphology could be rescued by overexpressing LRRK2 in heterozygous VPS35 deficient larvae. LRRK2 and VPS35 are both present at synaptic boutons but at different sites. They seem to both be regulating synaptic vesicles dynamics as similar phenotypes are found in VPS35 or LRRK2 deficient drosophila (Inoshita *et al.*, 2017).

VPS35 and the retromer seem to play an important role in both pre- and postsynaptic compartment. How VPS35 p.D620N exactly functions in this context remains elusive as the binding to DRD1 does not seem to be impaired for example. Overall, the mutation leads to decreased surface expression of important receptors and transporters for synaptic neurotransmission.

With its central role in protein trafficking, VPS35 p.D620N mutation affects many cellular pathways *e.g.* mitochondrial homeostasis, protein and organelle clearance and synaptic function most likely due to a loss-of-function. Also, VPS35 has been shown to interact with several PD-associated proteins such as LRRK2, α-synuclein, RME-8, auxilin, synaptojanin 1, and Parkin (reviewed in Cui *et al.*, 2018). All of these proteins are associated with the endosomal pathway. Furthermore, the mutation causes late-onset PD and the clinical phenotype of the patients resembles the sporadic PD and VPS35 levels are decreased in brains of sporadic PD patients. Together, all this makes the p.D620N VPS35 mutation a good model to study dysfunctional pathways such as mitochondrial dysfunction, clearance impairment and α-synuclein accumulation in PD. Also, the iPSC-derived neurons carrying p.D620N VPS35 could serve as a good screening model to find potential treatment for the disease, including Mdivi1 and the retromer chaperone.

4. Outlook

Further studies are needed to pinpoint exactly how p.D620N VPS35 causes mitochondrial impairment. Investigating whether MDVs play a role in this phenotype in DA neurons derived from patients would be essential, considering their potential role in regulating mitochondrial dynamics. Furthermore, correction of the point mutation by CRISPR-Cas9 mediated gene-editing would help strengthen the claim that the observed phenotypes are indeed caused by the p.D620N mutation and not solely by the PD genetic background. Indeed, Walter and collaborators have shown that introducing LRRK2 p.G2019S in a control iPSC line, did not fully recapitulate LRRK2 p.G2019S related phenotypes (Walter *et al.*, 2019). This shows the importance of patients genetic background on the cellular phenotypes observed.

Moreover, it would be interesting to treat the iPSC-derived neurons from patient carrying the p.D620N mutation in *VPS35* with the mitochondrial fission inhibitor Mdivi1. Indeed, we could test whether Mdivi1 also rescues mitochondrial functional and morphological impairment in our cellular model (Tang *et al.*, 2015*c*; Wang *et al.*, 2015; Zhou *et al.*, 2017). We could further

investigate whether it rescues autophagy and lysosomal clearance dysfunction and α-synuclein accumulation as well. Indeed, Mdivi1 treatment has been shown to rescue the DA neuronal degeneration in rat model carrying the p.D620N mutation in *VPS35* (Wang *et al.*, 2015) and in rat model carrying the p.A53T mutation in *SNCA* (Bido *et al.*, 2017). Furthermore, Mdivi1 has been demonstrated to be beneficial in AD transgenic mice models where it rescued mitochondrial impairment but also decreased β-amyloid deposition in the brain and improved learning and memory capacity (Baek *et al.*, 2017).

On the other hand, we could treat the iPSC-derived DA neurons from the patient carrying p.D620N mutation, with the retromer chaperone used in AD transgenic models to stabilise and increase the retromer complex (Mecozzi *et al.*, 2014). It would be interesting to see whether it rescues the mitochondrial impairment, lysosomal clearance dysfunction and α-synuclein accumulation observed in the patient-derived neurons carrying the p.D620N mutation.

Moreover, the cellular phenotypes observed in iPSC-derived neurons from patient carrying the p.D620N mutation in *VPS35* are similar to those seen in idiopathic PD cases. Also, the clinical phenotype is indistinguishable from idiopathic PD. Therefore, Mdivi1 and retromer chaperone treatments could be tested as well on iPSC-derived neurons from sporadic PD patients.

5. References

Amin N, Tan X, Ren Q, Zhu N, Botchway BOA, Hu Z, et al. Recent advances of induced pluripotent stem cells application in neurodegenerative diseases. Prog Neuro-Psychopharmacology Biol Psychiatry 2019; 95: 109674.

Andersen OM, Reiche J, Schmidt V, Gotthardt M, Spoelgen R, Behlke J, et al. Neuronal sorting protein-related receptor sorLA/LR11 regulates processing of the amyloid precursor protein. Proc Natl Acad Sci 2005; 102: 13461–13466.

Ando M, Funayama M, Li Y, Kashihara K, Murakami Y, Ishizu N, et al. VPS35 mutation in Japanese patients with typical Parkinson's disease. Mov Disord 2012; 27: 1413–1417.

Antony PMA, Diederich NJ, Krüger R, Balling R. The hallmarks of Parkinson's disease. FEBS J 2013; 280: 5981–5993.

Arighi CN, Hartnell LM, Aguilar RC, Haft CR, Bonifacino JS. Role of the mammalian retromer in sorting of the cation-independent mannose 6-phosphate receptor. J Cell Biol 2004; 165: 123–133.

Baek SH, Park SJ, Jeong JI, Kim SH, Han J, Kyung JW, et al. Inhibition of Drp1 Ameliorates Synaptic Depression, Aβ Deposition, and Cognitive Impairment in an Alzheimer's Disease Model. J Neurosci 2017; 37: 5099–5110.

Bandres-Ciga S, Saez-Atienzar S, Bonet-Ponce L, Billingsley K, Vitale D, Blauwendraat C, et al. The endocytic membrane trafficking pathway plays a major role in the risk of Parkinson's disease. Mov Disord 2019; 34: 460–468.

Baumuratov AS, Antony PMA, Ostaszewski M, He F, Salamanca L, Antunes L, et al. Enteric neurons from Parkinson's disease patients display ex vivo aberrations in mitochondrial structure. Sci Rep 2016; 6: 33117.

Berman DE, Ringe D, Petsko GA, Small SA. The Use of Pharmacological Retromer Chaperones in Alzheimer's Disease and other Endosomal-related Disorders. Neurotherapeutics 2015; 12: 12–18.

Bido S, Soria FN, Fan RZ, Bezard E, Tieu K. Mitochondrial division inhibitor-1 is neuroprotective in the A53T-α-synuclein rat model of Parkinson's disease. Sci Rep 2017; 7: 7495.

Bindoff LA, Birch-Machin M, Cartlidge NEF, Parker WD, Turnbull DM. MITOCHONDRIAL FUNCTION IN PARKINSON'S DISEASE. Lancet 1989; 334: 49.

Bloem BR, Hausdorff JM, Visser JE, Giladi N. Falls and freezing of gait in Parkinson's disease: A review of two interconnected, episodic phenomena. Mov Disord 2004; 19: 871–884.

Bolam JP, Pissadaki EK. Living on the edge with too many mouths to feed: Why dopamine neurons die. Mov Disord 2012; 27: 1478–1483.

Braak H, Bohl JR, Müller CM, Rüb U, de Vos RAI, Del Tredici K. Stanley Fahn Lecture 2005: The staging procedure for the inclusion body pathology associated with sporadic Parkinson's disease reconsidered. Mov Disord 2006; 21: 2042–2051.

Braschi E, Goyon V, Zunino R, Mohanty A, Xu L, McBride HM. Vps35 Mediates Vesicle Transport between the Mitochondria and Peroxisomes. Curr Biol 2010; 20: 1310–1315.

Braschi E, Zunino R, McBride HM. MAPL is a new mitochondrial SUMO E3 ligase that regulates mitochondrial fission. EMBO Rep 2009; 10: 748–754.

Brichta L, Greengard P. Molecular determinants of selective dopaminergic vulnerability in Parkinson's disease: an update [Internet]. Front Neuroanat 2014; 8Available from: http://journal.frontiersin.org/article/10.3389/fnana.2014.00152/abstract

Burbulla LF, Krebiehl G, Krüger R. Balance is the challenge - The impact of mitochondrial dynamics in Parkinson's disease. Eur J Clin Invest 2010; 40: 1048–1060.

Burbulla LF, Song P, Mazzulli JR, Zampese E, Wong YC, Jeon S, et al. Dopamine oxidation mediates mitochondrial and lysosomal dysfunction in Parkinson's disease. Science (80-) 2017; 357: 1255–1261.

Cai B, Xie S, Caplan S, Naslavsky N. GRAF1 forms a complex with MICAL-L1 and EHD1 to cooperate in tubular recycling endosome vesiculation [Internet]. Front Cell Dev Biol 2014; 2Available from: http://journal.frontiersin.org/article/10.3389/fcell.2014.00022/abstract

von Campenhausen S, Bornschein B, Wick R, Bötzel K, Sampaio C, Poewe W, et al. Prevalence and incidence of Parkinson's disease in Europe. Eur Neuropsychopharmacol 2005; 15: 473–490.

Cataldi S, Follett J, Fox JD, Tatarnikov I, Kadgien C, Gustavsson EK, et al. Altered dopamine release and monoamine transporters in Vps35 p.D620N knock-in mice. npj Park Dis 2018; 4: 27.

Cataldo AM, Peterhoff CM, Troncoso JC, Gomez-Isla T, Hyman BT, Nixon RA. Endocytic Pathway Abnormalities Precede Amyloid β Deposition in Sporadic Alzheimer's Disease and Down Syndrome. Am J Pathol 2000; 157: 277–286.

Choy RW-Y, Park M, Temkin P, Herring BE, Marley A, Nicoll RA, et al. Retromer Mediates a Discrete Route of Local Membrane Delivery to Dendrites. Neuron 2014; 82: 55–62.

Chung CY, Khurana V, Yi S, Sahni N, Loh KH, Auluck PK, et al. In Situ Peroxidase Labeling and Mass-Spectrometry Connects Alpha-Synuclein Directly to Endocytic Trafficking and mRNA Metabolism in Neurons. Cell Syst 2017; 4: 242-250.e4.

Cobb MM, Ravisankar A, Skibinski G, Finkbeiner S. iPS cells in the study of PD molecular pathogenesis. Cell Tissue Res 2018; 373: 61–77.

Cuervo AM, Stefanis L, Fredenburg R, Lansbury PT, Sulzer D. Impaired degradation of mutant alpha-synuclein by chaperone-mediated autophagy. Science 2004; 305: 1292–5.

Cui Y, Yang Z, Teasdale RD. The functional roles of retromer in Parkinson's disease. FEBS Lett 2018; 592: 1096–1112.

Dehay B, Ramirez A, Martinez-Vicente M, Perier C, Canron M-H, Doudnikoff E, et al. Loss of P-type ATPase ATP13A2/PARK9 function induces general lysosomal deficiency and leads to Parkinson disease neurodegeneration. Proc Natl Acad Sci 2012; 109: 9611–9616.

Deng H-X, Shi Y, Yang Y, Ahmeti KB, Miller N, Huang C, et al. Identification of TMEM230 mutations in familial Parkinson's disease. Nat Genet 2016; 48: 733–739.

Derivery E, Sousa C, Gautier JJ, Lombard B, Loew D, Gautreau A. The Arp2/3 Activator WASH Controls the Fission of Endosomes through a Large Multiprotein Complex. Dev Cell 2009; 17: 712–723.

Devi L, Raghavendran V, Prabhu BM, Avadhani NG, Anandatheerthavarada HK. Mitochondrial Import and Accumulation of α-Synuclein Impair Complex I in Human Dopaminergic Neuronal Cultures and Parkinson Disease Brain. J Biol Chem 2008; 283: 9089–9100.

Dodson MW, Zhang T, Jiang C, Chen S, Guo M. Roles of the Drosophila LRRK2 homolog in Rab7-dependent lysosomal positioning. Hum Mol Genet 2012; 21: 1350–1363.

Dorsey ER, Elbaz A, Nichols E, Abd-Allah F, Abdelalim A, Adsuar JC, et al. Global, regional, and national burden of Parkinson's disease, 1990–2016: a systematic analysis for the Global Burden of Disease Study 2016. Lancet Neurol 2018; 17: 939–953.

Ebrahimi-Fakhari D, Cantuti-Castelvetri I, Fan Z, Rockenstein E, Masliah E, Hyman BT, et al. Distinct Roles In Vivo for the Ubiquitin-Proteasome System and the Autophagy-Lysosomal Pathway in the Degradation of -Synuclein. J Neurosci 2011; 31: 14508–14520.

Edvardson S, Cinnamon Y, Ta-Shma A, Shaag A, Yim YI, Zenvirt S, et al. A deleterious mutation in DNAJC6 encoding the neuronal-specific clathrin-uncoating Co-chaperone auxilin, is associated with juvenile parkinsonism. PLoS One 2012; 7: e36458.

Fjorback AW, Seaman M, Gustafsen C, Mehmedbasic A, Gokool S, Wu C, et al. Retromer Binds the FANSHY Sorting Motif in SorLA to Regulate Amyloid Precursor Protein Sorting and Processing. J Neurosci 2012; 32: 1467–1480.

Follett J, Norwood SJ, Hamilton NA, Mohan M, Kovtun O, Tay S, et al. The Vps35 D620N Mutation Linked to Parkinson's Disease Disrupts the Cargo Sorting Function of Retromer.

Traffic 2014; 15: 230–244.

Freeman CL, Hesketh G, Seaman MNJ. RME-8 coordinates the activity of the WASH complex with the function of the retromer SNX dimer to control endosomal tubulation. J Cell Sci 2014; 127: 2053–2070.

Friedman JR, Lackner LL, West M, DiBenedetto JR, Nunnari J, Voeltz GK. ER Tubules Mark Sites of Mitochondrial Division. Science (80-) 2011; 334: 358–362.

Gómez-Suaga P, Rivero-Ríos P, Fdez E, Blanca Ramírez M, Ferrer I, Aiastui A, et al. LRRK2 delays degradative receptor trafficking by impeding late endosomal budding through decreasing Rab7 activity. Hum Mol Genet 2014; 23: 6779–6796.

Griffin CT, Trejo J, Magnuson T. Genetic evidence for a mammalian retromer complex containing sorting nexins 1 and 2. Proc Natl Acad Sci 2005; 102: 15173–15177.

Grossmann D, Berenguer-Escuder C, Bellet ME, Scheibner D, Bohler J, Massart F, et al. Mutations in RHOT1 disrupt ER-mitochondria contact sites interfering with calcium homeostasis and mitochondrial dynamics in Parkinson's disease. Antioxid Redox Signal 2019: ars.2018.7718.

Grünewald A, Kumar KR, Sue CM. New insights into the complex role of mitochondria in Parkinson's disease. Prog Neurobiol 2019; 177: 73–93.

Guardia-Laguarta C, Area-Gomez E, Rub C, Liu Y, Magrane J, Becker D, et al. -Synuclein Is Localized to Mitochondria-Associated ER Membranes. J Neurosci 2014; 34: 249–259.

Gustavsson EK, Trinh J, Guella I, Vilariño-Güell C, Appel-Cresswell S, Stoessl AJ, et al. DNAJC13 genetic variants in parkinsonism. Mov Disord 2015; 30: 273–278.

Henry AG, Aghamohammadzadeh S, Samaroo H, Chen Y, Mou K, Needle E, et al. Pathogenic LRRK2 mutations, through increased kinase activity, produce enlarged lysosomes with reduced degradative capacity and increase ATP13A2 expression. Hum Mol Genet 2015; 24: 6013–6028.

Hsieh CH, Shaltouki A, Gonzalez AE, Bettencourt da Cruz A, Burbulla LF, St. Lawrence E, et al. Functional Impairment in Miro Degradation and Mitophagy Is a Shared Feature in Familial and Sporadic Parkinson's Disease. Cell Stem Cell 2016; 19: 709–724.

Hu F, Padukkavidana T, Vægter CB, Brady OA, Zheng Y, Mackenzie IR, et al. Sortilin-

Mediated Endocytosis Determines Levels of the Frontotemporal Dementia Protein, Progranulin. Neuron 2010; 68: 654–667.

Hughes AJ, Daniel SE, Blankson S, Lees AJ. A clinicopathologic study of 100 cases of Parkinson's disease. Arch Neurol 1993; 50: 140–8.

Inoshita T, Arano T, Hosaka Y, Meng H, Umezaki Y, Kosugi S, et al. Vps35 in cooperation with LRRK2 regulates synaptic vesicle endocytosis through the endosomal pathway in Drosophila. Hum Mol Genet 2017; 26: 2933–2948.

Ishizu N, Yui D, Hebisawa A, Aizawa H, Cui W, Fujita Y, et al. Impaired striatal dopamine release in homozygous Vps35 D620N knock-in mice. Hum Mol Genet 2016: ddw279.

Jackson-Lewis V, Blesa J, Przedborski S. Animal models of Parkinson's disease. Parkinsonism Relat Disord 2012; 18 Suppl 1: S183-5.

Jankovic J. Parkinson's disease: clinical features and diagnosis. J Neurol Neurosurg Psychiatry 2008; 79: 368–376.

Jiang H, Ren Y, Yuen EY, Zhong P, Ghaedi M, Hu Z, et al. Parkin controls dopamine utilization in human midbrain dopaminergic neurons derived from induced pluripotent stem cells. Nat Commun 2012; 3: 668.

Kamp F, Exner N, Lutz AK, Wender N, Hegermann J, Brunner B, et al. Inhibition of mitochondrial fusion by α-synuclein is rescued by PINK1, Parkin and DJ-1. EMBO J 2010; 29: 3571–3589.

Kisos H, Ben-Gedalya T, Sharon R. The Clathrin-Dependent Localization of Dopamine Transporter to Surface Membranes Is Affected by α-Synuclein. J Mol Neurosci 2014; 52: 167–176.

Krebiehl G, Ruckerbauer S, Burbulla LF, Kieper N, Maurer B, Waak J, et al. Reduced basal autophagy and impaired mitochondrial dynamics due to loss of Parkinson's disease-associated protein DJ-1. PLoS One 2010; 5: e9367.

Krebs CE, Karkheiran S, Powell JC, Cao M, Makarov V, Darvish H, et al. The sac1 domain of SYNJ1 identified mutated in a family with early-onset progressive parkinsonism with generalized seizures. Hum Mutat 2013; 34: 1200–1207.

Krüger R, Klucken J, Weiss D, Tönges L, Kolber P, Unterecker S, et al. Classification of

advanced stages of Parkinson's disease: translation into stratified treatments. J Neural Transm 2017; 124: 1015–1027.

Langston JW, Ballard P, Tetrud JW, Irwin I. Chronic Parkinsonism in humans due to a product of meperidine-analog synthesis. Science 1983; 219: 979–80.

Larsen SB, Hanss Z, Krüger R. The genetic architecture of mitochondrial dysfunction in Parkinson's disease. Cell Tissue Res 2018; 373: 21–37.

Lautenschläger J, Kaminski CF, Kaminski Schierle GS. α-Synuclein – Regulator of Exocytosis, Endocytosis, or Both? Trends Cell Biol 2017; 27: 468–479.

Lesage S, Condroyer C, Klebe S, Honore A, Tison F, Brefel-Courbon C, et al. Identification of VPS35 mutations replicated in French families with Parkinson disease. Neurology 2012; 78: 1449–1450.

Li J-G, Chiu J, Praticò D. Full recovery of the Alzheimer's disease phenotype by gain of function of vacuolar protein sorting 35 [Internet]. Mol Psychiatry 2019Available from: http://www.nature.com/articles/s41380-019-0364-x

Linhart R, Wong S, Cao J, Tran M, Huynh A, Ardrey C, et al. Vacuolar protein sorting 35 (Vps35) rescues locomotor deficits and shortened lifespan in Drosophila expressing a Parkinson's disease mutant of Leucine-rich repeat kinase 2 (LRRK2). Mol Neurodegener 2014; 9: 23.

Little D, Luft C, Mosaku O, Lorvellec M, Yao Z, Paillusson S, et al. A single cell high content assay detects mitochondrial dysfunction in iPSC-derived neurons with mutations in SNCA. Sci Rep 2018; 8: 9033.

Lozza C, Marié R-M, Baron J-C. The metabolic substrates of bradykinesia and tremor in uncomplicated Parkinson's disease. Neuroimage 2002; 17: 688–99.

Macht M, Kaussner Y, Möller JC, Stiasny-Kolster K, Eggert KM, Krüger H-P, et al. Predictors of freezing in Parkinson's disease: A survey of 6,620 patients. Mov Disord 2007; 22: 953–956.

Di Maio R, Barrett PJ, Hoffman EK, Barrett CW, Zharikov A, Borah A, et al. α-Synuclein binds to TOM20 and inhibits mitochondrial protein import in Parkinson's disease. Sci Transl Med 2016; 8: 342ra78-342ra78.

Martinez-Vicente M, Talloczy Z, Kaushik S, Massey AC, Mazzulli J, Mosharov E V., et al. Dopamine-modified α-synuclein blocks chaperone-mediated autophagy [Internet]. J Clin Invest 2008Available from: http://content.the-jci.org/articles/view/32806

Martinez A, Lectez B, Ramirez J, Popp O, Sutherland JD, Urbé S, et al. Quantitative proteomic analysis of Parkin substrates in Drosophila neurons. Mol Neurodegener 2017; 12: 29.

Mazzulli JR, Xu YH, Sun Y, Knight AL, McLean PJ, Caldwell GA, et al. Gaucher disease glucocerebrosidase and α-synuclein form a bidirectional pathogenic loop in synucleinopathies. Cell 2011; 146: 37–52.

Mazzulli JR, Zunke F, Isacson O, Studer L, Krainc D. α-Synuclein–induced lysosomal dysfunction occurs through disruptions in protein trafficking in human midbrain synucleinopathy models. Proc Natl Acad Sci 2016; 113: 1931–1936.

McGough IJ, Steinberg F, Jia D, Barbuti PA, McMillan KJ, Heesom KJ, et al. Retromer Binding to FAM21 and the WASH Complex Is Perturbed by the Parkinson Disease-Linked VPS35(D620N) Mutation. Curr Biol 2014; 24: 1670–1676.

Mecozzi VJ, Berman DE, Simoes S, Vetanovetz C, Awal MR, Patel VM, et al. Pharmacological chaperones stabilize retromer to limit APP processing. Nat Chem Biol 2014; 10: 443–449.

Mir R, Tonelli F, Lis P, Macartney T, Polinski NK, Martinez TN, et al. The Parkinson's disease VPS35[D620N] mutation enhances LRRK2-mediated Rab protein phosphorylation in mouse and human. Biochem J 2018; 475: 1861–1883.

Mohan M, Mellick GD. Role of the VPS35 D620N mutation in Parkinson's disease. Parkinsonism Relat Disord 2017; 36: 10–18.

Moisoi N, Klupsch K, Fedele V, East P, Sharma S, Renton A, et al. Mitochondrial dysfunction triggered by loss of HtrA2 results in the activation of a brain-specific transcriptional stress response. Cell Death Differ 2009; 16: 449–464.

Munsie LN, Milnerwood AJ, Seibler P, Beccano-Kelly DA, Tatarnikov I, Khinda J, et al. Retromer-dependent neurotransmitter receptor trafficking to synapses is altered by the Parkinson's disease VPS35 mutation p.D620N. Hum Mol Genet 2015; 24: 1691–1703.

Murphy KE, Gysbers AM, Abbott SK, Tayebi N, Kim WS, Sidransky E, et al. Reduced

glucocerebrosidase is associated with increased α-synuclein in sporadic Parkinson's disease. Brain 2014; 137: 834–848.

Narendra D, Tanaka A, Suen DF, Youle RJ. Parkin is recruited selectively to impaired mitochondria and promotes their autophagy. J Cell Biol 2008; 183: 795–803.

Nguyen M, Krainc D. LRRK2 phosphorylation of auxilin mediates synaptic defects in dopaminergic neurons from patients with Parkinson's disease. Proc Natl Acad Sci 2018; 115: 5576–5581.

Nicklas WJ, Vyas I, Heikkila RE. Inhibition of NADH-linked oxidation in brain mitochondria by 1-methyl-4-phenyl-pyridine, a metabolite of the neurotoxin, 1-methyl-4-phenyl-1,2,5,6-tetrahydropyridine. Life Sci 1985; 36: 2503–2508.

Niu J, Yu M, Wang C, Xu Z. Leucine-rich repeat kinase 2 disturbs mitochondrial dynamics via Dynamin-like protein. J Neurochem 2012; 122: 650–658.

Norris A, Tammineni P, Wang S, Gerdes J, Murr A, Kwan KY, et al. SNX-1 and RME-8 oppose the assembly of HGRS-1/ESCRT-0 degradative microdomains on endosomes. Proc Natl Acad Sci 2017; 114: E307–E316.

Orenstein SJ, Kuo S-H, Tasset I, Arias E, Koga H, Fernandez-Carasa I, et al. Interplay of LRRK2 with chaperone-mediated autophagy. Nat Neurosci 2013; 16: 394–406.

Parihar MS, Parihar A, Fujita M, Hashimoto M, Ghafourifar P. Mitochondrial association of alpha-synuclein causes oxidative stress. Cell Mol Life Sci 2008; 65: 1272–1284.

Polymeropoulos MH, Lavedan C, Leroy E, Ide SE, Dehejia A, Dutra A, et al. Mutation in the alpha-synuclein gene identified in families with Parkinson's disease. Science 1997; 276: 2045–7.

Priya A, Kalaidzidis I V, Kalaidzidis Y, Lambright D, Datta S. Molecular Insights into Rab7-Mediated Endosomal Recruitment of Core Retromer: Deciphering the Role of Vps26 and Vps35. Traffic 2015; 16: 68–84.

Qiao L, Hamamichi S, Caldwell KA, Caldwell GA, Yacoubian TA, Wilson S, et al. Lysosomal enzyme cathepsin D protects against alpha-synuclein aggregation and toxicity. Mol Brain 2008; 1: 17.

Quadri M, Fang M, Picillo M, Olgiati S, Breedveld GJ, Graafland J, et al. Mutation in the

SYNJ1 gene associated with autosomal recessive, early-onset parkinsonism. Hum Mutat 2013; 34: 1208–1215.

Quinlan CL, Perevoshchikova I V., Hey-Mogensen M, Orr AL, Brand MD. Sites of reactive oxygen species generation by mitochondria oxidizing different substrates. Redox Biol 2013; 1: 304–312.

Rahman AA, Morrison BE. Contributions of VPS35 Mutations to Parkinson's Disease. Neuroscience 2019; 401: 1–10.

Ramonet D, Daher JPL, Lin BM, Stafa K, Kim J, Banerjee R, et al. Dopaminergic Neuronal Loss, Reduced Neurite Complexity and Autophagic Abnormalities in Transgenic Mice Expressing G2019S Mutant LRRK2. PLoS One 2011; 6: e18568.

Reinhardt P, Glatza M, Hemmer K, Tsytsyura Y, Thiel CS, Höing S, et al. Derivation and Expansion Using Only Small Molecules of Human Neural Progenitors for Neurodegenerative Disease Modeling. PLoS One 2013; 8: e59252.

Del Rey NL-G, Quiroga-Varela A, Garbayo E, Carballo-Carbajal I, Fernández-Santiago R, Monje MHG, et al. Advances in Parkinson's Disease: 200 Years Later [Internet]. Front Neuroanat 2018; 12Available from: https://www.frontiersin.org/article/10.3389/fnana.2018.00113/full

Rojas R, van Vlijmen T, Mardones GA, Prabhu Y, Rojas AL, Mohammed S, et al. Regulation of retromer recruitment to endosomes by sequential action of Rab5 and Rab7. J Cell Biol 2008; 183: 513–526.

Ryan BJ, Hoek S, Fon EA, Wade-Martins R. Mitochondrial dysfunction and mitophagy in Parkinson's: from familial to sporadic disease. Trends Biochem Sci 2015; 40: 200–210.

Sánchez-Danés A, Richaud-Patin Y, Carballo-Carbajal I, Jiménez-Delgado S, Caig C, Mora S, et al. Disease-specific phenotypes in dopamine neurons from human iPS-based models of genetic and sporadic Parkinson's disease. EMBO Mol Med 2012; 4: 380–395.

Schapira AHV, Chaudhuri KR, Jenner P. Non-motor features of Parkinson disease. Nat Rev Neurosci 2017; 18: 435–450.

Seaman MNJ, Michael McCaffery J, Emr SD. A Membrane Coat Complex Essential for Endosome-to-Golgi Retrograde Transport in Yeast. J Cell Biol 1998; 142: 665–681.

Sidransky E, Nalls MA, Aasly JO, Aharon-Peretz J, Annesi G, Barbosa ER, et al. Multicenter Analysis of Glucocerebrosidase Mutations in Parkinson's Disease. N Engl J Med 2009; 361: 1651–1661.

Small SA, Kent K, Pierce A, Leung C, Kang MS, Okada H, et al. Model-guided microarray implicates the retromer complex in Alzheimer's disease. Ann Neurol 2005; 58: 909–919.

Song P, Trajkovic K, Tsunemi T, Krainc D. Parkin Modulates Endosomal Organization and Function of the Endo-Lysosomal Pathway. J Neurosci 2016; 36: 2425–2437.

Soubannier V, McLelland GL, Zunino R, Braschi E, Rippstein P, Fon EA, et al. A vesicular transport pathway shuttles cargo from mitochondria to lysosomes. Curr Biol 2012; 22: 135–141.

Soukup S-F, Kuenen S, Vanhauwaert R, Manetsberger J, Hernández-Díaz S, Swerts J, et al. A LRRK2-Dependent EndophilinA Phosphoswitch Is Critical for Macroautophagy at Presynaptic Terminals. Neuron 2016; 92: 829–844.

Stamey W, Davidson A, Jankovic J. Shoulder Pain. JCR J Clin Rheumatol 2008; 14: 253–254.

Storch A, Hwang Y-I, Gearhart DA, Beach JW, Neafsey EJ, Collins MA, et al. Dopamine transporter-mediated cytotoxicity of beta-carbolinium derivatives related to Parkinson's disease: relationship to transporter-dependent uptake. J Neurochem 2004; 89: 685–694.

Strauss KM, Martins LM, Plun-Favreau H, Marx FP, Kautzmann S, Berg D, et al. Loss of function mutations in the gene encoding Omi/HtrA2 in Parkinson's disease. Hum Mol Genet 2005; 14: 2099–2111.

Su Y-C, Qi X. Inhibition of excessive mitochondrial fission reduced aberrant autophagy and neuronal damage caused by LRRK2 G2019S mutation. Hum Mol Genet 2013; 22: 4545–4561.

Surmeier DJ, Sulzer D. The pathology roadmap in Parkinson disease. Prion 2013; 7: 85–91.

Tang F-L, Erion JR, Tian Y, Liu W, Yin D-M, Ye J, et al. VPS35 in Dopamine Neurons Is Required for Endosome-to-Golgi Retrieval of Lamp2a, a Receptor of Chaperone-Mediated Autophagy That Is Critical for -Synuclein Degradation and Prevention of Pathogenesis of Parkinson's Disease. J Neurosci 2015; 35: 10613–10628.

Tang F-L, Liu W, Hu J-X, Erion JR, Ye J, Mei L, et al. VPS35 Deficiency or Mutation Causes Dopaminergic Neuronal Loss by Impairing Mitochondrial Fusion and Function. Cell Rep 2015; 12: 1631–1643.

Tang FL, Liu W, Hu JX, Erion JR, Ye J, Mei L, et al. VPS35 Deficiency or Mutation Causes Dopaminergic Neuronal Loss by Impairing Mitochondrial Fusion and Function. Cell Rep 2015; 12: 1631–1643.

Tanik SA, Schultheiss CE, Volpicelli-Daley LA, Brunden KR, Lee VMY. Lewy Body-like α-Synuclein Aggregates Resist Degradation and Impair Macroautophagy. J Biol Chem 2013; 288: 15194–15210.

Temkin P, Lauffer B, Jäger S, Cimermancic P, Krogan NJ, von Zastrow M. SNX27 mediates retromer tubule entry and endosome-to-plasma membrane trafficking of signalling receptors. Nat Cell Biol 2011; 13: 715–721.

Temkin P, Morishita W, Goswami D, Arendt K, Chen L, Malenka R. The Retromer Supports AMPA Receptor Trafficking During LTP. Neuron 2017; 94: 74-82.e5.

Tokarev AA, Alfonso A, Segev N. Overview of Intracellular Compartments and Trafficking Pathways. In: Trafficking Inside Cells. New York, NY: Springer New York; 2009. p. 3–14

Tsika E, Glauser L, Moser R, Fiser A, Daniel G, Sheerin U-M, et al. Parkinson's disease-linked mutations in VPS35 induce dopaminergic neurodegeneration. Hum Mol Genet 2014; 23: 4621–4638.

Unal Gulsuner H, Gulsuner S, Mercan FN, Onat OE, Walsh T, Shahin H, et al. Mitochondrial serine protease HTRA2 p.G399S in a kindred with essential tremor and Parkinson disease. Proc Natl Acad Sci 2014; 111: 18285–18290.

Usenovic M, Tresse E, Mazzulli JR, Taylor JP, Krainc D. Deficiency of ATP13A2 Leads to Lysosomal Dysfunction, -Synuclein Accumulation, and Neurotoxicity. J Neurosci 2012; 32: 4240–4246.

Vagnozzi AN, Praticò D. Endosomal sorting and trafficking, the retromer complex and neurodegeneration. Mol Psychiatry 2019; 24: 857–868.

Vardarajan BN, Bruesegem SY, Harbour ME, George-Hyslop P St., Seaman MNJ, Farrer LA. Identification of Alzheimer disease-associated variants in genes that regulate retromer function. Neurobiol Aging 2012; 33: 2231.e15-2231.e30.

Vargas KJ, Makani S, Davis T, Westphal CH, Castillo PE, Chandra SS. Synucleins Regulate the Kinetics of Synaptic Vesicle Endocytosis. J Neurosci 2014; 34: 9364–9376.

Vidyadhara DJ, Lee JE, Chandra SS. Role of the Endolysosomal System in Parkinson's disease. J Neurochem 2019: jnc.14820.

Vilariño-Güell C, Rajput A, Milnerwood AJ, Shah B, Szu-Tu C, Trinh J, et al. DNAJC13 mutations in Parkinson disease. Hum Mol Genet 2014; 23: 1794–1801.

Vilariño-Güell C, Wider C, Ross OA, Dachsel JC, Kachergus JM, Lincoln SJ, et al. VPS35 Mutations in Parkinson Disease. Am J Hum Genet 2011; 89: 162–167.

Walter J, Bolognin S, Antony PMA, Nickels SL, Poovathingal SK, Salamanca L, et al. Neural Stem Cells of Parkinson's Disease Patients Exhibit Aberrant Mitochondrial Morphology and Functionality. Stem Cell Reports 2019; 12: 878–889.

Wang C, Niu M, Zhou Z, Zheng X, Zhang L, Tian Y, et al. VPS35 regulates cell surface recycling and signaling of dopamine receptor D1. Neurobiol Aging 2016; 46: 22–31.

Wang H, Toh J, Ho P, Tio M, Zhao Y, Tan E-K. In vivo evidence of pathogenicity of VPS35 mutations in the Drosophila. Mol Brain 2014; 7: 73.

Wang W, Ma X, Zhou L, Liu J, Zhu X. A conserved retromer sorting motif is essential for mitochondrial DLP1 recycling by VPS35 in Parkinson's disease model. Hum Mol Genet 2016: ddw430.

Wang W, Wang X, Fujioka H, Hoppel C, Whone AL, Caldwell MA, et al. Parkinson's disease–associated mutant VPS35 causes mitochondrial dysfunction by recycling DLP1 complexes. Nat Med 2015; 22: 54–63.

Wang W, Wang X, Fujioka H, Hoppel C, Whone AL, Caldwell MA, et al. Parkinson's disease–associated mutant VPS35 causes mitochondrial dysfunction by recycling DLP1 complexes. Nat Med 2016; 22: 54–63.

Wauters F, Cornelissen T, Imberechts D, Martin S, Koentjoro B, Sue C, et al. LRRK2 mutations impair depolarization-induced mitophagy through inhibition of mitochondrial accumulation of RAB10. Autophagy 2019: 1–20.

Wen L, Tang F-L, Hong Y, Luo S-W, Wang C-L, He W, et al. VPS35 haploinsufficiency increases Alzheimer's disease neuropathology. J Cell Biol 2011; 195: 765–779.

Weykopf B, Haupt S, Jungverdorben J, Flitsch LJ, Hebisch M, Liu G-H, et al. Induced pluripotent stem cell-based modeling of mutant LRRK2-associated Parkinson's disease. Eur J Neurosci 2019; 49: 561–589.

Williams ET, Chen X, Moore DJ. VPS35, the Retromer Complex and Parkinson's Disease. J Parkinsons Dis 2017; 7: 219–233.

Williams ET, Glauser L, Tsika E, Jiang H, Islam S, Moore DJ. Parkin mediates the ubiquitination of VPS35 and modulates retromer-dependent endosomal sorting. Hum Mol Genet 2018; 27: 3189–3205.

Winslow AR, Chen C-W, Corrochano S, Acevedo-Arozena A, Gordon DE, Peden AA, et al. α-Synuclein impairs macroautophagy: implications for Parkinson's disease. J Cell Biol 2010; 190: 1023–1037.

Wu S, Fagan RR, Uttamapinant C, Lifshitz LM, Fogarty KE, Ting AY, et al. The Dopamine Transporter Recycles via a Retromer-Dependent Postendocytic Mechanism: Tracking Studies Using a Novel Fluorophore-Coupling Approach. J Neurosci 2017; 37: 9438–9452.

Xiong Y, Neifert S, Karuppagounder SS, Liu Q, Stankowski JN, Lee BD, et al. Robust kinase- and age-dependent dopaminergic and norepinephrine neurodegeneration in LRRK2 G2019S transgenic mice. Proc Natl Acad Sci 2018; 115: 1635–1640.

Yim Y-I, Sun T, Wu L-G, Raimondi A, De Camilli P, Eisenberg E, et al. Endocytosis and clathrin-uncoating defects at synapses of auxilin knockout mice. Proc Natl Acad Sci 2010; 107: 4412–4417.

Youle RJ, van der Bliek AM. Mitochondrial Fission, Fusion, and Stress. Science (80-) 2012; 337: 1062–1065.

Zambon F, Cherubini M, Fernandes HJR, Lang C, Ryan BJ, Volpato V, et al. Cellular α-synuclein pathology is associated with bioenergetic dysfunction in Parkinson's iPSC-derived dopamine neurons. Hum Mol Genet 2019; 28: 2001–2013.

Zavodszky E, Seaman MNJ, Moreau K, Jimenez-Sanchez M, Breusegem SY, Harbour ME, et al. Mutation in VPS35 associated with Parkinson's disease impairs WASH complex association and inhibits autophagy. Nat Commun 2014; 5: 3828.

Zhou L, Wang W, Hoppel C, Liu J, Zhu X. Parkinson's disease-associated pathogenic VPS35 mutation causes complex I deficits. Biochim Biophys Acta - Mol Basis Dis 2017; 1863: 2791–

2795.

Zimprich A, Benet-Pagès A, Struhal W, Graf E, Eck SH, Offman MN, et al. A mutation in VPS35, encoding a subunit of the retromer complex, causes late-onset parkinson disease. Am J Hum Genet 2011; 89: 168–175.

Zimprich A, Benet-Pagès A, Struhal W, Graf E, Eck SH, Offman MN, et al. A Mutation in VPS35, Encoding a Subunit of the Retromer Complex, Causes Late-Onset Parkinson Disease. Am J Hum Genet 2011; 89: 168–175.

6. Appendices

6.1. Preliminary phenotyping in patient-derived fibroblasts

Mitochondrial impairment has previously been showed in primary neuronal cultures and cell lines either overexpression p.D620N mutant or downregulating VPS35, as well as in patient-derived fibroblasts, reviewed in (Larsen *et al.*, 2018). Indeed, mitochondrial network was found to be fragmented and display a decreased MMP. Here, we investigated whether these findings could be replicated those results in our patient-derived fibroblasts.

Mitochondrial morphology was assessed by live cell imaging using MMP independent Mitotracker TM deep red (Thermo Fisher Scientific). Fibroblasts were cultured in DMEM supplemented with 1% Pen/Strep only for 4 hrs prior to the acquisition in a humidified chamber at 37°C and 5% CO_2. Z-stack images were acquired to allow a 3D analysis of mitochondrial network. Mitochondrial morphology was analysed with the same automated Matlab script used in the manuscript II, developed in house by Paul Antony. Briefly, a difference of Gaussian of convoluted foreground and background images was used for detecting all mitochondria in the field. Previews of mitochondrial mask of each image was saved as an image and all previews were checked by eye for quality control.
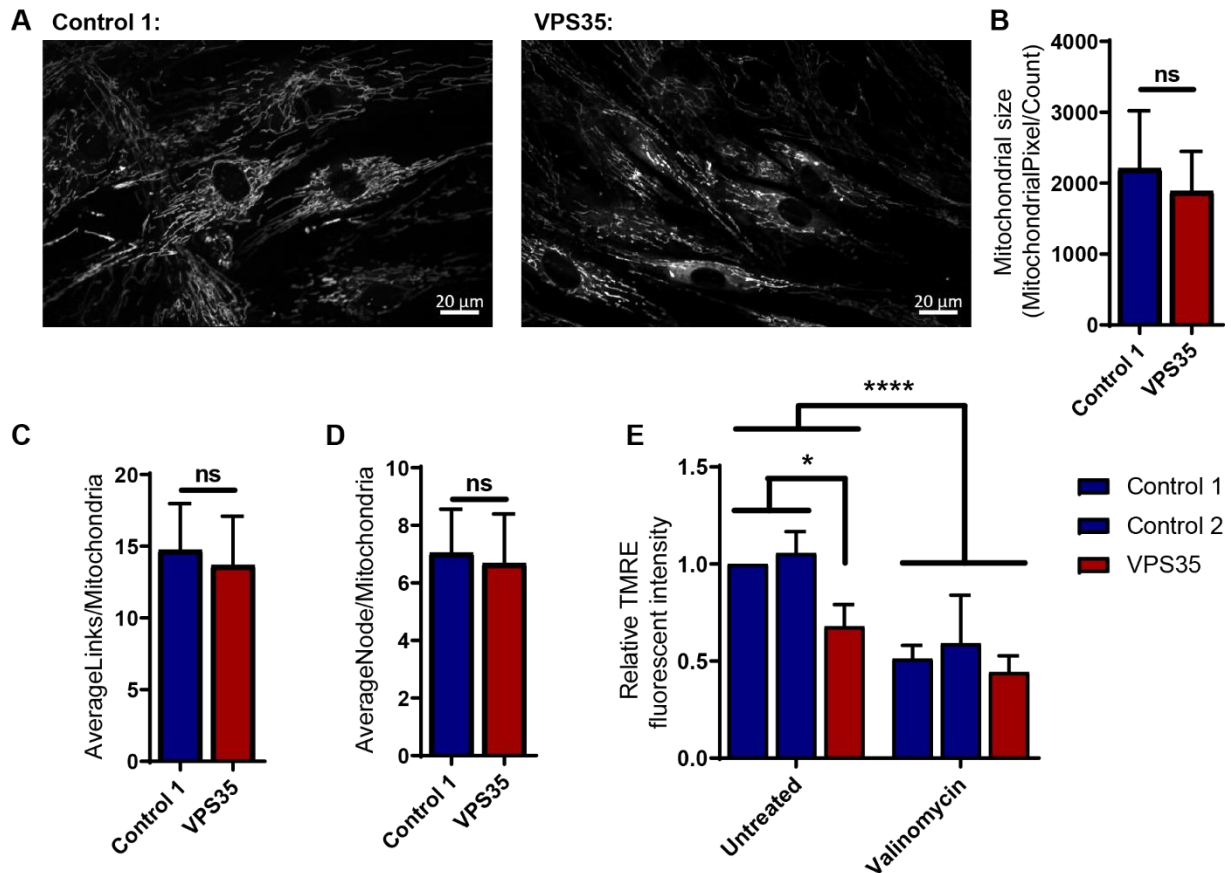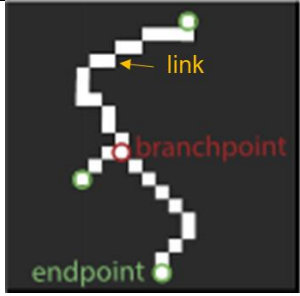
Figure S1: Patient fibroblasts have depolarised mitochondria with no morphological change. (**A**) Live cell imaging show mitochondrial labelled with Mitotracker Red, MMP independent. Mitochondrial size (**B**), average links per mitochondrion (**C**) and average nodes per mitochondrion (**D**) were calculated from four independent passages of Control 1 and patient VPS35 fibroblasts grown in DMEM + 1% Pen/Strep only for 4 hrs. (**E**) Mitochondrial membrane potential measured by TMRE mean fluorescence intensity from four independent passages of Control 1, Control 2 and VPS35 fibroblasts grown in DMEM + 1% Pen/Strep only for 4 hrs with or without 250 nM of Valinomycin. All statistical tests were Mann-Whitney tests to compare groups and One-way Anova followed by Sidak's multiple comparisons tests to compare groups and conditions. Error bars show standard deviation and ns $p>0.05$; * $p< 0.05$; *** $p<0.001$.

The parameters (Table S1) of each image were automatically calculated with the script and data was plotted and analysed using GraphPad Prism.

Table S1: Calculated parameters of automated mitochondrial network analysis (adapted from (Baumuratov *et al.*, 2016)).

Parameter	Definition	Pictogram
Mitochondrial size	Mitochondrial total surface by mitochondrial count	
Average Nodes per mitochondrion	Average number of nodes (branchpoint + endpoint) per mitochondrium	
Average Links per mitochondrion	Average number of links per mitochondrion	

We found no difference in mitochondrial size between patient-derived fibroblasts and control in baseline conditions (**Fig. S1B**). Furthermore, mitochondrial network was also shown to be unchanged with no differences in the average number of nodes and links per mitochondrion (**Fig. S1C, D**).

MMP was measured using TMRE (Thermo Fisher Scientific) staining, normalised to mitochondrial mass with MMP-independent Mitotracker TM Green (Thermo Fisher Scientific) by flow cytometry. Fibroblasts were grown in DMEM supplemented with 1% Pen/Strep only during 4 hrs with or without 250 nM Valinomycin treatment, which serves as positive control. 200 000 fibroblasts were stained and the mean TMRE fluorescence intensity was measured in 10 000 living fibroblasts (DAPI negative). The mean TMRE fluorescence intensity was normalised to the mean Mitotracker Green intensity representing mitochondrial mass.

Here, we found that patient-derived fibroblasts had significantly decreased MMP compared to age- and gender-matched healthy controls (**Fig. S1E**).

6.2. Preliminary phenotyping in patient-derived smNPCs

We used smNPCs for further analysis of phenotypic differences between the patient-derived cells and controls. Indeed, smNPCs have many advantages as they are mitotic cells that can be grown in high quantities and fast. Although it is a progenitor cell, smNPCs are already

specified toward a neuronal lineage, which is a more disease-specific model than dermal fibroblasts. All of this make smNPCs a good model for high throughput PD modelling.

First, we wanted to see whether the mitochondrial phenotype seen in dermal fibroblasts could be replicated in smNPCs. We did not analyse mitochondrial morphology as smNPCs have very little cytoplasm. Still, we measured MMP using TMRE (Thermo Fisher Scientific) staining, normalised to mitochondrial mass with MMP-independent Mitotracker TM Green (Thermo Fisher Scientific) by flow cytometry. smNPCs were grown in smNPC N2 medium, without antioxidants for 4 hrs prior to the experiment treated with or without 20 nM of Valinomycin (positive control). 200 000 smNPCs were stained and the mean TMRE fluorescence intensity was measured in 10 000 living smNPCs (DAPI negative). The mean TMRE fluorescence intensity was normalised to the mean Mitotracker Green intensity representing mitochondrial mass.
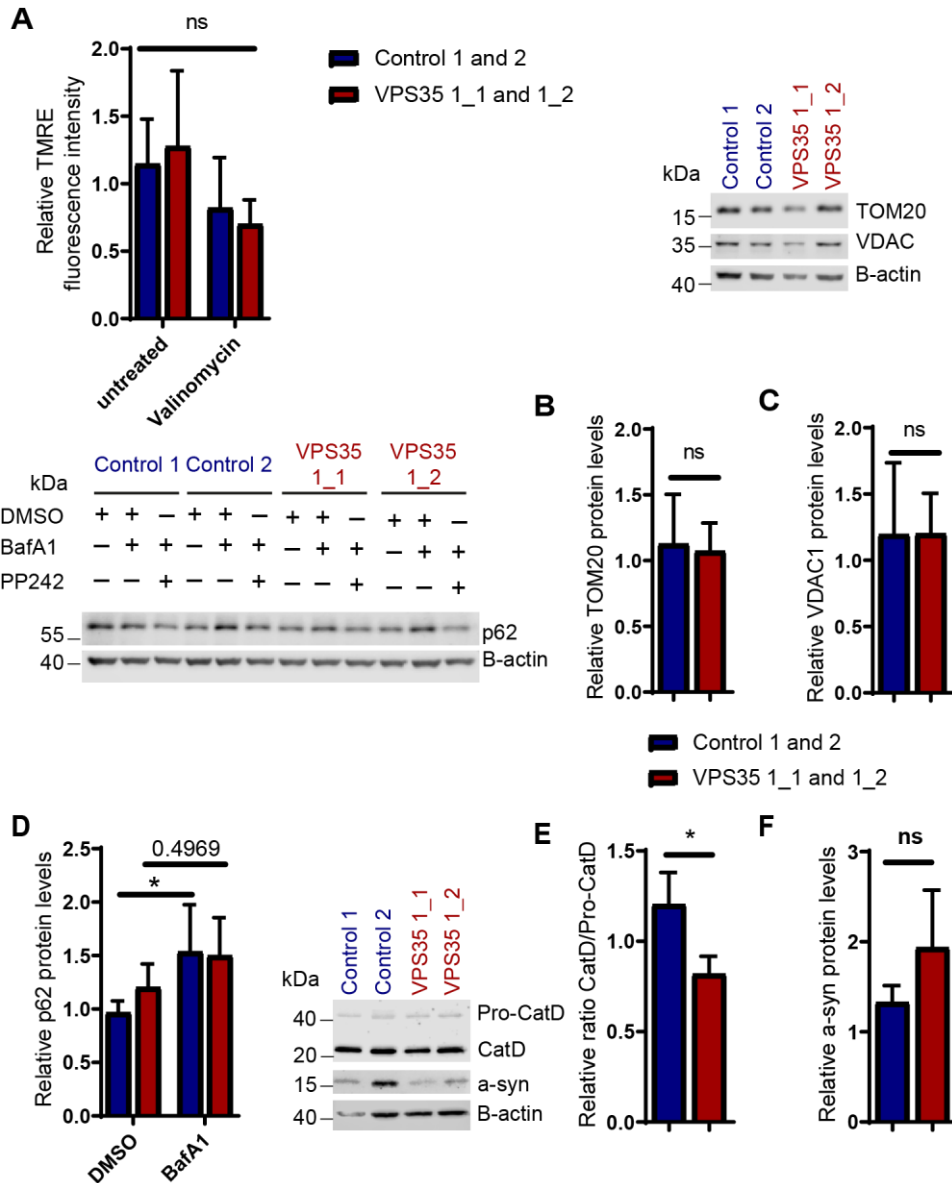
Figure S2: Patient-derived smNPCs display no difference in MMP, mitochondrial mass and α-synuclein level but impaired autophagic flux. (**A**) Mitochondrial membrane potential measured by TMRE mean fluorescence intensity from two independent passages of Control 1 and 2 and VPS35 1_1 and 1_2 smNPCs grown in smNPC N2 medium for 4 hrs with or without 20 nM of Valinomycin. (**B, C**) Western blot analysis of TOM20 (**A**), VDAC (**B**) and β-actin (loading control) from three independent passages of control (Control 1 and 2) and VPS35 D620N mutant (VPS35 clones 1_1 and 1_2) smNPCs under basal culture condition. (**D**) Western blot analysis of p62 and β-actin (loading control) from four independent passages of control (Control 1 and 2) and VPS35 D620N mutant (VPS35 clones 1_1 and 1_2) smNPCs under basal culture condition and Bafilomycin A1 (BafA1) 20 nM treatment for 24 hrs. (E) Western blot analysis of α-synuclein (α-syn) and β-actin (loading control) from four independent passages of control (Control 1 and 2) and VPS35 D620N mutant (VPS35 clones 1_1 and 1_2) smNPCs under basal culture condition. All statistical tests were Mann-Whitney tests to compare groups and One-way Anova followed by Sidak's multiple comparisons tests to compare groups and conditions. Error bars show standard deviation and ns p>0.05; * p< 0.05.

We found that upon Valinomycin treatment, MMP decreased, as expected in both controls and patient-derived smNPCs (**Fig. S2A**). No difference was measured between controls and patient-derived smNPCs. Mitochondrial mass, measured by TOM20 and VDAC1 protein level, was also found to be unchanged between patient and controls smNPCs (**Fig. S2B and C**).

The link between the retromer and macroautophagy has been found by the sorting of ATG9, an important protein for the induction of autophagy (Popovic and Dikic, 2014). Additionally, in cells overexpressing the mutant VPS35 p.D620N, ATG9 was missorted which leads to impaired autophagy (Zavodszky et al., 2014). Here, we measured the steady state level of the autophagy protein p62 (**Fig. S2D**) which was not different between patient and controls. We treated the smNPCs for 24 hrs with 20 nM Bafilomycin A1 to block the fusion between autophagosome and lysosome and measured the level of p62. p62 accumulated in controls smNPCs after Bafilomycin A1 treatment, however did not accumulate in the patient smNPCs. This shows that patient-derived smNPCs display an impaired autophagic flux.

The genetic architecture of mitochondrial dysfunction in Parkinson's disease

Simone B. Larsen[1], **Zoé Hanss**[1], Rejko Krüger[1,2]

S. B. Larsen and Z. Hanss contributed equally to this work

[1] Luxembourg Centre for Systems Biomedicine (LCSB), University of Luxembourg, Esch-sur Alzette, Luxembourg

[2] Parkinson Research Clinic, Centre Hospitalier de Luxembourg (CHL), Luxembourg City, Luxembourg